PhD degree in Systems Medicine (curriculum in Molecular Oncology)
European School of Molecular Medicine (SEMM),
University of Milan and University of Naples "Federico II"
Settore disciplinare: BIO/11

Metformin and glucose starvation attenuate the DNA-Damage Response through the activation of Protein Phosphatase 2A

Sebastiano Peri
European Institute of Oncology (IEO), Milan
Matricola n. R12443

Tutor: Prof. Saverio Minucci
European Institute of Oncology (IEO), Milan

PhD Coordinator: Prof. Saverio Minucci
European Institute of Oncology (IEO), Milan

Anno Accademico: 2021-2022

Table of Contents

Table of abbreviations

ABC: ATP-binding cassette
AC: anthracycline (doxorubicin) + cyclophosphamide
ACM: anthracycline (doxorubicin) + cyclophosphamide + metformin
AD: Alzheimer's disease
AMPK: AMP-activated protein kinase
AR: androgen receptor
BL: basal-like (referred to TNBC)
BLBC: basal-like breast cancer (referred to TNBC)
BLIA: basal-like immune-activated (referred to TNBC)
BLIS: basal-like immune-suppressed
BRCA1 and 2: breast cancer type 1 and 2 susceptibility genes
CIP2A: cancerous inhibitor of PP2A
CP: cyclophosphamide
CSC: cancer stem cell
DBD: DNA-binding domain
DDR: DNA-Damage Response
DOX: doxorubicin
EGFR: epidermal growth factor receptor
EMT: epithelial to mesenchymal transition
ER: estrogen receptor
FACS: fluorescence activated cell sorting
GS: glucose starvation (0,45 g/L or 2.5 mM)
HER2: human epidermal growth factor receptor 2
HG: high glucose (1,8 g/L or 10 mM)
IF: intermittent fasting
IHC: immunohistochemistry
KD: knock-down
KO: knock-out
LAR: luminal androgen receptor (referred to TNBC)
IM: immune-modulatory (referred to TNBC)
M: mesenchymal (referred to TNBC)
MET: metformin
MSL: mesenchymal stem-like (referred to TNBC)
mTORC1: mammalian target of rapamycin complex 1
PARP: poly (ADP-ribose) polymerase
pCR: pathologic complete response
PDX: patient-derived xenografts
PGR: progesterone receptor
PI: propidium iodide
PP2A: Protein Phosphatase 2A
PTM(s): post-translational modification(s)
RAPA: rapamycin

ROS: reactive oxygen species
TAD: transcriptional activation domain
TNBC: Triple Negative Breast Cancer
WB: western blot

Table of figures

Abstract

The DNA-Damage Response (DDR) mediates DNA-damage sensing and repair. Protein Phosphatase 2A (PP2A) is a major phosphatase in eukaryotes and plays a critical role in countless cellular processes. Among them, PP2A has been shown to modulate the DDR, although many aspects of this regulation remain to be better characterized. PP2A integrates metabolic sensing with the DDR in yeast. Through a pharmacological and genetic approach, our group found that the combination of metformin (the most commonly used drug for type 2 diabetes) with glucose starvation increased PP2A activity. In Triple Negative Breast Cancer (TNBC) cell lines and patient-derived tumors, metformin and glucose starvation enhanced the efficacy of low-dose, DNA-damaging chemotherapy. We demonstrated that PP2A, over-activated by metformin and glucose starvation, attenuated the DDR triggered by chemotherapy, thus preventing the cell cycle arrest necessary for DNA repair and increasing genomic fragmentation, which finally led to cell death. We showed that metformin and glucose starvation increased PP2A recruitment on the chromatin; this could stabilize PP2A catalytic subunit and increase its phosphatase activity. In mouse models of TNBC, metformin and cycles of intermittent fasting (which lowered blood glucose) increased the efficacy of low-dose chemotherapy and induced tumor regression. Targeting the DDR is considered an attractive therapeutic opportunity, based on the intrinsic genomic instability of tumor cells. Here we provide a metabolic strategy to mitigate the DDR at multiple levels, which is safe, tolerable and immediate.

Introduction

1. Tumor metabolism

1.1 The hallmarks of tumor metabolism.

Aberrant metabolism is considered one of the hallmarks of cancer, which are features unique to the tumor but also putative targets for novel therapies (Hanahan & Weinberg, 2000, 2011). The first insights on tumor metabolic alterations date back nearly a century ago: Otto Warburg and colleagues observed that tumor slices exposed to high concentrations of glucose and oxygen converted the surplus pyruvate in lactate, missing the bioenergetic benefits of coupling glycolysis with the tricarboxylic acid (TCA) cycle (WARBURG, 1956). Now it's well established that the Warburg effect is a regulated metabolic state, rather than an adaptation to mitochondrial defects, and may be advantageous during a time of increased biosynthetic demand. Indeed, even though aerobic glycolysis is disadvantageous in terms of adenosine 5′-triphosphate (ATP) production, it facilitates the uptake and incorporation of nutrients into biomass and the reducing potential in the form of the cofactor NADPH (Cairns et al., 2011; Vander Heiden et al., 2009).

Aerobic glycolysis is one of the hallmarks of cancer metabolic reprogramming (Pavlova & Thompson, 2016), which is defined as the up- or down-regulation of conventional metabolic pathways as a consequence of oncogenic drive from within (activation of oncogenes and loss of tumor suppressors) and environmental pressure from without (hypoxia, pH, vascularization and nutrient availability) (reviewed in Cairns et al., 2011; DeBerardinis & Chandel, 2016). Metabolic reprogramming is one of the first steps necessary for malignant transformation and, as the tumor progresses, it must address three fundamental needs of the tumor cell, i.e., meeting bioenergetic

requirements, ensuring the biomass required to sustain a high proliferation rate and maintaining an appropriate redox balance. These will be discussed in detail in the following paragraphs, with references to the oncogene(s) which govern pathway-specific reprogramming.

Following Warburg's observations, it was thought that glycolysis was the process that produced the most ATP in cancer cells; now it is known that the greatest amount of ATP is produced by mitochondrial respiration, unless there are mutations in mitochondrial enzymes (for instance, fumarate hydratase, FH), but even then, alternative ways to circumvent the obstacle have been described (Guzy et al., 2008; Lussey-Lepoutre et al., 2015; Mullen et al., 2012; L. Zheng et al., 2015). Even in condition of low availability of oxygen and nutrients, cancer cells do not give up on mitochondrial respiration and have evolved alternative methods to supply the TCA cycle with precursors (mainly Acetyl-CoA from fatty acid oxidation and glutamine) (Fan et al., 2013; Mayers et al., 2014) (**Figure 1**). If the nutrient scarcity persists, conservative mechanisms are implemented such as: use of opportunistic ways for nutrient acquisition (Kamphorst et al., 2013; Nieman et al., 2011), inhibition of mammalian target of rapamycin (mTORC1) and consequential initiation of autophagy (J. Y. Guo et al., 2011; Strohecker & White, 2014) and activation of adenosine 5′ monophosphate (AMP)-kinase (AMPK), which curbs anabolic processes in favor of catabolic processes (for instance, fatty acid oxidation) (reviewed in Hardie et al., 2016). This is due to a certain flexibility of tumor cells and adaptability to change in nutrient availability (metabolic plasticity) (Jia et al., 2019).

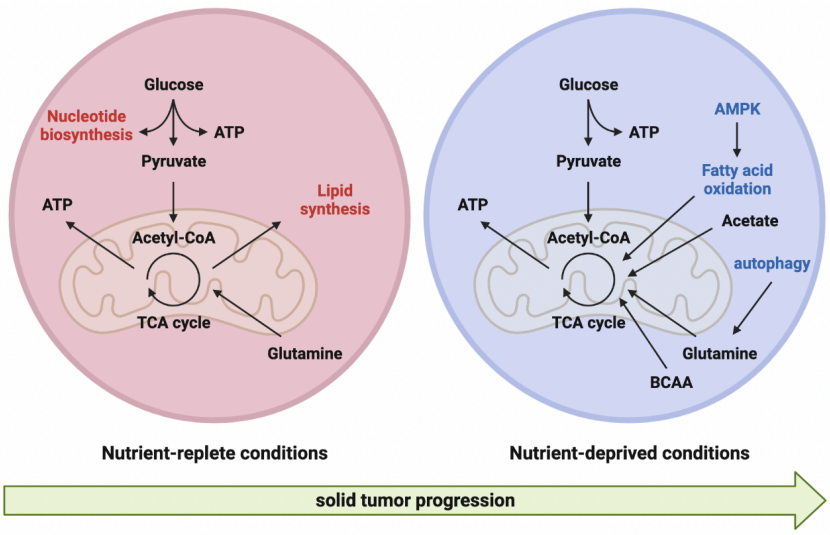

Figure 1: metabolic plasticity allows cancer cells to adapt to changes in nutrient availability.

Metabolic pathways in cancer cells under nutrient availability and deprivation. Adapted from DeBerardinis & Chandel, 2016.

In addition to glucose, to sustain high replicative rate, tumors need huge amounts of proteins, lipids, and nucleic acids. Many pathways necessary for the production of macromolecules are branched from glycolysis, hence the advantage of a high glycolytic rate even in presence of oxygen (**Figure 2**): the pentose phosphate pathway (PPP), the hexosamine synthesis pathway, the glycogenesis and the serine biosynthesis (reviewed in Hay, 2016). Tumor cells maximize the yield from glycolysis by: i) trapping glucose in glycolysis through the over-expression of glucose channel (GLUT-1) and hexokinase 2 (HK2) (Mathupala et al., 2001; Robey & Hay, 2006; J. E. Wilson, 2003); ii) mitigating the last step of glycolysis (conversion of phospho-enol-pyruvate to pyruvate) to diverge as many metabolites as possible to the branches (Israelsen & Vander Heiden, 2015); iii) maximizing the conversion of pyruvate to lactate through lactate dehydrogenase A (LDHA), which is then secreted (Doherty & Cleveland, 2013; Valvona et al., 2016); the NAD+ formed in the process is used in the first steps of

serine synthesis for the production of essential amino acids. Sill, cancer cells have enough pyruvate to enter the TCA cycle, further facilitated by glutamine from outside (Hensley et al., 2013). Lactate itself promotes tumorigenesis: it increases extracellular vascular endothelial growth factor A (VEGFA) (Fukumura et al., 2001; Shi et al., 2001), is used by stromal cells to produce pyruvate then internalized by tumor cells and inhibits tumor-infiltrating lymphocytes (Fischer et al., 2007).

Cancer cells acquire amino acids from the extracellular environment, which keeps mTORC1 activity high, thus promoting protein synthesis and ribosome biogenesis (reviewed in Laplante & Sabatini, 2012). Non-essential amino acids are synthesized from glutamine-derived glutamate; glutamine can itself be exported in exchange for essential amino acids.

Acetyl-CoA (derived mainly from glucose but also from glutamine) and NADPH (from the PPP) are needed for fatty acid synthesis (DeBerardinis et al., 2007; Fan et al., 2014). The transcription factors sterol regulatory element binding protein 1 and 2 (SREBP-1 and 2), contributed by mTORC1, regulate genes involved in fatty acid synthesis (Horton et al., 2002; T. R. Peterson et al., 2011). Lipids and fatty acids can be also internalized from the extracellular environment with the contribution of the phosphoinositide 3-kinases (PI3K) signaling pathway.

The synthesis of nucleotides requires NADPH, glutamate, TCA cycle-derived oxaloacetate and precursors from the PPP and from the one carbon/folate metabolism. Little is known about the contribution of oncogenes, but mTORC1 appears to play an important role (Ben-Sahra et al., 2013).

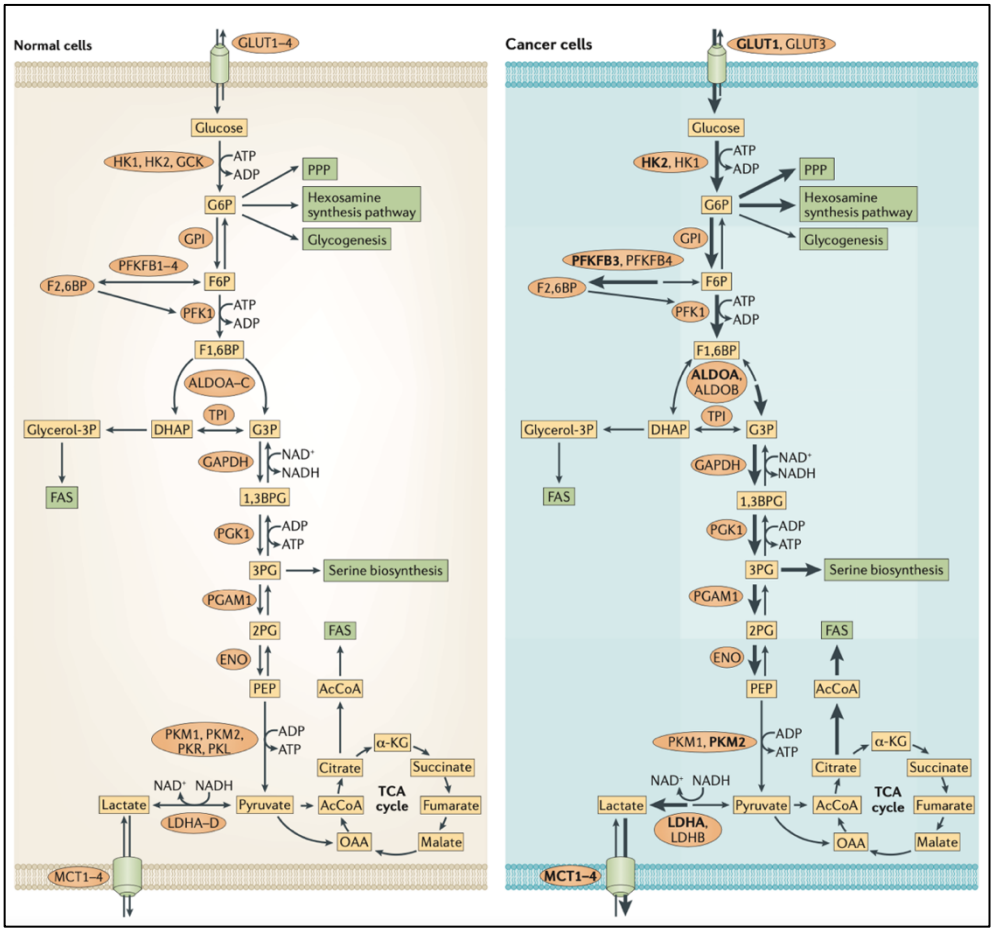

Figure 2: metabolic changes and enhanced metabolic flux in glucose metabolism from normal to cancer cells.

1,3BPG, 1,3-bisphosphoglycerate; 2PG, 2-phosphoglycerate; 3PG, 3-phosphoglycerate; α-KG, α-ketoglutarate; Ac-CoA, acetyl-CoA; ALDO, aldolase; DHAP, dihydroxyacetone-phosphate; ENO, enolase; F1,6BP, fructose-1,6-bisphosphate; F2,6BP, fructose-2,6-bisphosphate; F6P, fructose-6-phosphate; FAS, fatty acid synthesis; G3P, glyceraldehyde-3-phosphate; G6P,glucose-6-phosphate; HK, hexokinase; LDH, lactate dehydrogenase; GAPDH, glyceraldehyde- 3-phosphate dehydrogenase; GCK, glucokinase; GLUT, glucose transporter; glycerol-3P, glycerol-3-phosphate; GPI, glucose-6-phosphate isomerase; MCT, monocarboxylate transporter; OAA, oxaloacetate; PEP, phosphoenolpyruvate;PFK1, phosphofructokinase1; PFKFB, 6-phosphofructo2-kinase/fructose-2,6-bisphosphatase; PGAM1, phosphoglycerate mutase 1; PGK1, phosphoglycerate kinase 1; PK, pyruvate kinase; PPP, pentose phosphate pathway; TCA, tricarboxylic acid; TPI, triosephosphate isomerase.

Pathways or enzymes over-activated or over-expressed in tumors compared with healthy cells are highlighted in bold. Adapted from Hay, 2016.

From early stage to metastasis, cancer cells have to maintain a proper balance between (over-)production of ROS and anti-oxidant defenses to prevent high level of ROS from damaging DNA, proteins and lipids, as exemplified in **Figure 3**. Tumor cells exhibit higher ROS levels than healthy tissue due to over-activation of oncogenes and loss of tumor suppressors. In the early stages of malignant transformation, low levels of ROS promote tumor progression through activation of the PI3K and mitogen-activated protein kinase (MAPK) pathways, and the transcription factors hypoxia-inducible factor 1 (HIF1) and nuclear factor kB (NF-kB). At this stage, the uncontrolled increase in ROS is buffered by the induction of nuclear factor (erythroid-derived 2)–related factor 2 (NFR2)-dependent genes and through NADPH produced by the PPP (DeNicola et al., 2011, 2015; Harris et al., 2015; Ye et al., 2014). As tumor mass increases, nutrient and oxygen availability decreases; this causes a further increase in ROS. Under the condition of glucose shortage, the PPP is unable to provide sufficient levels of NADPH, which is then replenished by one-carbon metabolism. Low levels of ATP activate AMPK, which, as anticipated, blocks NADPH-consuming anabolic processes (Jeon et al., 2012; Saito et al., 2015). The detachment from the matrix for the metastatic phase results in a further increase in ROS, which are buffered primarily through NADPH by one-carbon metabolism (Jiang et al., 2016; Schafer et al., 2009). It is important to consider that too high or too low levels of ROS are equally incapable of sustaining tumor progression.

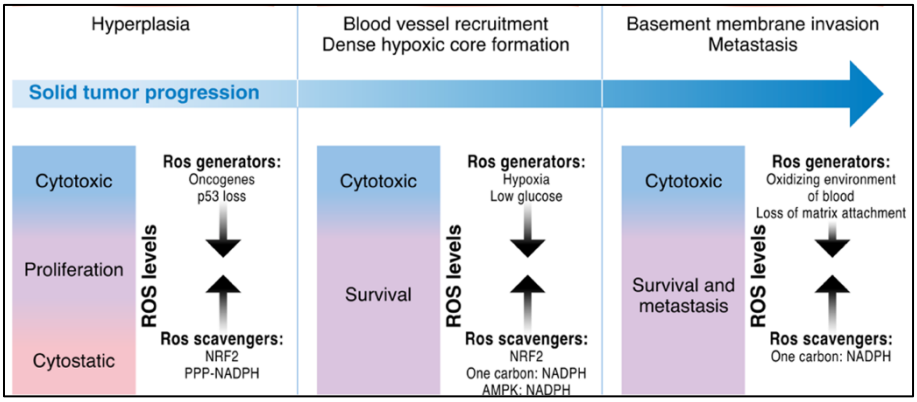

Figure 3: tumor cells maintain a favorable REDOX balance.

Balance between ROS production and anti-oxidant defenses in cancer cells correlated with solid tumor progression. Sources and ROS scavengers are indicated. Adapted from DeBerardinis & Chandel, 2016.

1.2 Tackling tumor metabolism.

When it comes to metabolism, identifying the perfect molecular target is not easy, since inhibition of a specific pathway could cause both systemic toxicity and for fast cycling cells (such as immune cells) (K. Ito & Suda, 2014; Pearce et al., 2013). There are excellent examples already used in the clinic: antifolates inhibit nucleotide synthesis and are the standard of many chemotherapy regimens. The glycolytic enzymes LDHA and HK2 were the first metabolic targets whose inhibition showed encouraging results in animal models (even though the effects on the immune system could not be assessed since immune-deficient mice were principally used) (Fantin et al., 2006; Le et al., 2010; Y.-H. Wang et al., 2014; Xie et al., 2014). Also, serine metabolism supports tumor growth and may become a drug target (Kim et al., 2015; Labuschagne et al., 2014).

Metformin (which is the most widely used drug in the world for type 2 diabetes) is a good example of drug repositioning: from epidemiological data, the use of metformin

has been associated with a lower onset of tumors and a longer survival in oncologic patients (Daugan et al., 2016; Evans et al., 2005; Memmott et al., 2010). Mechanistically, metformin inhibits mitochondrial complex I in cells expressing organic cation transporters (OCTS), found in the liver, kidneys and some types of tumors (Bridges et al., 2014; El-Mir et al., 2000; Owen et al., 2000). The anti-cancer effect of metformin is supposed to be due to both a systemic hypoglycemic effect (consequence of gluconeogenesis inhibition in the hepatocytes), and by direct actions on the tumor cells; in this contest, metformin works best when combined with strategies that inhibit glycolysis, the second largest source of ATP (Birsoy et al., 2014; Elgendy et al., 2019; Griss et al., 2015; Pollak, 2014; Wheaton et al., 2014)]. Metformin has also been shown to be effective in targeting cancer stem cells and preventing relapse (Janzer et al., 2014; Roesch et al., 2013).

As previously anticipated, one strategy could be to lower the cancer's antioxidant defenses and allow ROS to irreversibly damage cancer cells. Eliminating NADPH-producing systems would cause systemic toxicity, except for the two enzymes Glucose-6-phosphate de-hydrogenase (G6PDH, whose deficiency causes favism and is compatible with survival) and MTHFD2. Another approach lies in saturating glutathione (GSH) with high levels of oxidized vitamin C (Y. Ma et al., 2014; Tagde et al., 2014).

2. Protein Phosphatase 2A

2.1 Protein phosphatases.

In all types of cells, a vast number of processes are carried out through phosphorylation and de-phosphorylation events, by kinases and phosphatases, respectively. The

formers have been more extensively investigated during the past decades given the high number of oncogenes in the kinase family, while the latter have only recently attracted the scientific interest, not only in cancer research. There are more than 650 kinases and about 190 phosphatases (M. J. Chen et al., 2017; X. Li et al., 2013); this has led to the mistaken belief that kinases mediated more selective reactions while phosphatases were more promiscuous. In contrast, the catalytic sites of phosphatases can associate with different regulatory proteins giving rise to an enormous range of enzyme complexes. Today we talk about the "phosphatase code" whereby each specific protein or enzyme complex recognizes a unique and precise motif on the phosphatase target (M. J. Chen et al., 2017). Phosphatases can be constituted by single catalytic units or by enzymatic complexes. As with kinases, there are serine, serine/threonine and tyrosine phosphatases, and they both use water to cleave a phosphomonoester into a phosphate ion and an alcohol.

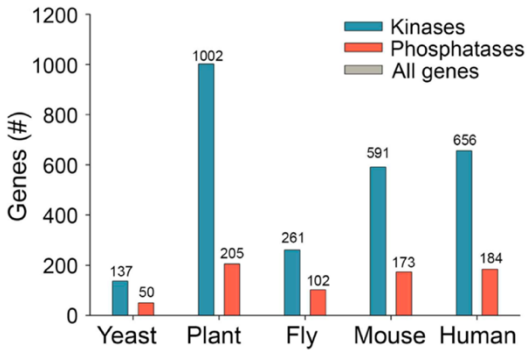

Figure 4: kinase and phosphatase encoding genes in five eukaryotic genomes.

Adapted from Smoly, 2016.

2.2 Protein Phosphatase 2A: structure.

PP2A is a ubiquitously expressed Ser/Thr phosphatase which is responsible for most the de-phosphorylation events in eucaryotes. PP2A is not a single protein but rather an enzymatic complex consisting of a dimeric core (composed by the scaffold A subunit and the catalytic C subunit) and several regulatory B subunits (grouped in 4 sub-families with at least 15 members) which confer localization and target specificity (Janssens & Goris, 2001) (**Figure 5 - 6**).

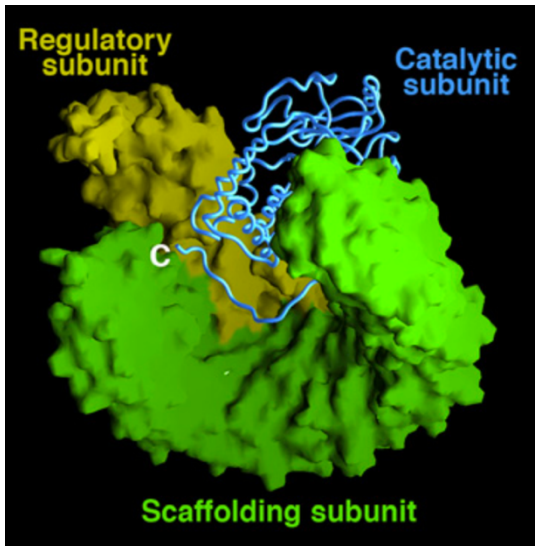

Figure 5: crystal structure of PP2A holoenzyme.

The scaffold A subunit is shown in green, the catalytic C subunit in blue and the regulatory B subunit in yellow. Adapted from Xu, 2006.

The catalytic C subunit (PP2Ac) has a globular structure, with the C-terminus containing the binding domain for the scaffold and the regulatory subunits. In mammals, the existence of two PP2Ac isoforms, α and β, has been described, encoded by two different genes, *PPP2CA* and *PPP2CB*, respectively, with a sequence identity of 97% (T. A. Jones et al., 1993); they are both ubiquitous but Cα is the most abundant,

with expression levels 10 times higher than Cβ. PP2Ac is evolutionary conserved from lower organism to mammals (drosophila, plants and yeast). Knock-down (KD) or knock-out (KO) of the C subunit is (embryonically) lethal.

The 65 KDa scaffold subunit A (PP2Aa) presents a horseshoe shape with 15 tandem HEAT repeats that give it flexibility when interacting with the catalytic subunit C and regulatory subunits (Cho & Xu, 2007; Xing et al., 2006; Xu et al., 2006). As the catalytic, also the scaffold subunit has two isoforms, Aα and Aβ, encoded by two distinct genes, *PPP2R1A* and *PPP2R1B*, respectively; again, the Aα is more abundant and is present in 90% of all the PP2A assemblies.

The PP2A-B regulatory subunits encompass 26 different transcripts and splicing variants from four different families: B (B55/PR55), B′ (B56/PR61), B″ (PR72/PR48/ /PR130), and B‴ (STRN/PR93/PR110). The width of diversity reflects the role of the B subunits in target and compartment identification and allows the generation of more than 90 enzymatic complexes (Janssens & Goris, 2001). In mammals, the B family comprises 55 KDa proteins (PR55α, β, γ, δ) encoded by four genes with little sequence similarity; PR55β and γ is highly enriched in the brain, while the others have a more widespread tissue distribution.

The B′ family comprises five proteins (PR56α, β, γ, δ, ε) with a molecular weight of 56 KDa. The B′ subunits share 80% similarity and redundancy between their functions and localization is thought to occur. Studies demonstrated the existence of a shared consensus motif recognized by the B56 family (LxxIxE) (Hertz et al., 2016; Kruse et al., 2020), confirming the fact that phosphatases are not as promiscuous as previously thought, but each family or regulatory subunits has a specific binding preference. The B‴ is far less studied compared to the B and B′ families and encompasses three subunits with different tissue distribution; B″ subunits have calcium binding motif,

suggesting that calcium could be a mediator for B″ subunits-containing complexes (Janssens et al., 2003). The B‴ family significantly differs from the others families and includes calmodulin-binding proteins. Striatins (STRN) belong to this family. Based on the target they recognize, B and B′ family form tumor suppressor complexes, while B″ and B‴ have oncogenic properties.

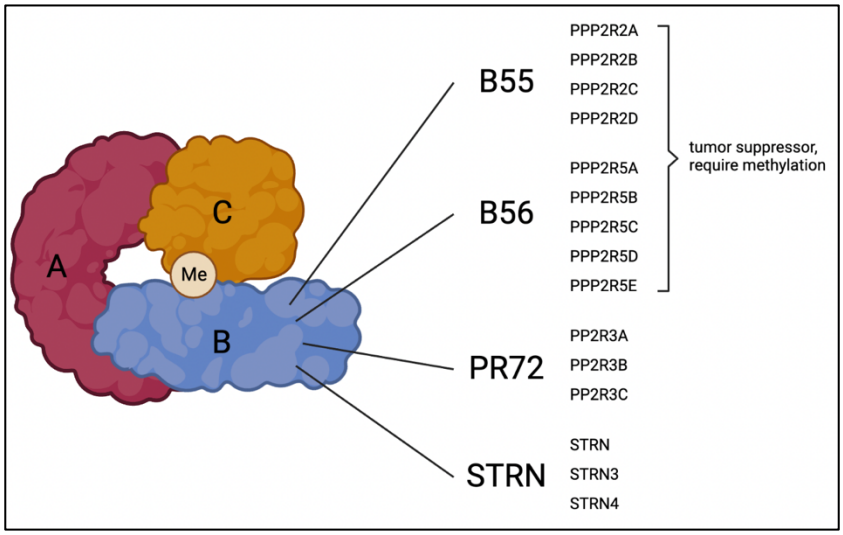

Figure 6: PP2A "canonical" complexes.

PP2A trimeric holoenzyme composed by the scaffold A, the catalytic C and one of the fifteen B subunits divided into four families. Adapted from Westermarck & Neel, 2020.

The heterotrimers assembly through a multi-step process described in **Figure 7**: PP2A phosphatase activator (PTPA) stabilizes the catalytic subunit while ATP enhances binding of metal ions (Mn^{2+}) necessary for the phosphatase activity (F. Guo et al., 2014). Then, leucine-carboxyl methyl transferase (LCMT) methylates PP2Ac at Leu309, which is required for the assembly with B55 and B56 tumor suppressor subunits; this process is reversed by PP2A methyl-esterase (PME-1) (Sangodkar et al., 2016). In cancer cells the activity of LCMT is low compared to PME-1, thus leading to the incorporation of other B subunits (as striatins) that do not require methylation and

sometimes give rise to complexes with oncogenic activity. Also, endogenous inhibitors of PP2A (which will be described in detail in the next section) can sequester B55 and B56 subunits, even when PP2Ac is properly methylated (W. Chen et al., 2004; Fowle et al., 2019).

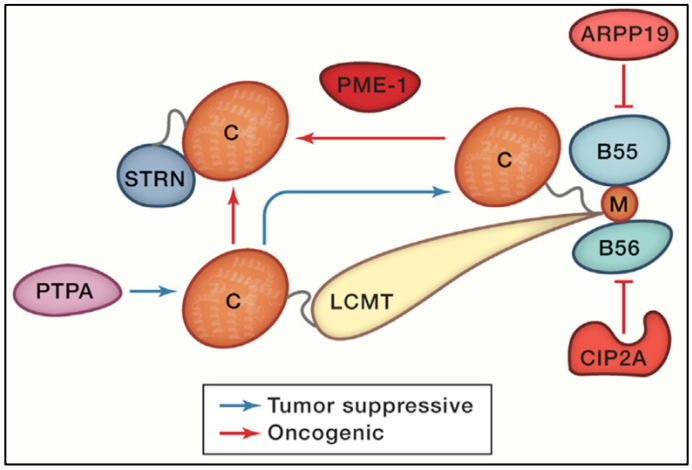

Figure 7: multistep biogenesis of PP2A tumor suppressor complexes.

PTPA, PP2A phosphatase activator; LCMT, leucine-carboxyl methyl transferase; PME-1, PP2A methyl-esterase; CIP2A, cancerous inhibitor of PP2A. STRN, Striatins. Adapted from Westermarck & Neel, 2020.

2.3 Protein Phosphatase 2A: inhibitors.

PP2A is considered a crucial tumor suppressor for the following reasons: i) its inactivation (with okadaic acid or by endogenous inhibitors) is a necessary step for tumor transformation, together with the loss of essential tumor suppressors (p53 and RB), the expression of telomerases, and the activation of oncogenes (Ras) (Junttila et al., 2007; Sablina et al., 2007); ii) it counteracts the major oncogenic pathways, including MEK, MYC and AKT (Arnold & Sears, 2006; W. Chen et al., 2004; Mumby, 2007). Not many PP2A genetic mutations have been described and only in certain

types of tumors (Calin et al., 2000; Kauko & Westermarck, 2018) (e.g., mutation of B55α in AML blasts (Ruvolo et al., 2011)), thus suggesting that other mechanisms prevent the activity of PP2A as tumor suppressor. Indeed, a considerable number of endogenous inhibitors of PP2A have been described from human cells to viruses; some generically inhibit all holoenzymes, while others are more selective.

PP2A inhibitor 1 (ANP32a) and 2 (SET) inhibit the C subunit alone or complexed either with the A or the A and the B subunits, indicating no selectivity towards a specific holoenzyme. Both their activity and cytosol/nucleus retention are governed by phosphorylation events (Irie et al., 2012; ten Klooster et al., 2007; Yu et al., 2013). SET is over-expressed in various cancers like chronic myelogenous leukemia and Wilms tumor. Beyond the cancer field, a potent example of SET aberrant activity is Alzheimer's disease (AD), in which a strong inhibition of PP2A leads to maintenance of an hyperphosphorylated Tau protein (H. Wei et al., 2020).

TIPRL (TOR signaling pathway regulator) allosterically inhibits the C subunit alone or complexed with the A subunit (McConnell et al., 2007; Smetana & Zanchin, 2007). TIPRL negatively regulates nuclear PP2A involved in the DNA-Damage Response (DDR), as well in mTORC1 pathway regulation (Nakashima et al., 2013).

Cancerous inhibitor of PP2A (CIP2A) (first described in Junttila et al., 2007) sequesters the B56 subunits preventing assembly of the holoenzyme (J. Wang et al., 2017). The over-expression of CIP2A in many tumor types appears to be due to the transcription factors MYC (A. Khanna et al., 2009), ETS (A. Khanna et al., 2011) and E2F (Laine et al., 2013). CIP2A increases the stability of MYC (and its phosphorylated form on serine 62) (Junttila et al., 2007; Myant et al., 2015), the signaling of AKT, the anchorage-independent growth and the activation of the mTORC1 pathway (Puustinen et al., 2014; Puustinen & Jäättelä, 2014).

PP2A mitotic inhibitors include: ENSA, ARP-19 and BOD1. All are selective for PP2A complexes containing B55 subunits and all are activated by major cell cycle kinases through phosphorylation events (Dupré et al., 2014; Gharbi-Ayachi et al., 2010; Manchado et al., 2010; Mochida et al., 2010; Porter et al., 2013).

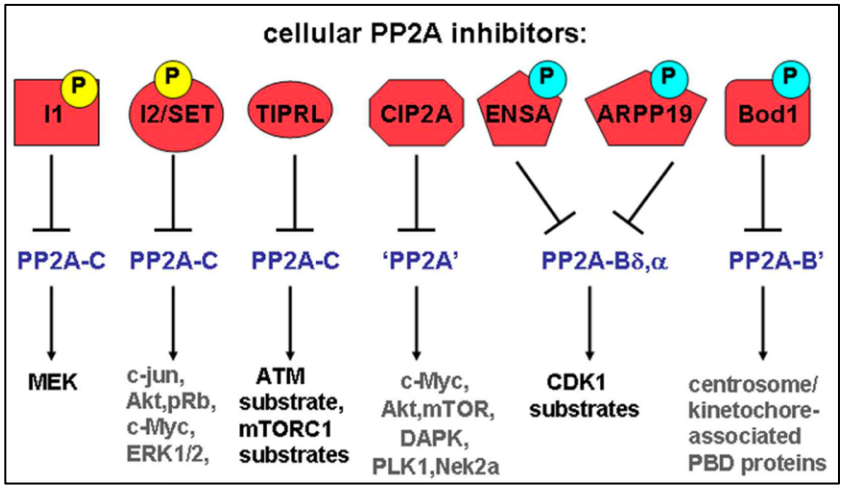

Figure 8: PP2A endogenous inhibitors.

Schematic representation of endogenous PP2A inhibitors, their subunit/holoenzyme specificity, and the PP2A target they affect. PP2A inhibitor 1 and 2 are regulated by phosphorylation (yellow), while PP2A mitotic inhibitors are strictly dependent on phosphorylation (blue). Adapted from Haesen, 2014.

2.4 Protein Phosphatase 2A: functions.

Given the complexity of the holoenzyme and the wide range of substrates, it is not surprising that PP2A is involved in countless cellular processes, of which, in the following section, some specific examples are given with a particular focus on the tumor suppressor role of PP2A.

First of all, PP2A is essential during embryogenesis and KO of the catalytic (PP2Acα) subunit is embryonically lethal. Indeed, PP2A controls proliferation and apoptosis through the de-phosphorylation of AKT (Kuo et al., 2008), Wnt signaling pathway (X. Li et al., 2001), the pro-apoptotic BAD (Chiang et al., 2001) and anti-apoptotic BCL2 proteins (X. Li et al., 2002; S. S. Lin et al., 2006). PP2A de-phosphorylates MYC at Ser62 leading to MYC destabilization and growth defects in different types of tumors; CIP2A over-expression counteracts MYC destabilization (Junttila et al., 2007; Myant et al., 2015). PP2A inhibits and is itself inhibited by mTORC1 (R. T. Peterson et al., 1999; Yan et al., 2010); also, PP2A negatively controls the MAPK pathway (Lao et al., 2007; Letourneux et al., 2006; Ugi et al., 2002).

PP2A regulates the cell cycle at multiple levels. PP2A decreases β-catenin signaling through the stabilization of Glycogen-Synthase kinase 3β (GSK3β), which phosphorylates and targets β-catenin for degradation (Kumar et al., 2012; Mitra et al., 2012). To enter mitosis, cells have to activate CDK1 and inactivate PP2A, which otherwise would inhibit CDC25, necessary for cell-cycle progression (Margolis et al., 2006; Mochida et al., 2009); cyclin A-CDK2 also contributes to PP2A inactivation by phosphorylating Greatwall kinase, which in turns activate the PP2A mitotic inhibitor ENSA (Mochida et al., 2010). PP2A is important for both entry and exit from mitosis as it stabilizes kinetochore-microtubules attachments (Foley et al., 2011), induces the reassembly of the Golgi apparatus (Lowe et al., 2000; Schmitz et al., 2010) and promotes chromosome de-condensation (Afonso et al., 2014).

PP2A maintains cell adhesion and its disruption leads to loss of cell polarity, enhances cell motility and invasiveness (A. Ito et al., 2000; Young et al., 2002, 2003). Furthermore, PP2A controls the DNA-Damage Response (DDR) in unperturbed

conditions or after the DNA lesions have been solved (Freeman et al., 2010; C. Y. Guo et al., 2002; X. Li et al., 2015; Petersen et al., 2006; Shimada & Nakanishi, 2013).

PP2A also plays a role in cellular metabolism as it negatively regulates insulin metabolic signaling by dephosphorylating AKT and Protein Kinase C (PKC) (Ugi et al., 2004). Recently, our group proposed a model of synthetic lethality achieved by the combination of metformin with hypoglycemia, obtained *in vitro* by lowering of glucose in the medium, and *in vivo* by cycles of intermittent fasting. The anti-tumor effect was not simply the result of a metabolic catastrophe but it was mediated by PP2A upstream of GSK3β and MCL1, and did not depend on AMPK (Elgendy et al., 2019). Furthermore, a growing body of evidence agrees that PP2A not only regulates cell metabolism, but is itself regulated by certain metabolites: ceramides, a class of sphingolipids, activate PP2A through inhibition of SET (Ferrari et al., 2017; Mukhopadhyay et al., 2009; Perry et al., 2012).

2.5 Strategies to activate PP2A in cancer.

Given the role of PP2A as tumor suppressor, the (recent) efforts to release its anti-proliferative potential in cancer are not surprising. Phenothiazines (PPZs), which are anti-psychotic drug, have off-target effect as PP2A activator, even though the molecular mechanism was unclear (Gutierrez et al., 2014). Thanks to the small molecule activator of PP2A (SMAP) DT-061, it was possible to study the precise molecular mechanism: DT-061 functions as a molecular glue that stabilizes B56α-containing PP2A (Leonard et al., 2020), in a context of dynamic exchange between different B subunits (Westermarck & Neel, 2020). Another recent work proposed the use of a different molecule, improved heterocyclic activator of PP2A, or iHAP, which,

unlike phenothiazines, has no dopamine D2 receptor (DRD2) binding activity and promotes the assembly of a B56ε-containing PP2A (Morita et al., 2022). This work has recently been retracted given the toxicity of iHAP on microtubule polymerization, which prevents an objective assessment of the efficacy in *vivo*.

Since malignant transformation requires both the over-activation of oncogenes and the down-regulation of PP2A, a recent work demonstrated that the simultaneous activation of PP2A (e.g., with DT-061) and inhibition of oncogenic pathways, such as that of MAPKs (specifically, inhibition of RAS) induced cell death both in *vitro* and in *vivo* (Kauko et al., 2018). Other strategies to activate PP2A imply counteracting the activity of PP2A endogenous inhibitors: to date, no selective inhibitors of CIP2A are available, but ceramides (and in particular a synthetic derivative, FTY720) inhibit SET thereby activating PP2A.

3. The DNA-Damage Response

3.1 The DNA Damage Response: description.

The term DNA-Damage Response (DDR) indicates the large set of intra- and inter-cellular events that begin with the detection of a DNA lesion and lead to different consequences depending on the type and magnitude of the damage and the stage of the cell cycle at which it occurs. These include cell cycle arrest, DNA-damage repair, and, if this is not possible, death or senescence (d'Adda di Fagagna et al., 2003).

For each type of DNA injury there is a specific repair system (J. H. Hoeijmakers, 2001) (**Figure 9**), and one system can compensate for the lack of another, albeit less efficiently. Through a mechanism known as direct repair, O^6-methylguanine DNA methyltransferase (MGMT) demethylates O^6-methylguanine lesions which are formed

as a result of incorrect methylation or following chemotherapy (Tubbs et al., 2007). Base-excision repair (BER) pathway repairs abnormal bases and abasic sites that can give rise to DNA single-strand breaks (SSB) during replication (Caldecott, 2014). Nucleotide excision repair (NER) removes DNA adducts from exposure to UV-light and chemical agents (as platinum salts) (J. H. J. Hoeijmakers, 2009). The mismatch repair (MMR) pathway recognizes and repairs mismatch base-pairing, and nucleotide insertions/deletions (Jiricny, 2006). DNA double strand breaks (DSB) are repaired by: homologous recombination (HR), which uses the undamaged sister chromatid as a template and is therefore more accurate (Moynahan & Jasin, 2010) or non-homologous end-joining (NHEJ) which does not need the sister chromatid but is less accurate and introduces errors (Ceccaldi et al., 2016; Lieber, 2010). The phase of the cell-cycle at which the DNA-damage occurs influences the choice of repair system; for example, DSBs occurring before the S-phase can only be repaired through NHEJ.

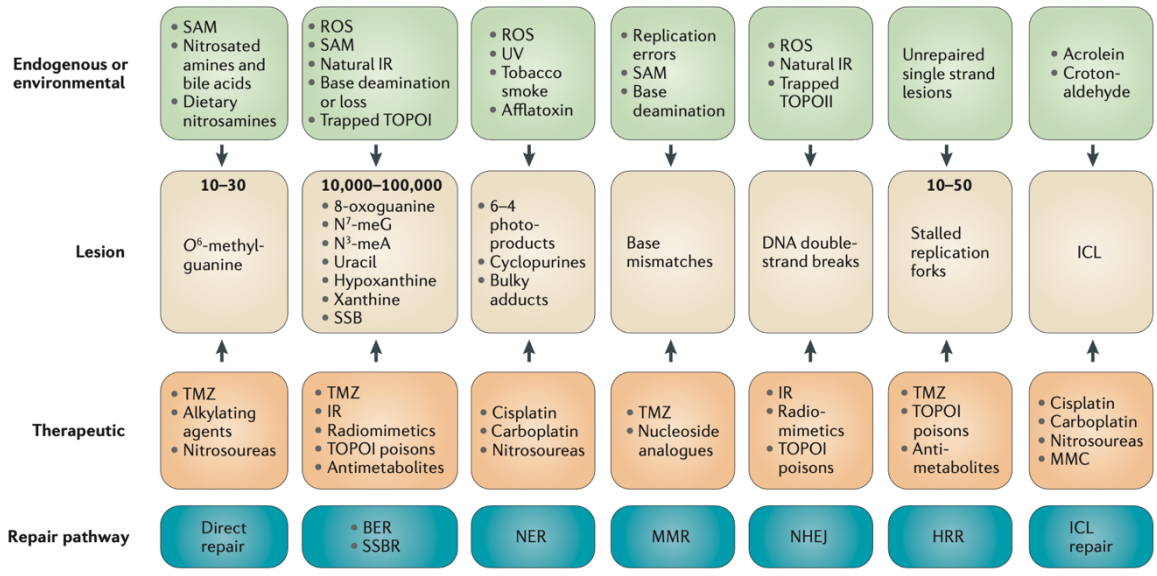

Figure 9: DNA-damage sources and repair processes.

Endogenous or environmental sources of DNA-damage are listed in green boxes, with the lesion they cause in beige boxes. The orange boxes list the therapeutic agents that cause that

specific injury. DNA repair pathways are shown in blue boxes. BER, base excision repair; HRR, homologous recombination repair; ICL, interstrand crosslink; IR, ionizing radiation; MMC, mitomycin C; MMR: mismatch repair; NER, nucleotide excision repair; NHEJ, non-homologous end joining; ROS, reactive oxygen species; SAM, S-adenosyl methionine; SSB, single-strand break; SSBR, SSB repair; TMZ, temozolomide; TOPO, topoisomerase; UV, ultraviolet. Adapted from: Curtin, 2012.

Specific checkpoints recognize the DNA-damage and initiate its repair, thus preventing it from being passed to the next phase of the cycle. In particular, G1/S checkpoints (ATM, CHK2 and to a lesser extent p53) give time to repair DNA before replication begins; the S-phase checkpoints (ATR, CHK1, DNA-PK and WEE1) delay the replication to repair any lesions that have not yet been repaired or that occur during replication itself; the G2/M checkpoints (CHK1, MYT1, WEE1) represent the last opportunity to repair any injuries before they can be carried into mitosis and cause mitotic catastrophe and cell death (Castedo, Perfettini, Roumier, Andreau, et al., 2004; Castedo, Perfettini, Roumier, Valent, et al., 2004).

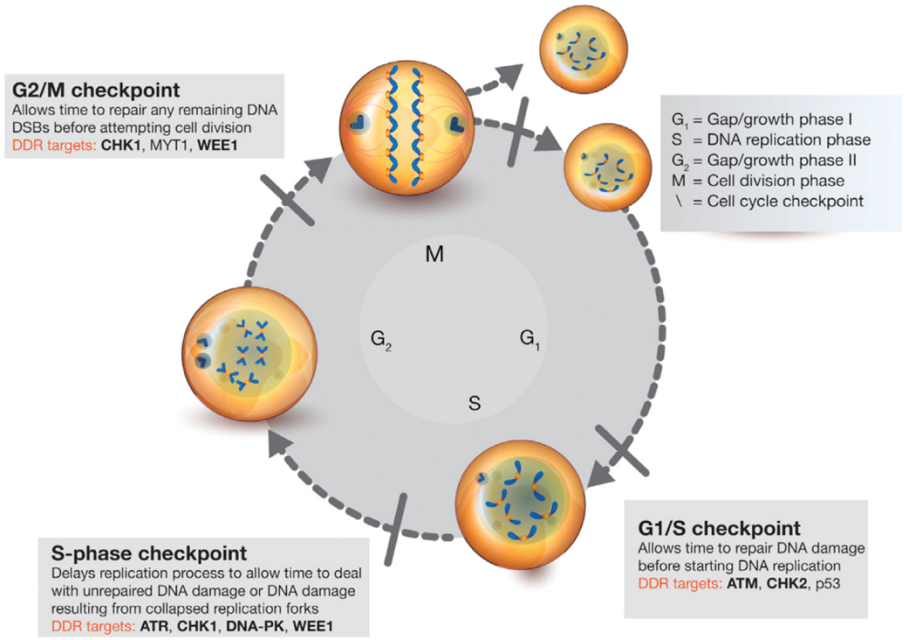

Figure 10: the DDR checkpoints controls genome integrity.

APE1, AP endonuclease 1; ATM, ataxia-telangiectasia mutated; ATR, ataxia-telangiectasia and Rad3-related; DNA-PK, DNA-dependent protein kinase; PARP, poly (ADP-ribose) polymerase. Adapted from O'Connor, 2015.

3.2 The DNA-Damage Response checkpoints.

The Ataxia-telangiectasia-mutated (ATM) and Ataxia-telangiectasia and Rad3-related (ATR) kinases belong to the class-IV phosphoinositide 3-kinase-related kinase (PIKK) family together with mTOR, DNA-PK, suppressor of morphogenesis in genitalia-1 (SGM-1) and transformation/transcription-associated protein (TRAPP); differently from other members of the family, ATM and ATR lack lipid kinase activity and possess Ser/Thr kinase activity (Bakkenist & Kastan, 2004). They both exist as homo- or hetero-dimer; in particular, ATM forms homo-dimers under unperturbed conditions and monomers are released following DSBs. ATR forms a hetero-dimer with its obligate partner, ATR-interacting protein (ATRIP) (Bakkenist & Kastan, 2003).

The activation of ATM at the sites of DSBs is strictly dependent on the MRE11-RAD50-NBS1 (MRN) complex, which first interacts with the DNA (Falck et al., 2005; Hartlerode et al., 2015; J.-H. Lee & Paull, 2005; Paull, 2015). In addition, post-translational modifications (PTMs) such as autophosphorylation at Ser1981 and acetylation at Lys3016 are necessary for ATM monomerization, stabilization, and interaction with the MRN complex and the DNA (Bakkenist & Kastan, 2003; So et al., 2009; Y. Sun et al., 2005, 2007). ATM immediately phosphorylates the histone variant H2Ax (which accounts for 10-25% of the H2A histones) at Ser139 (γHA2x); this PTM serves to anchor other proteins of the DDR, thus amplifying exponentially the DNA-damage signal (X. Huang et al., 2004). In response to DSBs, ATM recruits either BRCA1 or P53 Binding Protein 1 (53BP1), depending on the phase of the cell cycle, to favor HR or NHEJ, respectively (Bouwman et al., 2010). CHK2 is phosphorylated at Thr68 and is the main mediator of the ATM early response (Cai et al., 2009). CHK2 phosphorylates several targets including CDC25A, which upon phosphorylation is degraded, thus preventing activation of the CDK1-cyclin B complex and cell cycle progression, and P53, which reinforces G1-phase arrest. P53 is also phosphorylated directly by ATM at Ser15. Transcription of P53-target genes counts as late modulation by ATM and leads to further cell cycle arrest (by the CDK inhibitor P21) or initiation of apoptotic processes (Turenne et al., 2001).

The activation of ATR in response to persistent single-stranded DNA (ssDNA) is a multi-step process that requires several effectors. Normally, ssDNA occurs during replication and is rapidly solved by the DNA-damage repair pathways (mostly, NER and BER). ATR-ATRIP binding on the ssDNA depends on Replication Protein A (RPA) (Zou & Elledge, 2003), and on the RAD9-RAD1-HUS1 (9-1-1) complex, which interacts extensively with ATRIP although the loading mechanisms are different and

independent. Also, the RAD17-RFC-TOBP1 complex participates (Choi et al., 2010; Cimprich & Cortez, 2008; St Onge et al., 2003). Once activated, ATR i) ensures controlled replication by stabilizing replicative forks so that they do not degenerate in DSBs (Couch et al., 2013; Paulsen & Cimprich, 2007), ii) maintains a low firing of replicative origins (Y.-H. Chen et al., 2015; Shechter et al., 2004), iii) pairs replication with transcription (Bermejo et al., 2011), iv) starts the replication stress response (Flynn & Zou, 2011) and v) favors the increase of Ribonucleotide Reductase M2 (Buisson et al., 2015). Downstream of ATR, CHK1, phosphorylated on residues Ser317 and Ser345, contributes to the S-phase effects of ATR (Brown & Baltimore, 2003; Maya-Mendoza et al., 2007; Petermann et al., 2006, 2010; Segurado & Diffley, 2008; Zhao & Piwnica-Worms, 2001); it also phosphorylates and thereby down-regulates CDC25A, while sequestering CDC25C in the cytosol, which in turn does not activate the CDK1-cyclin B complex, avoiding G2/M progression (Nghiem et al., 2001).

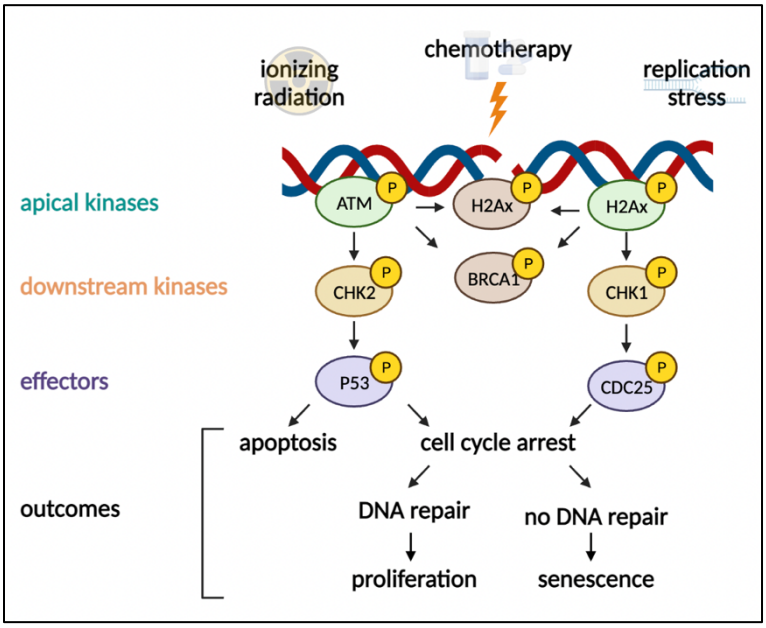

Figure 11: the DDR signaling cascade.

3.3 Targeting the DNA-Damage Response in cancer.

Given the critical role of DDR in preserving genomic integrity, one wonders why targeting it is a therapeutic opportunity in cancer therapies. Mark O'Connor explains it well in his review (M. J. O'Connor, 2015). In particular, he makes a distinction between healthy and cancer cells, highlighting three aspects of the DDR that differ between the former and the latter: i) loss of one or more DDR pathways, ii) increased levels of replication stress and iii) increased levels of endogenous DNA damage.

Regarding the first point, it has been shown that, in pre-cancerous cells, activation of the DDR (mainly the ATM and ATR pathways) is a barrier to tumor transformation (Bartkova et al., 2005, 2010; Gorgoulis et al., 2005). The inactivation of a specific pathway is therefore necessary for complete tumor transformation, but, at the same time, it makes the cancer cell dependent on the remaining pathway, which becomes its "Achilles heel" (Ashworth, 2008; Curtin, 2012). Targeting that one remaining pathway - a concept described as synthetic lethality - has proven to be an effective approach; see in this regard the recent approval of olaparib (Lynparza), an inhibitor of PARP, which is necessary for SSBs repair, in Breast Cancer type 1 and 2 susceptibility genes (*BRCA1* and *BRCA2*)-mutated tumors [EMA, 2014; FDA, 2015]. Both BRCA1 and BRCA2 participate in the repair of DSBs in the process of HR (Prakash et al., 2015) and their loss of function predisposes to greater genomic instability and cancer risk (Venkitaraman, 2014). PARP inhibitors (PARPi) block inactive PARP on SSBs that evolve to DSBs (Helleday, 2011; Murai et al., 2012); since they are unable to repair the damage by HR, BRCA1- and BRCA2-mutated tumors rely on NHEJ alone, which, having less fidelity, increases genomic instability to the point of being unbearable (Patel et al., 2011).

Moving on to the second point, replication stress is defined as the "uncoupling of the DNA polymerase from the replisome helicase activity" (Byun et al., 2005; Zeman & Cimprich, 2014), and can be the consequence of intrinsic and extrinsic factors. Intrinsic factors include loss of tumor suppressor genes (RB and P53) and oncogenic drive (*KRAS* mutation and *MYC* or cyclins genes amplification) (R. M. Jones et al., 2013; Rohban & Campaner, 2015), but also over-production of ROS, which damage nucleotide (Sabharwal & Schumacker, 2014). Extrinsic factors mainly include chemotherapeutic drugs that create secondary structures that encumber polymerase (as platinum salts), or that decrease the nucleotide pool (as gemcitabine) (Ewald et al., 2008). As previously described, ATR pathway is mainly involved in protecting cells from the deleterious effects of replication stress; thus, the pharmacological inhibition of ATR and CHK1 was a promising strategy to induce premature entry into mitosis and mitotic catastrophe [ATR clinical trial identifiers: NCT01955668; NCT02223923; NCT02264678; NCT02567409; NCT02487095; NCT02567422] [CHK1 clinical trial identifiers: NCT01564251; NCT01870596]. To date, it is reasoned that, rather than the single, it is the dual inhibition of ATR-CHK1 and WEE1-CDK1/2 that causes mitotic catastrophe and cell death (Aarts et al., 2012; Beck et al., 2012; Do et al., 2013). This dual inhibition is necessary since CHK1 appears to be activated not only by ATR but also by ATM (Buisson et al., 2015).

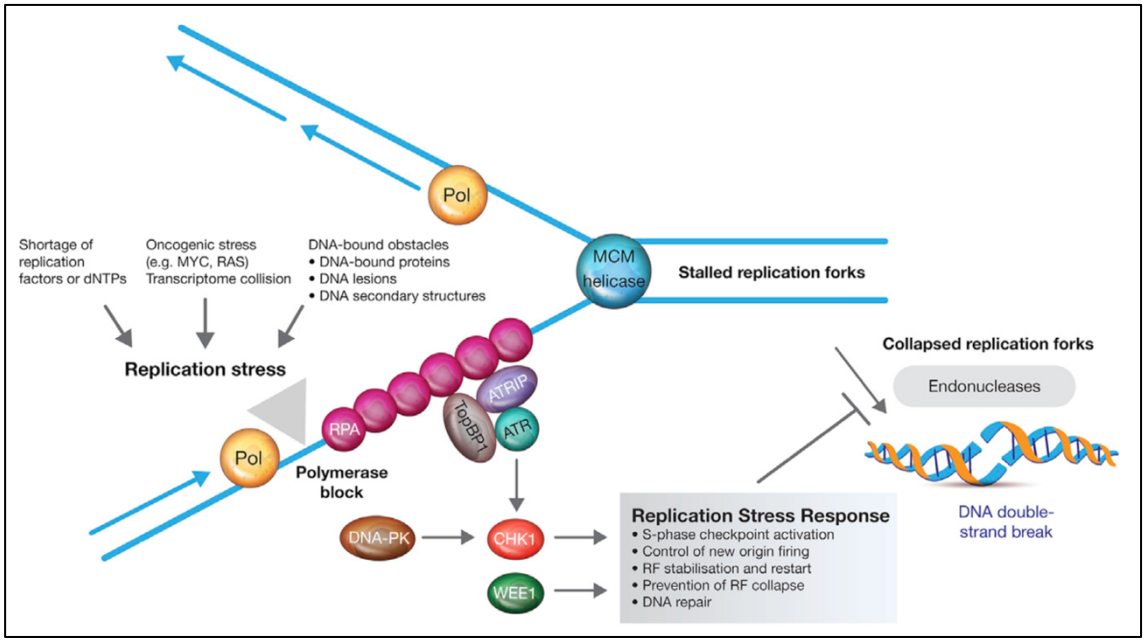

Figure 12: the replication stress response.

Schematic representation of sources, consequences and proteins involved in the replication stress response. Once activated the replication stress response prevents replication forks collapse and generate toxic DSBs. Adapted from O'Connor, 2015.

These two features of cancer cells, i.e., loss of one or more DDR pathways and increased replicative stress (Macheret & Halazonetis, 2015), also explain the third difference in the DDR dependency between normal and cancer cells, i.e., the increased levels of endogenous DNA damage. The causes are those previously listed along with metabolic stress, which was not considered in this chapter but which has a major impact on DNA-damage levels. Metabolic stress refers to a condition characterized by low nutrient availability (due to difficulty in supply and high consumption by cancer cells) and over-production of ROS which damage DNA, proteins, and lipids.

In conclusion, the DDR is a barrier to tumor transformation since it safeguards genomic integrity, arrests the cell cycle when any DNA-damage is detected, and initiates its repair. Not surprisingly, most, if not all, DDR proteins are considered tumor

suppressors. Loss of one or more of the DDR pathways, continued replicative stress, and, consequently, increased levels of endogenous DNA-damage, make cancer cells much more dependent on DDR than "healthy" cells; this makes the DDR an attractive therapeutic target. Many DDR inhibitors have shown encouraging results in *vitro* and have entered clinical trials in combination with standard chemotherapy, or as monotherapy. Advances in diagnostic tools - such as sequencing of tumor DNA from each individual patient - and stratification of patients not by tissue of origin but by specific mutations in the DDR genes are needed for both strategies. This has particular relevance with a view to using the DDR inhibitors as monotherapy to achieve synthetic lethality on tumor cells alone and not on healthy tissue.

4. Triple Negative Breast Cancer (TNBC)

4.1 TNBC: a definition.

TNBCs are defined as tumors that lack the expression (assessed primarily by immunohistochemistry) of estrogen receptor (ER), progesterone receptor (PgR) and over-expression/amplification of human epidermal growth factor receptor 2 (HER2) (Hudis & Gianni, 2011). Besides being a diagnostic marker, ER, PgR, and HER2 are also therapeutic targets, which makes TNBCs insensitive to endocrine therapies and HER2 monoclonal antibodies.

TNBCs are responsible for 15-20% of all breast cancers (Sporikova et al., 2018) with a homogeneous distribution by age group; the 5-years survival rate is around 70%, with differences depending on the age of patient, the stage and the spread at the time of diagnosis (Dent et al., 2007). Approximately one in two patients has distal metastases (with a median survival of 13.3 months) and one in four patients goes on

to recurrence, with a mortality rate of 75% within three months after recurrence (N. U. Lin et al., 2008). The median time for recurrence is 35-67 months for non-TNBC patients and 19-40 months for TNBC patients (Foulkes et al., 2010; Gluz et al., 2009).

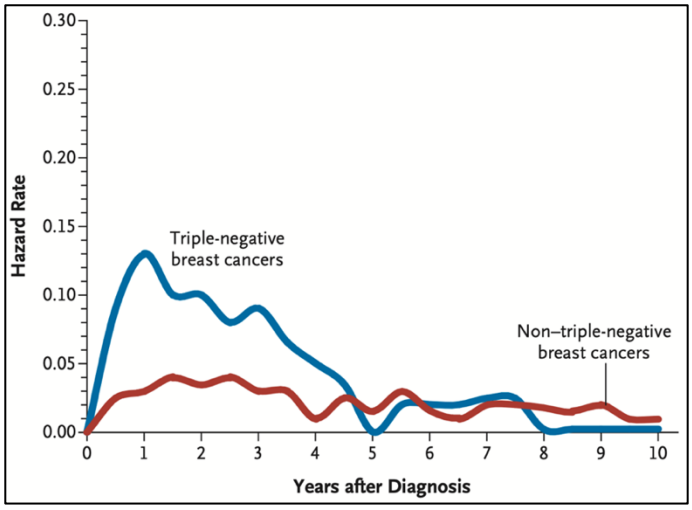

Figure 13: hazard rate for distant recurrence of TNBC and non-TNBC patients.

Data from Dent, 2007. Adapted from Foulkes, 2010.

TNBCs comprise a very heterogeneous class of diseases, and many attempts have been made to divide them into subtypes. The first studies of gene expression profiles described five breast-cancer "intrinsic" subtypes (Parker et al., 2009; Perou et al., 2000; Sørlie et al., 2001), with more than 90% basal-like breast cancers (BLBC) being TNBCs (Cheang et al., 2015). To date, one of the most widely used system is that proposed by Lehmann and colleagues, who described 6 TNBC subtypes (TNBCtypes) based on gene expression profiles (**Figure 14**) (Lehmann et al., 2011).

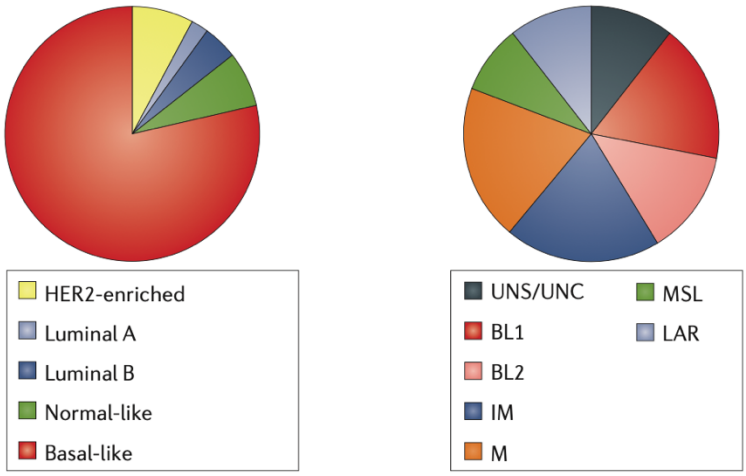

Figure 14: gene expression-based classifications of TNBC.

Left panel: gene expression-based classification of TNBC according to the PAM50. Right panel: gene expression-based classification by Lehmann and colleagues. BL: basal-like-related subgroups; M: mesenchymal-related subgroups; MSL: mesenchymal stem-like; IM: immunomodulatory subgroup; LAR: luminal androgen receptor subgroup. Adapted from Bianchini, 2016.

Lehmann again, in 2014, and Bareche, in 2018, identified specific biomarkers for each subtype which can also direct the choice of appropriate medication (Bareche et al., 2018; Lehmann & Pietenpol, 2014). BL1 subtype is characterized by amplification of cell-cycle regulator genes (among others *MYC, CDK6, CDKN2A/B, KRAS, PI3KCA* and *AKT1/2*) and deletion of DDR genes (*BRCA1/2, RB1, TP53*); thus, patients with BL1 tumors could benefit from standard chemotherapy, antimitotic drugs (taxanes) (Bauer et al., 2010), CDK4/6 inhibitors and PARPi. BL2 subtype presents activation of growth factors signaling and metabolic pathways (Wnt-β-catenin, EGFR, IGF-R1, MET); patients could benefit from growth factor inhibitors (cetuximab), PI3K, AKT and mTORC1 inhibitors. The IM subtype is characterized by immune response-associated gene profiles and inhibitory checkpoints genes (*CTLA-4, PD-1* and *PDL-1*); patients

could benefit from immune checkpoints blockade. The M subtype presents cell motility and epithelial to mesenchymal transition (EMT)-associated genes profile; M tumors tend to develop resistance to classic chemotherapeutics, and patients could benefit from the use of anti-angiogenesis drugs (bevacizumab) (Miller et al., 2007). The MSL is similar to the M subtype but expresses fewer proliferation-related genes and more stemness-related genes; patients could benefit from the same therapies listed for the M subtype. The LAR subtype has luminal-like gene expression profile (highly activated hormone-related signaling pathway) even though it is ER-negative; LAR tumors express high levels of androgen receptor (AR) and AR-related metabolic genes. Compared with IM, the LAR subtype is associated with a worse prognosis, but patients could benefit from anti-AR therapy.

TNBC subtype	Therapeutic strategies	Therapeutic targeted drugs
BL1 (basal-like 1)	Inhibit cell proliferation and DNA damage response	**Mitosis inhibitors** (Paclitaxel, Docetaxel, Ixabepilone, Nab-Paclitaxel, Vinorelbine) **Cytostatics** (Cisplatin, Carboplatin, Nedaplatin, Eptaplatin, Oxaliplatin, Lobaplatin, Satraplatin, Mercaptopurine) **PARP inhibitors** (Olaparib, Rucaparib, Talazoparib, Niraparib) **DNA Synthetic inhibitors** (Topotecan, Irinotecan, Camptothecin, Doxorubicin, Daunorubicin, Mitomycin)
BL2 (basal-like 2)	Inhibit TP63, EGFR, and MET signaling	**Cytostatics** (Cisplatin, Carboplatin, Nedaplatin, Eptaplatin, Oxaliplatin, Lobaplatin, Satraplatin, Mercaptopurine) **PARP inhibitors** (Olaparib, Rucaparib, Talazoparib and Niraparib) **Growth Factor inhibitors** (Erlotinib, Gefitinib, Afatinib, Osimertinib, Olmutinib, Nazartinib, Avitinib, lapatinib, Cetuximab, Panitumumab, Vandetanib, Bevacizumab, Pertuzumab, Ramucirumab, Trastuzumab, Axitinib, Cabozantinib, Ceritinib, Crizotinib, Lenvatinib, Nilotinib, Pazopanib, Regorafenib, Sorafenib, Sunitinib) **mTOR inhibitors** (rapamycin, everolimus, RapaLink-1)
IM (immunomodulatory)	Inhibit immune signaling	**Cytostatics** (Cisplatin, Carboplatin, Nedaplatin, Eptaplatin, Oxaliplatin, Lobaplatin, Satraplatin, Mercaptopurine) **PARP inhibitors** (Olaparib, Rucaparib, Talazoparib and Niraparib) **Immune checkpoint inhibitors** (Ipilimumab, Nivolumab)
M (mesenchymal)	Inhibit EMT, Wnt, PI3K, mTOR, Scr, TGFβ, IGF1R, Notch	**Growth Factor inhibitors** (Erlotinib, Gefitinib, Afatinib, Osimertinib, Olmutinib, Nazartinib, Avitinib, lapatinib, Cetuximab, Panitumumab, Vandetanib, Bevacizumab, Pertuzumab, Ramucirumab, Trastuzumab, Axitinib, Cabozantinib, Ceritinib, Crizotinib, Lenvatinib, Nilotinib, Pazopanib, Regorafenib, Sorafenib, Sunitinib) **mTOR inhibitors** (Rapamycin, Everolimus, RapaLink-1) **Scr inhibitors** (Bosutinib, Dasatinib) **PI3K inhibitors** (Idelalisib)
MSL (mesenchymal stem-like)	Inhibit EMT, Wnt, TGFβ, MAPK, Rac, PI3K, mTOR, Scr, PDGF	**Growth Factor inhibitors** (Erlotinib, Gefitinib, Afatinib, Osimertinib, Olmutinib, Nazartinib, Avitinib, lapatinib, Cetuximab, Panitumumab, Vandetanib, Bevacizumab, Pertuzumab, Ramucirumab, Trastuzumab, Axitinib, Cabozantinib, Ceritinib, Crizotinib, Lenvatinib, Nilotinib, Pazopanib, Regorafenib, Sorafenib, Sunitinib) **mTOR inhibitors** (rapamycin, everolimus, RapaLink-1) **PI3K inhibitors** (Idelalisib) **MAPK inhibitors** (Trametinib, Dabrafenib) **Scr inhibitors** (Bosutinib, Dasatinib)
LAR (luminal androgen receptor)	Inhibit AR signaling, FOXA1, and ERBB4 signaling	**Nonsteroidal antiandrogens** (bicalutamide) **mTOR inhibitors** (rapamycin, everolimus, RapaLink-1) **PI3K inhibitors** (Idelalisib)

Figure 15: Lehmann classification and biomarkers and therapeutic strategies.

BL: basal-like-related subgroups; M: mesenchymal-related subgroups; MSL: mesenchymal stem-like; IM: immunomodulatory subgroup; LAR: luminal androgen receptor subgroup. Adapted from Yin, 2020.

Since Lehmann's TNBCtypes were not representative of all patients across different studies, in 2015 Burstein and colleagues introduced a novel, four-groups classification (Burstein et al., 2015): LAR, (expression of AR and MUC1); M (expression of growth factor receptors); BLIS, basal-like immune-suppressed (expression of the immune-suppressive molecule *VTCN1*); BLIA, basal-like immune-activated (expression of *STAT* and release of cytokines). Patients with BLIA tumors are generally characterized by a better prognosis, followed by the M, the LAR and, lastly, the BLIS subtype. One year later, Liu and colleagues proposed a different classification based on both mRNA and long non-coding RNA (lncRNA) levels, and the interaction between the two, which they named the FUSCC classification, shown in **Figure 16** (Y.-R. Liu et al., 2016).

FUSCC classification	GO terms/canonical pathway	Most upregulated lncRNAs	Correlated mRNA	TNBC cell line
IM	Cytokine-cytokine receptor interaction↑ T cell receptor signaling pathway ↑ B cell receptor signaling pathway ↑ Chemokine signaling pathway ↑ NF-kappa B signaling pathway ↑	ENST00000443397	LOC100653210, LOC100653245, IGHV3-20, IGHV4-31, IGHJ1, IGKV3-7.	MDA-MB-231
LAR	Steroid hormone biosynthesis ↑ Porphyrin and chlorophyll metabolism ↑ PPAR signaling pathway ↑ Androgen and estrogen metabolism ↑	ENST00000447908	TRIM2, SDR16C5, C1QTNF3, KRT17, SERPINB5, TFAP2B, FAR2, CYP39A1, KIAA1467, EDDM3B.	HS578T
MES	ECM-receptor interaction ↑ Focal adhesion ↑ TGF-beta signaling pathway ↑ ABC transporter ↑ Adipocytokine signaling pathway ↑	NR_003221	SELP, CNN1, ADH1B.	HCC1937
BLIS	Mitotic cell cycle↑ Mitotic prometaphase↑ M phase of mitotic cell cycle↑ DNA replication↑ DNA repair↑ Immune response↓ Innate immune response ↓ T cell receptor signaling ↓	TCONS_00000027	RNASE6, MS4A6A, MTBP, FGFR2, CXor161, DHTKD1, IGLV6-57, BARD1, PRTFDC1.	MDA-MB-436

Figure 16: TNBC FUSCC classification.

Data from Liu, 2016. One cell line for each subgroup is listed. Adapted from Yin, 2020.

4.2. Treatment of TNBC.

As previously described, TNBCs are negative for ER, PgR and HER2 over-expression/amplification; therefore, they are insensitive to hormonal therapies, and pharmacological inhibition of HER2. Chemotherapy remains the standard of clinical care for TNBC patients, either before (neo-adjuvant) or after (adjuvant) surgery. Even though they are characterized by a worse prognosis (Liedtke et al., 2008; D. S. P. Tan et al., 2008), TNBC patients benefit from chemotherapy more than non-TNBC patients (TNBC paradox) (Carey et al., 2007); about 30-40% of early-stage TNBC patients achieve pathologic complete response (pCR) after a neo-adjuvant regimen with anthracyclines and taxanes (von Minckwitz et al., 2012). Unfortunately, pCR does not always result in increased survival. Currently, therapies are based on the combination of taxanes (paclitaxel/docetaxel), anthracyclines (doxorubicin), cyclophosphamide, fluorouracil and cisplatin (the BSL-1 subtype is particularly sensitive to treatment with platinum-derived agents (Jovanović et al., 2017)). Chemotherapy is particularly effective for early-stage disease and ineffective for advanced, metastatic disease, which has a survival rate of 12% at 5 years after diagnosis (Bonotto et al., 2014).

The major problem about chemotherapy is resistance, inherent or acquired. Here are reported the major resistance mechanisms for TNBCs: i) over-expression of ATP-binding cassette (ABC)-transporters, in particular, multidrug-resistant protein-1 and 8 (ABCC1/MRP1 and MRP8) and breast cancer resistance protein (ABCG2/BCRP) (Arumugam et al., 2019; Yamada et al., 2013); ii) presence of cancer stem cells (CSCs) that resist chemotherapy because of their slower proliferation and high expression of ABC-transporters (H. E. Lee et al., 2011; F. Ma et al., 2014; S. Y. Park et al., 2010; S. Zhou et al., 2001); iii) hypoxic environment, which promotes the stem cell phenotype and immunosuppression (Cosse & Michiels, 2008; E. Y. Tan et al., 2009; W. R. Wilson

& Hay, 2011); iv) *TP53* mutations, that abolish the G1/S checkpoint in favor of less efficient shelter systems that introduce mutations (Friboulet et al., 2019); v) constitutive activation of the PI3K-AKT-mTORC1 pathway (Steelman et al., 2008; Ueng et al., 2012).

Given the enormous intra-tumor heterogeneity and among different tumors (even of the same subtype), identifying actionable therapeutic biomarkers has proven arduous, and when it has been successful, clinical trials have not always confirmed the theory. The next section will report the best examples of targeted therapy in the context of TNBC. The first case is that of the anti-EGFR target therapy: three out of four patients have high levels of EGFR (Livasy et al., 2006). However, a phase II clinical trial (NCT00232505) showed that the use of cetuximab (EGFR inhibitor) carried very little benefit; patients treated with cetuximab still had robust activation of the EGFR downstream pathway, suggesting that other mechanisms may override its inhibition (Carey et al., 2012). Wang and colleagues identified an ER variant, ER-α36, which lacks the transcriptional activation domains (TADs) but retains the DNA-binding domains (DBDs) and transduces estrogen signaling in both ER-positive and ER-negative breast cancer cells (Z. Wang et al., 2005, 2006). In TNBC cell lines, the ER-α36 variant participates in a positive feedback loop with the EGFR, explaining possible resistance to cetuximab and other EGFR inhibitors; ER-α36 can also be considered a putative therapeutic target (X. T. Zhang et al., 2011).

Similar results have been obtained with PARP inhibition: about 20% of TNBC patients carry mutations on *BRCA1/2* genes, and are therefore eligible for treatment with PARPi (Gonzalez-Angulo et al., 2011). Unfortunately, clinical studies have not shown significant differences between BRCA-wild type (BRCA-wt) and BRCA-mutated tumors (Gelmon et al., 2011). Some encouraging results have been obtained in patients with

metastatic TNBC through the combination of PARPi and "conventional" chemotherapy. In this regard it is worth mentioning a work in which Ibrahim and colleagues demonstrated that PI3K inhibition leads to down-regulation of BRCA1/2, supporting the rationale for combining PI3K inhibitors with PARP inhibitors (Ibrahim et al., 2012); a clinical trial based on this finding is currently ongoing (NCT01623349). AR receptor antagonists (flutamide, bicatulimide or enzalutamide) were effective in both AR-positive cell lines, patient samples (Doane et al., 2006), and the portion of TNBC patients belonging to the LAR subtype, which corresponds to 10-15% of TNBC patients (Bardia et al., 2018; Gucalp et al., 2013).

Immunotherapy, which has proven effective in some cancer models such as advanced stage melanoma, has not confirmed in clinical trials the promising results obtained in *vitro* or in preclinical models. The numbers about the expression of PD-L1, PD1 or both (which are used as discriminatory criteria to benefit from immunotherapy) in TNBC patients are encouraging (W. Y. Sun et al., 2016); nevertheless, clinical trials with anti PD-1 or anti PD-L1 antibodies have shown modest response in TNBC patients ("Atezolizumab Extends Survival for Breast Cancer.," 2017; Nanda et al., 2016). In preclinical mouse models, the combination of anti-CTLA-4 with other agents significantly extended animal survival (Bernier et al., 2018; L. Liu et al., 2018), suggesting that combination therapies are needed to enhance the effects of immunotherapy. Chimeric antigen receptor (CAR)-T cells engineered to target the folate receptor (FR) or mesothelin have proven equally effective in *vitro* and in mouse models (Pastan & Hassan, 2014; Song et al., 2016).

To conclude, we have described in this chapter how TNBCs represent an unsolved medical challenge: the enormous heterogeneity of TNBCs required several sub-classifications over the years, each improving or enriching the previous one.

Nonetheless, molecular biomarkers that can either predict the efficacy of classical chemotherapy and direct the choice of the right regimen, or identify vulnerabilities for targeted therapies, are still lacking. Currently, considerable efforts are focused on identifying molecular biomarkers and improving chemotherapy regimens.

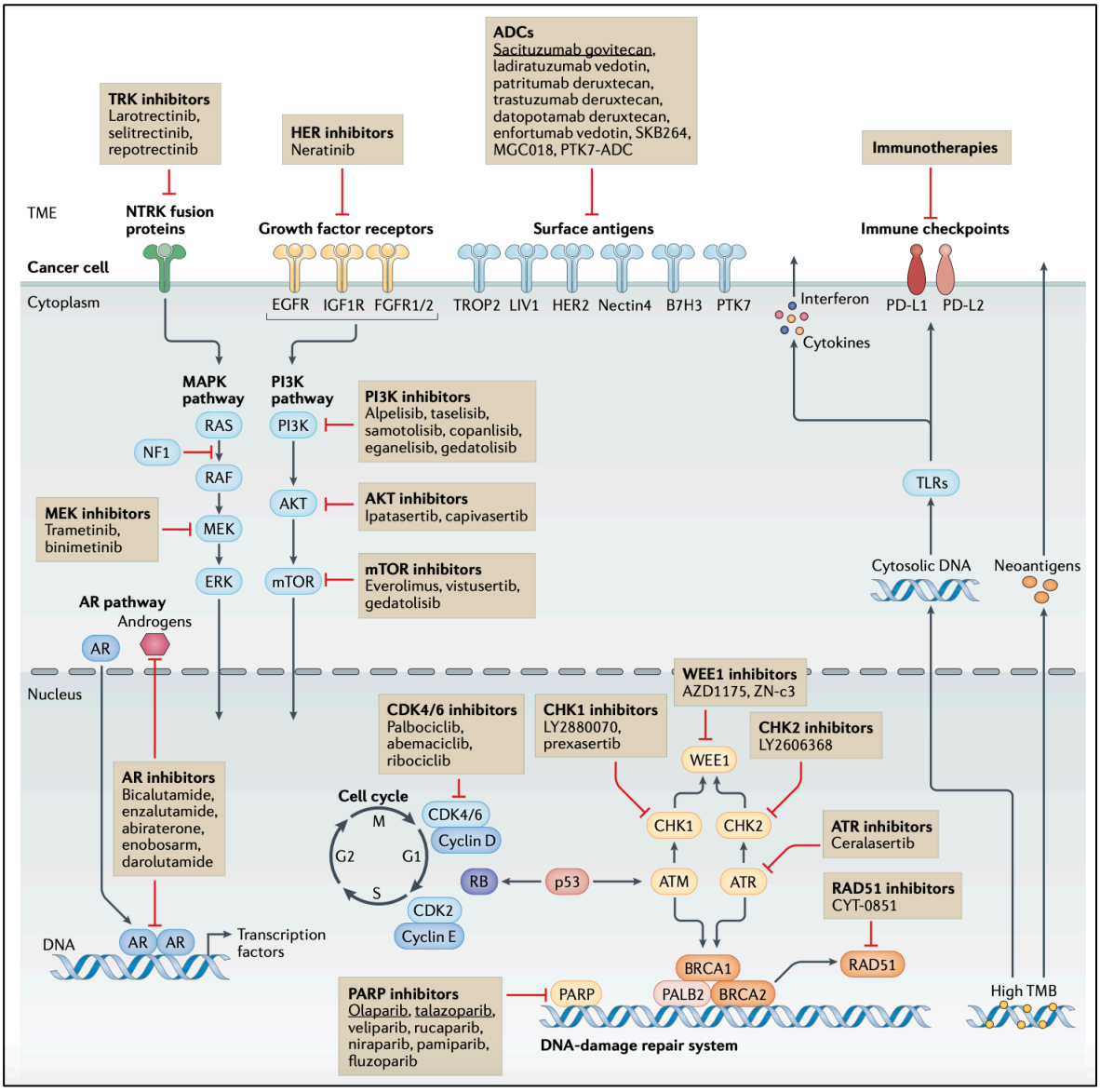

Figure 17: therapeutic strategies targeting the oncogenic vulnerabilities in TNBC.

Already approved agents are underlines, while the remaining are under clinical investigation. ADCs, antibody–drug conjugates; AR, androgen receptor; PARP, poly (ADP-ribose) polymerase; TLR, Toll-like receptor; TMB, tumour mutational burden; TME, tumour microenvironment; TROP2, trophoblast cell-surface antigen 2. Adapted from Bianchini, 2022.

Aim of the project

PP2A, which is one of the major phosphatases in eukaryotic cells, has long been known as a critical tumor suppressor: its inhibition leads to tumor initiation, and while it is not often mutated at the genetic level, its endogenous inhibitors are over-expressed in many types of tumors. Disregarding these early observations, for the past decades the study of PP2A has been relatively neglected, and greater emphasis was placed on oncogenic kinases, which have been successfully targeted in many cases by drugs. PP2A and other phosphatases are considered much more difficult to tackle: in this regard, recently described small-molecule activators of PP2A (SMAPs) have been proven efficacious in reducing tumor growth in *vitro* and in animal models.

Our group has recently demonstrated that PP2A is over-activated by the combination of metformin (anti-diabetic drug and mitochondrial complex I inhibitor) and hypoglycemia (achieved in *vitro* by lowering glucose in culture medium, and in *vivo* by cycles of intermittent fasting, and resulting in reduced glycolysis). The activation of PP2A upstream of GSK3β and MCL1 led to cell death in different tumor models. In parallel, Marco Foiani's lab (IFOM) in collaboration with our group demonstrated that, in yeast, PP2A integrated metabolic sensing (including glucose metabolism) with the DDR; specifically, under metabolic stress, PP2A attenuates the DDR.

The purpose of the present work is: i) to test whether the combination of metformin and glucose starvation is also effective in TNBCs, for which target therapies are ineffective and ii) to evaluate how this metabolic stress influences DNA-damaging chemotherapy, which for TNBC patients often remains the only suitable option. Therefore, we want to test whether and to what extent any combined effect depends on PP2A and the underlying molecular mechanism.

Materials and Methods

Cellular Biology procedures

Cell lines

All TNBC cell lines used in the present work were cultured according to ATCC recommendations and cultured at 5% CO_2 at 37°C. All the TNBC cell lines used in the present work are listed in **Table 1**. MDA-MB-231 cells, which was mainly used in the present work, were maintained in Dulbecco's modified Eagle's medium (DMEM) supplemented with 10% fetal bovine serum North American (NA), penicillin (100 U/mL)/streptomycin (1000 mg/mL), 2 mM of L-glutamine. MDA-MB-231 cells stably expressing CIP2A mutants (kindly provided by Jukka Westermarck's laboratory, Turku, Finland) were maintained in Dulbecco's modified Eagle's medium (DMEM) supplemented with 10% fetal bovine serum North American (NA), penicillin (100 U/mL)/streptomycin (1000 mg/mL), 2 mM of L-glutamine. HEK293T (Phoenix Ectotrophic human embryonic kidney packaging cell line from Nolan Lab) were maintained in DMEM supplemented with 10% fetal bovine serum South American (SA), penicillin (100 U/mL)/streptomycin (1000 mg/mL), 2 mM of L-glutamine. Patient-derived cells 197TX18 were maintained in "mammary epithelial basal medium modified" consisting of Dulbecco's modified Eagle's medium (DMEM) + Ham's F12 (1:1) supplemented with penicillin (100 U/mL)/streptomycin (1000 mg/mL), 2 mM of L-glutamine, 5 µg/ml insulin, 0.5 µg/ml hydrocortisone, 2% B27 (fresh), 20 ng/ml EGF and hFGF (fresh), 4 µg/ml heparin (fresh).

name	source	subtype	medium
MDA-MB-231	TNBC	Basal B/Mesenchimal Stem Like	90% DMEM+10% FBS (NA) +2mM L-Glutamine
MDA-MB-453	TNBC	Luminal Andorgen Receptor	90% DMEM+10% FBS (NA) +2mM L-Glutamine
MDA-MB-436	TNBC	Basal B/Mesenchimal Stem Like/Luminal Andorgen Receptor	90% DMEM/Ham's F12 (1:1) +10% FBS (SA) +2mM L-Glutamine
MDA-MB-468	TNBC	Basal A	90% DMEM/Ham's F12 (1:1) +10% FBS (SA) +2mM L-Glutamine
BT20	TNBC	Basal A	90% MEM with Earle's Salts+10% FBS (NA)+2mM L-Glutamine+1mM Sodium Pyruvate (NaP)+ 0.1mM Non-Essential Amino Acids (NEAA)
Hs578T	TNBC	Basal B	90% DMEM+10% FBS (NA)+0.01 mg/ml human insulin+2mM L-Glutamine
BT549	TNBC	Basal B/Mesenchimal	90% DMEM+10% FBS (SA) +2mM L-Glutamine
HCC1187	TNBC	Basal A/Immunomodulatory	90% RPMI 1640+10% FBS (NA) +2mM L-Glutamine
HCC1937	TNBC	Basal A	90% RPMI 1640+10% FBS (NA) +2mM L-Glutamine
HCC1599	TNBC	Basal A	90% RPMI 1640+10% FBS (NA) +2mM L-Glutamine
HCC1143	TNBC	Basal A	80% RPMI 1640+20% FBS (NA) +2mM L-Glutamine
DU4475	TNBC	Immunomodulatory	90% RPMI 1640+20% FBS (NA)+1mM Sodium Pyruvate (NaP)+10mM HEPES+2mM L-Glutamine+ 2.5 g/l D-Glucose

Table 1: TNBC cell lines used in the present work and relative culture medium.

Cell survival assay

Cell lines were plated in triplicate at a density of 200.000 cells/well in 6 wells plates. The day after, culture medium was replaced with fresh medium supplemented with 10% fetal bovine serum North American (NA), penicillin (100 U/mL)/streptomycin (1000 mg/mL), 2 mM of L-glutamine, and glucose according to the desired concentration (high glucose = 1,8 g/L; glucose starvation = 0,45 g/L). Specific treatments were added at the indicated concentrations. Cells were cultured in humidified atmosphere at 5% CO_2 at 37°C for 96 hours. Medium was replaced after 48 hours. After 96 hours cells were harvested and counted using the Burker's counting chamber or subjected to Propidium Iodide (PI) staining and FACS analysis. Patient-derived primary tumor cells were plated in triplicate at a density of 50.000 cells/well in 24 wells plates. Every condition was plated in the specific culture medium. After 96 hours cells were harvested and counted using the Burker's counting chamber.

Colony forming assay

At the end of the 96 hours treatment, MDA-MB-231 cells were plated in triplicate at a density of 200 single cells/well in 6 wells plates. Cells were cultured for 14 days in DMEM supplemented with 10% fetal bovine serum North American (NA), penicillin (100 U/mL)/streptomycin (1000 mg/mL), 2 Mm of L-glutamine, in humidified atmosphere at 5% CO_2 at 37°C. Medium was replenished every 3/4 days. Colonies were fixed with Gram's crystal violet solution (Merck, #1.09218) and scored.

Flow cytometry

MDA-MB-231 cells were harvested, washed and resuspended in 250 µL PBS. Next, cells were fixed by adding 750 µL EtOH dropwise while vortexing. Fixed cells were washed in PBS 1% BSA and resuspended in 1 mL PI (50 µg/mL) and RNAse and incubated overnight. Samples were acquired with BD FACSCelesta VBY FACSDiva Software v8.01.1. Samples were analyzed using FLOWJO software. For cell death measurement by PI exclusion, MDA-MB-231 cells were harvested, collected, washed and resuspended in 500 µL of PBS containing 1 µL of PI (50 µg/mL) and acquired with BD FACSCelesta VBY FACSDiva Software v8.01.1.

Infection procedures

For infection procedures, 250.000 MDA-MB-231 cells were plated in 6-wells plate into a final volume of 2 mL/well. Each well was inoculated with 200 µL of viral concentrated solution with polybrene 8 mg/mL. 8 hours later, virus-containing

medium was removed and fresh medium was added. The morning after, a second round of infection was performed under the same conditions. Infected cells were selected with puromycin (1 µg/mL) for 72 hours.

PP2A overexpression procedures

To over-express PP2Ac, HEK 293T and MDA-MB-231 cells were transfected through the calcium-phosphate transfection protocol with the pcDNA 3.1 expression vector expressing flag-tagged PP2Ac (kindly provided by Alessandro Gardini's laboratory, Wistar Institute Cancer Center, Pennsylvania).

Transformation procedure

10 µL of the ligation product (for details refer to the section: *cloning into pLKO.1 vector*) were used to transform *E. coli* competent cells (STBL3). STBL3 cells were incubated with the plasmid for 30 minutes in ice, then subjected to heat shock for 30 seconds at 42°C, followed by 5 minutes in ice and 30 minutes at 37°C in LB. Cells were then plated on LB agar plates supplemented with 50 µg/µL ampicillin and incubated at 37°C overnight. Ampicillin selected colonies (5 to 10) were inoculated in 5 mL of LB supplemented with Ampicillin 500X (100 µg/mL) and incubated overnight at 37°C. The DNA extraction was performed using QIAprep Miniprep kit (QIAGEN, Venlo, NL), according to manufacturer's instructions. Enzymatic digestion was performed to verify the presence of DNA of interest.

Viral production

Lentiviruses were produced through the calcium-phosphate transfection protocol in HEK 293T packaging cells. The day before transfection HEK293T cells were plated at a density of 50%, so that the day of transfection cells were in exponential growth (80-90% confluence). Two different solutions were prepared as follows:

components	**quantities**
Plasmidic lentiviral DNA	10 µg/plate
Plasmidic p-CMV-VSV-g	5 µg/plate
Plasmidic p-CMV-dr8.2 dvpr	8 µg/plate
$CaCl_2$	62 µL
ddH_2O	Up to 500 µL

Solution A

components	**quantities**
2X HBS (250mM Hepes pH7, 250mM NaCl and 150mM Na_2PO_4)	500 µL

Solution B

48 hours post transfection, viral supernatant was collected, filtered (0,45 µm) and incubated overnight at 4ºC with PEG solution 5X (120 g PEG 8000, 2.7 g NaCl, 200 mL H2O). The day after, samples were centrifuged at 1500g at 4ºC for 1 hour. Viral pellet was resuspended in PBS to obtain a 100X concentrated viral solution that could be stored at -80ºC or used immediately.

Molecular Biology procedures

Cloning into pLKO vectors

1.1 Digestion of pLKO vectors.

To Knock-Down (KD) PP2Ac and the B55 and B56 subunits, oligonucleotides were cloned into tet_pLKO_puro (PP2Ac) and pLKO_puro_TRC (B55/B56 subunits) vector which both express puromycin resistance cassette.

Plasmids were digested according to the following scheme at 37°C for 2 hours:

components	**quantities**
Plasmid	3 µg
10X buffer	5 µL
Restriction enzyme *	5 U
ddH_2O	up to 50 µL

Digestion mix. *For pLKO vectors we used AgeI-EcoRI.

The plasmid was dephosphorylated with 1 µL of Antarctic Phosphatase (New England Biolabs, Ipsiwich, MA) with its specific 10X buffer directly into digestion mixture, at 37°C for 30 minutes. Antarctic phosphatase was inactivated at 70°C for 5 minutes. To separate plasmid from digested DNA, the entire sample was subjected to agarose gel electrophoresis (TAE 1X 1% agarose). The bands of interest were extracted from gel with the commercial gel extraction kit QIAquick Gel Extraction Kit" (QIAGEN, Venlo, NL), according to manufacturer's instructions.

1.2 Cloning synthetic oligonucleotides into pLKO.1 vector.

Synthetic oligonucleotides were produced and purchased from Life Technologies and designed as short hairpin RNA (shRNA) with forward and reverse oligonucleotides prepared according to the following scheme:

- Forward oligo: 5′CCGG-sense21bp-CTCGAG-antisense21bp-TTTTTG 3′
- Reverse oligo: 5′AATTCAAAAA-sense21bp-CTCGAG-antisense21bp 3′

Synthetic oligonucleotides were resuspended in ddH_2O to a final concentration of 100 µM. The annealing mix (scheme) was incubated at 95°C for 4 minutes, then cooled down at room temperature (1 hour).

components	**quantities**
Forward oligonucleotides	5 µL
Reverse oligonucleotides	5 µL
NEB BUFFER 2 (Biolabs)	5 µL
ddH_2O	up to 50 µL

Annealing mix

After the annealing process, synthetic oligonucleotides and pLKO vector were ligated at a molar ratio vector:insert = 1:6 with 1 µL T4 DNA Ligase (New England Biolabs) at RT for 15 minutes.

components	**quantities**
Dephosphorylated vector	1 µL (10 ng/µL)
Synthetic oligonucleotides	1 µL (0,43 ng/µL)
T4 Ligase buffer 10X	2 µL
ddH_2O	Up to 20 µL

Ligation mix

10 µL of ligation product were used to transform *E. Coli* competent cells as described in the section *Transformation procedures*.

Immunoblotting

Whole cell extracts were prepared using Urea 8M with protease inhibitor. Cell lysates were sonicated (20", 15% Amplitude) and centrifuged at 13.000 RPM at 4ºC for 30 minutes to eliminate debris. Total protein concentration was determined using the Bradford assay (Bio-Rad). 1 volume of Bradford reagent was diluted with 4 volumes of MilliQ water to prepare a 1X working Bradford solution; urea 8M was used as blank. 30 µg of proteins were mixed with 5X Laemmli loading buffer (10% SDS, 50% glycerol, 25% 2-β-mercaptoethanol, 0.02% bromophenol blue and 0.3125 M Tris HCl) and denatured for 6 minutes at 95°C. Proteins were resolved in SDS-PAGE gel and transferred into nitrocellulose membranes (100V for 2 hours at 4°C or at 30V overnight at 4°C in Transfer Buffer containing 20% methanol, depending on the size of the protein of interest). Correct transfer of proteins to nitrocellulose membrane was evaluated using Ponceau S staining. Membranes were blocked for 1 hour at room temperature using PBS with 0,1% Tween-20 complemented with 5% BSA powder (blocking buffer). Primary antibodies were diluted in blocking buffer and applied overnight. Mouse or rabbit secondary antibodies were diluted in blocking buffer and applied for 1 hour at room temperature; signal was detected using ECL (Enhanced Chemi-Luminescence) staining for 5 minutes. Images were acquired with image scanning methods for chemiluminescence and colorimetric detection (Bio-Rad molecular imager Gel-Doc XR).

Neutral Comet Assay

MDA-MB-231 cells were harvested, washed and resuspended in cold PBS to the final concentration of 100.000 cells/mL. 10.000 cells (in 100 µL) were mixed with 200 µL low melting agarose and 60-80 µL of the final mix were plated on pre-coated slides (with agarose 1%). After agarose has gelled, samples were lysed in lysis buffer [NaCl (2,5 M); EDTA (100 mM); Tris-HCl pH 10,5 (10 mM); N- lauroylsarcosine (1%); Tryton™ X-100 (1%)] for 1 hour at 4ºC. After lysis, electrophoresis was performed in TBE for 25 minutes at 25 V in cold TBE in cold room. Slides were then washed in EtOH (70%, then 100%, 5 minutes each). Next day, slides were rehydrated with water for 30 minutes RT, and stained with DAPI (1:2000) for 20 minutes at RT. Samples were acquired with DM6B (Leica Microsystems) equipped with Zyla4.2 (Andor) camera. Comets were scored with the Fiji software; tail moments were calculated with the Fiji software (OpenComet plugin).

RNA extraction and RT-qPCR

Total RNA was extracted and purified from MDA-MB-231 cells with the RNeasy kit (QIAGEN) and quantified at spectrophotometer (ND NanoDrop 1000). Reverse transcription was performed with the Superscript II Kit (Invitrogen), according to the manufacturer's instructions. Quantitative PCRs (qPCRs) were performed in a final reaction volume of 20 µL containing 20 ng of cDNA, SYBR green buffer (Applied Biosystem) and 0,4 µM of each primer mix. qPCR amplifications were performed with the ViiA™7 Real-Time PCR system (4453534). mRNA levels were normalized to RPLP0.

Subcellular fractionation

MDA-MB-231 cells were harvested, washed twice in cold PBS and resuspended in ice-cold hypotonic buffer [Hepes pH 7 (10 mM; NaCl (50 mM); sucrose (0,3 M); NP40 (0,1 %); NEM (10 mM); protease and phosphatase cocktail inhibitors] for 15 minutes on ice to allow the lysis and the release of the cytosolic fraction. Nuclei were washed once in hypotonic buffer and resuspended in Nuclear Extraction Buffer [10 mM HEPES (pH 7); NaCl (200 mM): NP40 (0,5 %); NEM (10 mM): protease and phosphatase cocktail inhibitors] for 20 minutes on ice to allow the lysis and the release of the nucleosolic fraction.

- Pellets containing the chromatin-bound proteins were resuspended in UREA 8M and sonicated for 10-20 seconds in ice (15% amplitude), then centrifuged max speed for 2 minutes.
- Pellets containing the chromatin-bound proteins were resuspended RIPA buffer [Tris-HCl pH 7.5 50 mM, 150 mM NaCl, DOC 0.5 %, SDS 0.1 %, NP-40 1%] on ice for 20 minutes to allow the lysis of nuclear lamina; after centrifuge, pellets containing the chromatin-bound proteins were then resuspended in chromatin extraction buffer [Tris-HCl pH 7.5 (50mM); NaCl (150 mM); $MgCl_2$ (2 mM)] and incubated in presence of Benzonase 100X (Millipore) [280 U/mL], on ice for 40 minutes, then centrifuged max speed for 2 minutes.

The supernatant containing the chromatin-bound proteins was transferred to a new tube and quantified using Bradford's method. A total amount of 10-30 µg of protein was used for immunoblotting analysis as described above.

Biochemical assay: PP2A phosphatase assay

PP2A phosphatase activity was measured using the PP2A immunoprecipitation Phosphatase Assay kit (Merck Millipore) with minor modifications. MDA-MB-231 cells wild-type or stably expressing flag-tagged PP2Ac were treated for 24 hours with metformin (1 mM) in glucose starvation (0,45 g/L). Cells were washed and lysed with CoIP buffer [Tris-HCl pH 8 (50 mM); NP-40 (1%); NaCl (50 mM); Glycerol 50% (10%)]. Total protein concentration was determined using the Bradford assay (Bio-Rad) as described above, and 500 µg of proteins were then incubated with:

- 30 µL of DynaBeads-protein pre-equilibrated in PBS and supplemented with 0.5% BSA conjugated with antibody for PP2Ac (Merck, n. 05-421, clone 1D6) at 4ºC with constant rocking for 1 hour.
- 30 µL of ANTI-FLAG M2 magnetic beads (Merck, M8823) at 4ºC with constant rocking for 1 hour.

Beads-bound immune complexes were collected and then washed with 700 µL TBS (three times) and 500 µL Ser/Thr buffer (final wash), before they were resuspended in 20 µL Ser/Thr buffer. A phosphopeptide (amino acid sequence: K-R-pT-I-R-R) was added (60 µL, final concentration: 750 µM) as a substrate for PP2Ac, and samples were incubated at RT in a shaking incubator for 30 minutes. Supernatants (25 µL) were then transferred onto 96-well plate, and released phosphate was measured by adding 100 µL malachite green phosphate detection solution. Absorbance was read with Glomax Multi Plus Detection system (Promega) at 620 nm. Phosphate concentrations were calculated from a standard curve generated from serial dilutions of standard phosphate solution (0–2000 pMol).

In vivo experiments

Experiments have been done in accordance with the Italian Laws (D.L.vo 26/14 and following amendments), the Institutional Animal Care and Use Committee and the institutional guidelines at the European Institute of Oncology. Mice have been housed accordingly to the guidelines set out in Commission Recommendation 2007/526/EC - June 18, 2007 on guidelines for the accommodation and care of animals used for experimental and other scientific purposes. The protocol was approved by the Italian Ministry of Health (Authorization 71/2019-PR). *In vivo* studies were carried out in immunodeficient CD1-nude (Foxn1 nu/nu) female mice (Charles River, Italy), 8-10 weeks old. Mice were bred and housed under pathogen-free conditions in the animal facilities at the European Institute of Oncology – Italian Foundation for Cancer Research (FIRC) Institute of Molecular Oncology (IEO–IFOM, Milan, Italy) campus. Prior to injection, MDA-MB-231 cells were harvested, washed, and resuspended in PBS to a final concentration of 250.000 cells/10 µL. Cell suspension was then mixed 1:1 with growth factor–reduced matrigel and maintained in ice until injection. Female CD1 nude mice (8-10 weeks old) were anesthetized with 0.2% avertin and injected with 20 µL cell-matrigel suspension directly in the fourth mammary fat pad through the nipple with a Hamilton syringe. Tumor growth was monitored weekly, by bi-dimensional measurements using a caliper. Tumor volume was measured according to the formula: $w^2 \times W/2 = mm^3$, where "w" and "W" are "minor side" and "major side" (in mm), respectively. When the "W" reached 15 mm, mice were sacrificed. After the tumors appeared as established palpable masses (~10 days after cell injection), mice were randomized in different groups, and kept on the feeding/fasting protocols. Fasting cycles were achieved by complete removal of food while allowing free access to water for 24 hours from 6 pm to 6 pm of the following day when food

was re-supplied *ad libitum*, from Sunday to Friday for 4 weeks. Metformin (200 mg/kg dissolved in water) was administered three times a week (on Monday, Wednesday and Friday) at 9 am via oral gavage, for 4 weeks. Doxorubicin (0,5 mg/kg dissolved in saline solution) and Cyclophosphamide (50 mg/kg dissolved in saline solution) were administered once a week (on Monday) via intraperitoneal, for 4 weeks.

name	sequence
shRNA#1 for PP2A-C forward	CCGGACCGGAATGTAGTAACGATTTCTCGAGAAATCGTTACTACATTCCGGTTTTTTG
shRNA#1 for PP2A-C reverse	AATTCAAAAAACCGGAATGTAGTAACGATTTCTCGAGAAATCGTTACTACATTCCGGT
shRNA#2 for PP2A-C forward	CCGGGGCAAATCACCAGATACAAATCTCGAGATTTGTATCTGGTGATTTGCCTTTTTG
shRNA#2 for PP2A-C reverse	AATTCAAAAAGGCAAATCACCAGATACAAATCTCGAGATTTGTATCTGGTGATTTGCC
shRNA#3 for PP2A-C forward	CCGGTGGAACTTGACGATACTCTAACTCGAGTTAGAGTATCGTCAAGTTCCATTTTTG
shRNA#3 for PP2A-C reverse	AATTCAAAAATGGAACTTGACGATACTCTAACTCGAGTTAGAGTATCGTCAAGTTCCA

Table 2: oligonucleotides for PP2Ac RNA interference.

name	sequence
shRNA#1 for B55α forward	CCGGGATCCCAGTAACAGGTCATTTCTCGAGAAATGACCTGTTACTGGGATCTTTTTG
shRNA#1 for B55α reverse	AATTCAAAAAGATCCCAGTAACAGGTCATTTCTCGAGAAATGACCTGTTACTGGGATC
shRNA#2 for B55α forward	CCGGGCAAGTGGCAAGCGAAAGAAACTCGAGTTTCTTTCGCTTGCCACTTGCTTTTTG
shRNA#2 for B55α reverse	AATTCAAAAAGCAAGTGGCAAGCGAAAGAAACTCGAGTTTCTTTCGCTTGCCACTTGC
shRNA#1 for B55γ forward	CCGGCCGCTCATTCTTCTCGGAAATCTCGAGATTTCCGAGAAGAATGAGCGGTTTTTG
shRNA#1 for B55γ reverse	AATTCAAAAACCGCTCATTCTTCTCGGAAATCTCGAGATTTCCGAGAAGAATGAGCGG
shRNA#2 for B55γ forward	CCGGGCCGGAGTTTGACTATCTCAACTCGAGTTGAGATAGTCAAACTCCGGCTTTTTG
shRNA#2 for B55γ reverse	AATTCAAAAAGCCGGAGTTTGACTATCTCAACTCGAGTTGAGATAGTCAAACTCCGGC
shRNA#1 for B55δ forward	CCGGGCTGCCACCAATAACTTGTACCTCGAGGTACAAGTTATTGGTGGCAGCTTTTTG
shRNA#1 for B55δ reverse	AATTCAAAAAGCTGCCACCAATAACTTGTACCTCGAGGTACAAGTTATTGGTGGCAGC
shRNA#2 for B55δ forward	CCGGCGGGTCCTATAACAACTTCTTCTCGAGAAGAAGTTGTTATAGGACCCGTTTTTG
shRNA#2 for B55δ reverse	AATTCAAAAACGGGTCCTATAACAACTTCTTCTCGAGAAGAAGTTGTTATAGGACCCG

Table 3: oligonucleotides for B55 subunits RNA interference.

name	sequence
shRNA#1 for B56α forward	CCGGCCTCACATACAGTTGGTATATCTCGAGATATACCAACTGTATGTGAGGTTTTTG
shRNA#1 for B56α reverse	AATTCAAAAACCTCACATACAGTTGGTATATCTCGAGATATACCAACTGTATGTGAGG
shRNA#2 for B56α forward	CCGGGCTTACAACATGCACAGTATTCTCGAGAATACTGTGCATGTTGTAAGCTTTTTG
shRNA#2 for B56α reverse	AATTCAAAAAGCTTACAACATGCACAGTATTCTCGAGAATACTGTGCATGTTGTAAGC
shRNA#1 for B56β forward	CCGGCCGCATGATCTCAGTGAATATCTCGAGATATTCACTGAGATCATGCGGTTTTTG
shRNA#1 for B56β reverse	AATTCAAAAACCGCATGATCTCAGTGAATATCTCGAGATATTCACTGAGATCATGCGG
shRNA#2 for B56β forward	CCGGCCGCATGATCTCAGTGAATATCTCGAGATATTCACTGAGATCATGCGGTTTTTG
shRNA#2 for B56β reverse	AATTCAAAAACCGCATGATCTCAGTGAATATCTCGAGATATTCACTGAGATCATGCGG
shRNA#1 for B56γ forward	CCGGCCAGAAGTAGTCCATATGTTTCTCGAGAAACATATGGACTACTTCTGGTTTTTG
shRNA#1 for B56γ reverse	AATTCAAAAACCAGAAGTAGTCCATATGTTTCTCGAGAAACATATGGACTACTTCTGG
shRNA#2 for B56γ forward	CCGGCGGGAAGAAGCATGGGTTAAACTCGAGTTTAACCCATGCTTCTTCCCGTTTTTG
shRNA#2 for B56γ reverse	AATTCAAAAACGGGAAGAAGCATGGGTTAAACTCGAGTTTAACCCATGCTTCTTCCCG
shRNA#1 for B56δ forward	CCGGCATCGCATCTATGGCAAGTTTCTCGAGAAACTTGCCATAGATGCGATGTTTTTG
shRNA#1 for B56δ reverse	AATTCAAAAACATCGCATCTATGGCAAGTTTCTCGAGAAACTTGCCATAGATGCGATG
shRNA#2 for B56δ forward	CCGGTGCACTCTACAGGAACTCCAACTCGAGTTGGAGTTCCTGTAGAGTGCATTTTTG
shRNA#2 for B56δ reverse	AATTCAAAAATGCACTCTACAGGAACTCCAACTCGAGTTGGAGTTCCTGTAGAGTGCA
shRNA#1 for B56ε forward	CCGGCCTCCTAGTGACAGCAATGAACTCGAGTTCATTGCTGTCACTAGGAGGTTTTTG
shRNA#1 for B56ε reverse	AATTCAAAAACCTCCTAGTGACAGCAATGAACTCGAGTTCATTGCTGTCACTAGGAGG
shRNA#2 for B56ε forward	CCGGGTCGCAAAGTTCCTCACAGTTCTCGAGAACTGTGAGGAACTTTGCGACTTTTTG
shRNA#2 for B56ε reverse	AATTCAAAAAGTCGCAAAGTTCCTCACAGTTCTCGAGAACTGTGAGGAACTTTGCGAC

Table 4: oligonucleotides for B56 subunits RNA interference.

name	sequence
PP2A C forward	AAGCAGCTGTCCGAGTCCCA
PP2A C reverse	TGGACATCGAACCTCTTGCACG
PP2A A forward	ACCCCATCGCGGTGCTCATA
PP2A A reverse	CCAAGGCGATGGTGGACAGC
B55α forward	AGGGTCACCATTTGCAGCGC
B55α reverse	GCTCCTTTCACCTGAGAAAAACACCA
B55β forward	TAGCGACAGGGGACAAGGGG
B55β reverse	CGGGTTCATGGCTCTGGAATGT
B55γ forward	GACGTCACTGCAGGTGCCAG
B55γ reverse	GGCAAAGATCCTCCGAGGGC
B55δ forward	AAGACTTCGAGACCCATTTAGGA
B55δ reverse	CGTGGACTCGCTTCTACCATA
B56α forward	AGAGCCCTGATTTCCAGCCTA
B56α reverse	TTTCCCATAAATTCGGTGCAGA
B56β forward	GCCCGTCTACCCAGACATC
B56β reverse	TCAAGATTGGGCTCATCCTCT
B56γ forward	GAAGATCCTCGGGAGAGAGATT
B56γ reverse	TCTGCTATGCCATTATGATGCTC
B56δ forward	CCACCCTCAGCTGGCATA
B56δ reverse	CTTGGGCCAAAACTTGAGAA
B56ε forward	AGAATTCCAACCCAGCATTGCCA
B56ε reverse	GTCCCGTTCCCGAGGGTCTT
RPP0 forward	TTCATTGTGGGAGCAGAC
RPLP0 reverse	CAGCAGTTTCTCCAGAGC

Table 5: expression primers for RT-qPCR.

name	sequence
ATR	Cell Signaling Technology, n. E153S, clone 13934S
p-ATR (T1989)	GeneTex, n. GTX128145, clone 42396
CHK1	Cell Signaling Technology, n. 2G1D5, clone 2360S
p-CHK1 (S345)	Cell Signaling Technology, n. 133D3, clone 2348S
H2Ax	Cell Signaling Technology, n. D17A3, clone 7631S
γH2Ax (S139)	Cell Signaling Technology, n. 20E3, clone 9718S
ATM	Cell Signaling Technology, n. D2E2, clone 2873S
p-ATM (S1981)	Cell Signaling Technology, n. D25E5, clone 13050S
CHK2	Cell Signaling Technology, n. D9C6, clone 6334S
p-CHK2 (T68)	Cell Signaling Technology, n. C13C1, clone 2197T
PP2A A	Santa-Cruz, n. sc-81604, clone C1908 Cell signaling 2039S
PP2A C	Merck, n. 05-421, clone 1D6 Cell Signaling 2038S
CIP2A	Santa-Cruz, n. sc-80662
B55α	Cell Signaling Technology Cat# 5689S; RRID:AB_10827877
B56β	Invitrogen Cat# PA5-29262; RRID:AB_2546738
B55γ	Abcam Cat# ab27269; RRID:AB_2170097
B55δ	Invitrogen Cat# PA5-30763; RRID:AB_2548237
B56α	Invitrogen Cat# PA1-31436; RRID:AB_2170404
B56β	Santa Cruz Biotechnology Cat# sc-515676
B56γ	Invitrogen Cat# 39-3600; RRID:AB_2533409
B56δ	Santa-Cruz, n. sc-81605, clone B2117
B56ε	Invitrogen Cat# PA5-17981; RRID:AB_10982672
vinculin	Sigma-Aldrich, n. V9131, clone hVIN-1
actin	Sigma-Aldrich, n. A4700, clone AC-40
tubulin	Santa Cruz Biotechnology, n. sc-32356
H3	Abcam, n. 1791
P70S6K	Cell Signaling Technology, clone 9202S
pP70S6K (T389)	Cell Signaling Technology, clone 9205S
RPS6	Cell Signaling Technology, n. 54D2, clone 2317S
pRPS6 (S235/236)	Cell Signaling Technology, clone 2211S
4EBP1	Cell Signaling Technology, n. 53H11 clone 9644S
p4EBP1 (T37/46)	Cell Signaling Technology, 236B4, clone 2855S
P54-nrb	Santa Cruz SC-376865

Table 6: antibodies.

Results

1. TNBC cell lines are resistant to the combination of metformin and glucose starvation.

Our group has previously found that metformin and glucose starvation (75% reduction compared to high glucose) induced cell death in different cell lines and primary tumors (Elgendy et al., 2019).

We tested whether the same metabolic combination was effective in TNBCs, and we found that several TNBC cell lines were more resistant to high-dose metformin (10 mM) and glucose starvation (0,45 g/L), compared to both HeLa and HCT116 cells, which were primarily used in the afore-mentioned paper (**Figure 18**).

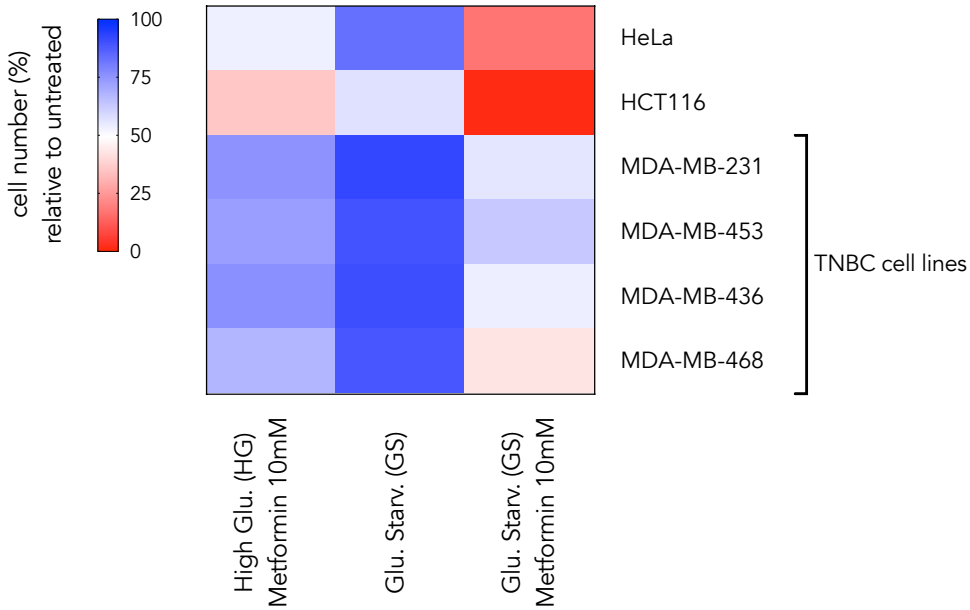

Figure 18: TNBC cell lines are resistant to high-dose metformin and glucose starvation.

Viability of HeLa, HCT116 and four TNBC cell lines after 2 days of treatment as follows: High Glucose (HG: 1,8 g/L); Glucose Starvation (GS: 0,45 g/L) ± metformin 10 mM (high dose). Values are relative to HG. N = 3 replicates. TNBC cell lines are indicated.

Both in HeLa and HCT116 cells, metformin induced the down-regulation of CIP2A, which is one of the endogenous inhibitors of PP2A, thus activating PP2A, while glucose starvation favored the assembly of a specific B56δ-PP2A complex upstream of GSK3β and MCL1 (Elgendy et al., 2019). In the TNBC cell line MDA-MB-231 (hereafter taken as reference cell line) the decrease of CIP2A was modest compared to HeLa and HCT116 and the protein level was not abolished by high-dose metformin (**Figure 19, left panel**); moreover, we did not observe any increase of B56δ (both protein and RNA level) after one day of glucose starvation (**Figure 19**).

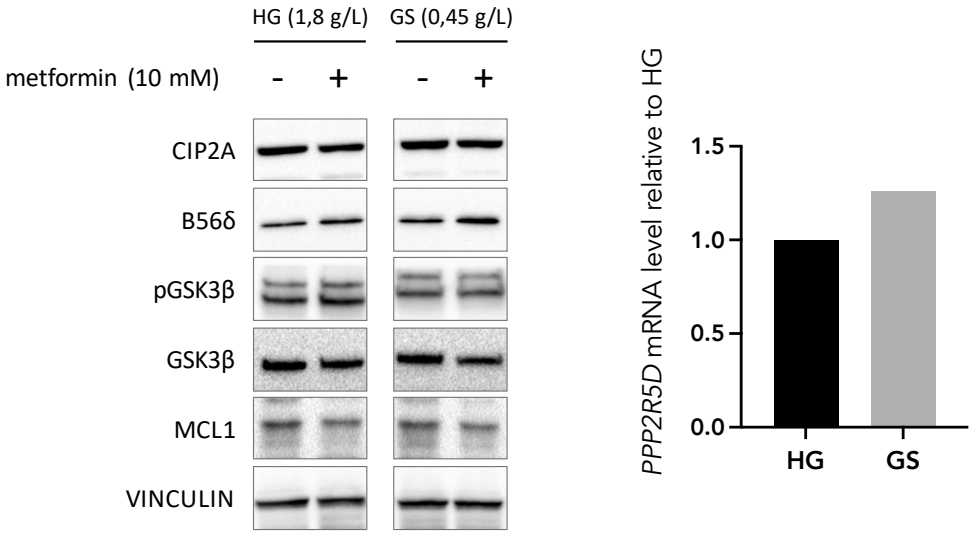

Figure 19: high-dose metformin and glucose starvation do not affect CIP2A and B56δ.

Left panel: western blot analysis showing the phosphorylation and the total levels of the indicated proteins after 1 day of treatment as follows: HG (1,8 g/L); GS (0,45 g/L), ± metformin (10 mM). Vinculin was used as loading control. N = 3 replicates. Right panel: analysis of PPP2R5D (gene encoding for B56δ) mRNA levels in MDA-MB-231 cells after 1 day of treatment as follows: HG (1,8 g/L); GS (0,45 g/L). Values are normalized against RPLP0 and referred as fraction of control (HG). N = 3 replicates.

A possible explanation for the decreased/absent effect of metformin on CIP2A levels is that the amount of CIP2A was much higher in MDA-MB-231 (and in the other TNBC cell lines previously screened in viability assays) compared to both HCT116 and HeLa cell lines (**Figure 20**). Our findings are in line with previous publications which described high CIP2A content in TNBC, both cell lines and primary tumors (H. Liu et al., 2017). However, we could not demonstrate a correlation between the levels of CIP2A and the response to the combination of metformin and glucose starvation.

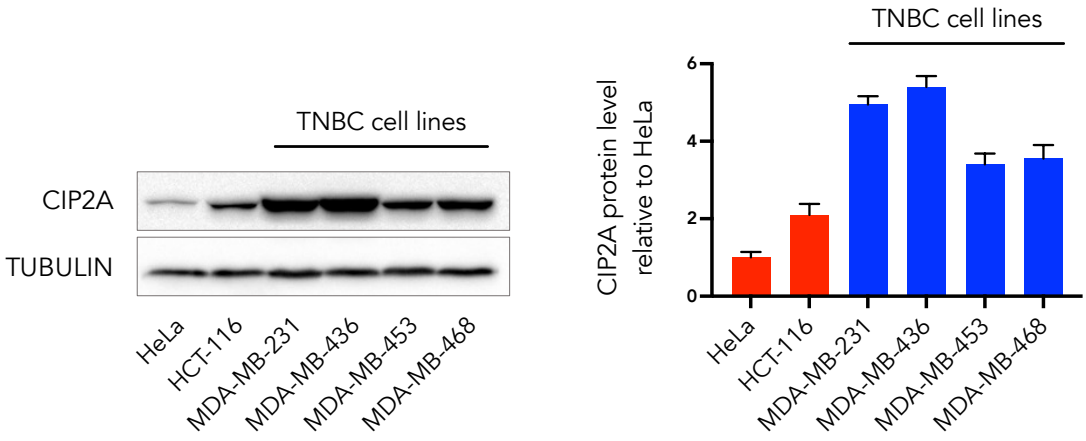

Figure 20: CIP2A is highly expressed in TNBC cell lines.

Western blot analysis (left panel) and band quantification (right panel) showing the total amount of CIP2A in different cell lines relative to HeLa cells (reference). Tubulin was used as loading control. N = 3 replicate. TNBC cell lines are highlighted.

Despite the lower efficacy in reducing cell viability, the combination of metformin and glucose starvation increased PP2A phosphatase activity after one day of treatment, measured by immunoprecipitation of endogenous PP2A followed by commercial phosphatase assay [Merck 32161000]. Not only was the combination effective, but lower doses of metformin (down to 0,1 mM) were sufficient to increase PP2A phosphatase activity, with a plateau around 1 mM (**Figure 21, left panel**). A recent

work has questioned several antibodies used for immune-precipitate PP2A catalytic subunit, including the monoclonal antibody 1D6 that was part of the commercial phosphatase assay kit (Frohner et al., 2020). To solve the problem of the non-specificity of the antibody, we over-expressed a flag-tagged PP2A catalytic subunit (exogenous flag-PP2Ac) in MDA-MB-231 cell line and we confirmed the results obtained with the endogenous subunit, thus excluding the off-target effect of the antibody (**Figure 21, right panel**). However, despite the activation of global PP2A activity, we failed to detect the dephosphorylation of GSK3β, observed in other responsive cell lines, which is a necessary step for the down-regulation of MCL-1 levels (**Figure 19, left panel**).

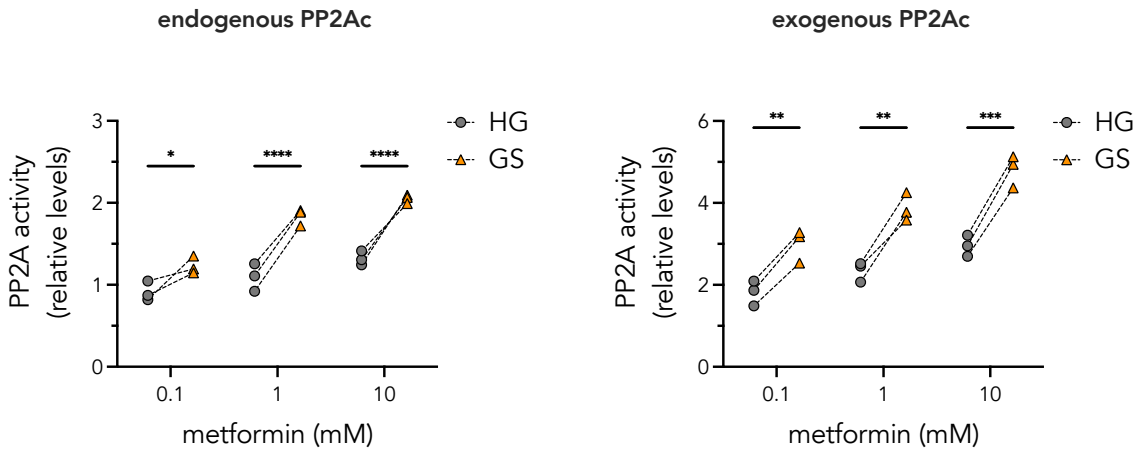

Figure 21: metformin and glucose starvation increase PP2A phosphatase activity.

*Result of the phosphatase assay performed in MDA-MB-231 cells, wild-type (left panel) or stably expressing flag-tagged PP2Ac (right panel), after 1 day of treatment as follows: HG (1,8 g/L); GS (0,45 G/L) with the indicated concentrations of metformin. Values are relative to HG (untreated, that is, no metformin). N = 3 replicates. Significances were calculated with one-way ANOVA. *p<0,05; **p<0,01; ***p<0,001; ****p<0,0001.*

2. Metformin and glucose starvation enhance the efficacy of chemotherapy in TNBC cell lines.

Given the intrinsic resistance of the TNBC cell lines to the combination of metformin and glucose starvation we investigated other (clinically relevant) therapeutic strategies. In this regard, the clinical trial BREAKFAST started at the Istituto Nazionale dei Tumori (Milan, Italy): TNBC patients undergoing neo-adjuvant chemotherapy (with doxorubicin and cyclophosphamide first, then paclitaxel) are subjected to a fasting mimicking diet (FMD) regimen with or without metformin. Thus, we inquired the impact of metformin and glucose starvation on chemotherapy treatment. On the basis of our previous findings in yeast, we also investigated mechanistically the impact of PP2A activation following metabolic stimuli on the DDR induced by chemotherapy. For this reason, we opted for doxorubicin and cyclophosphamide (and not paclitaxel), which are the first line therapy in the BREAKFAST clinical trial and directly trigger the DDR. We choose the MDA-MB-231 cell line (that was more resistant to high-dose metformin and glucose starvation and expressed high levels of CIP2A) and we set up a protocol as shown in **Figure 22** (timing of different experiments are listed). Cells were counted after 4 days and culture medium was changed after 2 days to keep glucose levels as stable as possible.

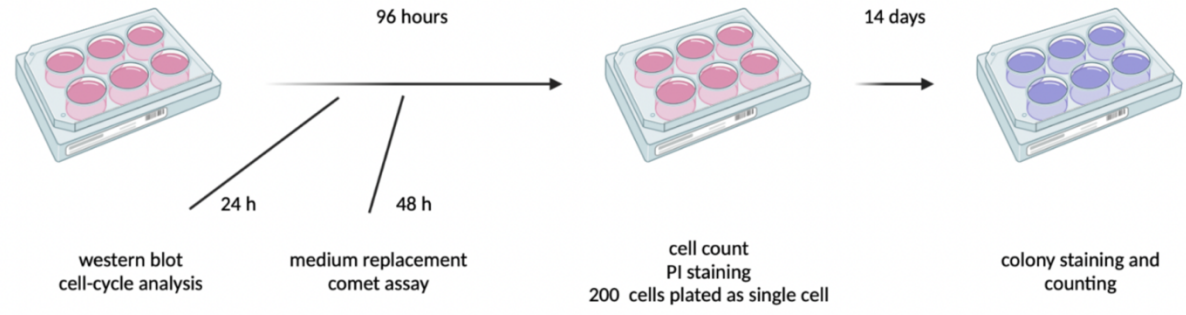

Figure 22: schematic representation of the experimental setup.

Cells were seeded and as soon as they attached, different media were added for 48 hours. After 48 hours media were replaced. After 96 hours cells were harvested and subjected to manual cell counting, PI-staining and FACS analysis. 200 living cells were then collected and plated as single cell for colony forming assay. For western blot and cell cycle analysis, cells were harvested after 24 hours. For comet assay, cells were harvested after 48 hours.

After 4 days, glucose starvation by itself had a little effect on cell proliferation without inducing cell death (**Figure 23**) and produced a slowdown in the doubling time (36,4 hours and 39,7 hours in high glucose and glucose starvation, respectively). This confirmed that tumor cells are (metabolically) plastic and adapt their metabolism to changes in nutrient availability.

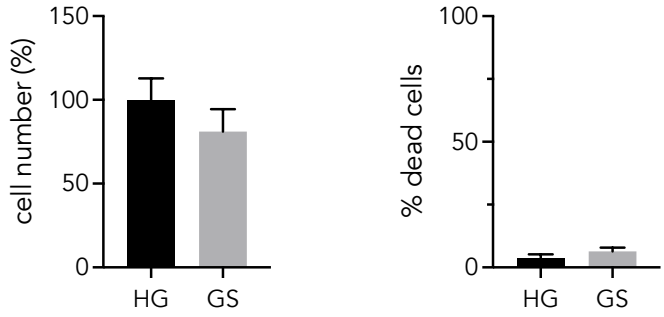

Figure 23: glucose starvation does not impact on cell viability.

Viability (left panel) and percentage of PI-positive (right panel) MDA-MB-231 cells after 4 days of treatment as follows: HG (1,8 g/L) or GS (0,45 g/L). Values are relative to HG. N = 3 replicates.

Based on the results of PP2A phosphatase assay, we opted for a metformin concentration of 1 mM. As previously stated, MDA-MB-231 cells are relatively resistant to metformin and glucose starvation: indeed, even with a lower concentration

of metformin, the combination modestly decreased cell viability compared to glucose starvation alone, with 40% reduction in cell proliferation and 20% increase in the percentage of PI-positive cells after 4 days (**Figure 24**).

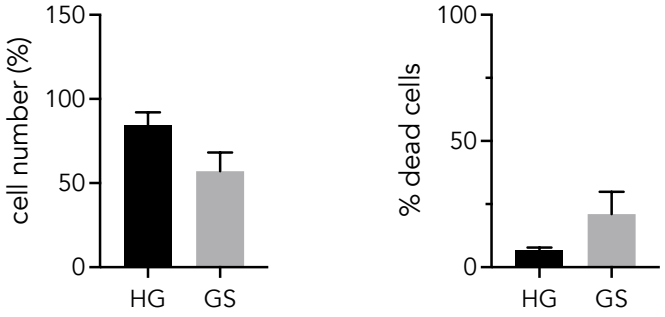

Figure 24: metformin and glucose starvation slightly impact cell viability.

*Viability (left panel) and percentage of PI-positive (right panel) MDA-MB-231 cells after 4 days of treatment as follows: HG (1,8 g/L) or GS (0,45 g/L) ± metformin (1 mM). Values are relative to untreated (HG of **Figure 23**). N = 3 replicates.*

Then, we combined metformin and glucose starvation with doxorubicin (dox) and cyclophosphamide (cp), which are the standard of clinical care for TNBC patients and they both interfere with the DNA structure and replication. In particular, dox is an intercalating agent and inhibits topoisomerase II (Pommier et al., 2010; Tacar & Dass, 2013), while cp forms inter- and intra-strand cross-linkages (Emadi et al., 2009). Since cyclophosphamide is converted to the active drug in the liver, for the *in vitro* experiments we used the active metabolite 4-hydro-peroxy-cyclophosphamide. In high glucose, metformin made no contribution to the effect of chemotherapeutics (**Figure 25**). Intriguingly, metformin and glucose starvation increased the anti-proliferative effect of both doxorubicin and cyclophosphamide (**Figure 25**).

Effectively, the IC_{50} for both the chemotherapeutic agents was significantly lower when combined with metformin and glucose starvation (**Figure 26**). Of note, chemotherapy was more effective if administered in glucose starvation, partially confirming observations by other groups and reiterating that a crosstalk exists between glucose metabolism and the sensitivity to DNA-damaging agents (D'Aronzo et al., 2015; C. Lee et al., 2012; Raffaghello et al., 2008; Shim et al., 2015).

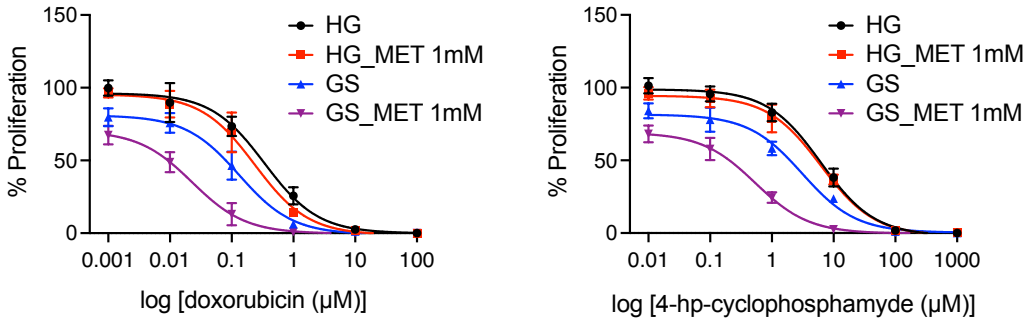

Figure 25: metformin and glucose starvation synergize with dox and cp.

Viability of MDA-MB-231 after 4 days as follows: HG (1,8 g/L) or GS (0,45 g/L) ± metformin 1 mM with chemotherapeutic drugs at the indicated concentrations. Left panel: doxorubicin. Right panel: 4-hp-cyclophosphamide. For cell survival procedures see material and methods. Values are normalized to HG (that is, without drugs, glucose starvation or metformin). N = 3 replicates.

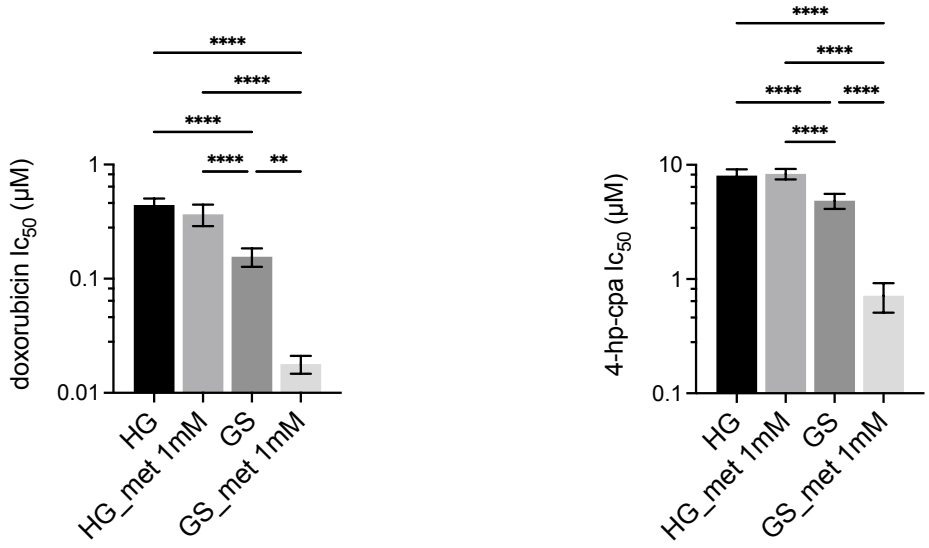

Figure 26: metformin and glucose starvation reduce the IC50 of dox and cp.

*IC_{50} of dox and cp was calculated at day 4. N = 3 replicates. Significances were calculated with one-way ANOVA. *p<0,05; **p<0,01; ***p<0,001; ****p<0,0001.*

We selected and combined two doses for each agent, referred as high-dose chemotherapy (HD: dox 1 µM + cp 20 µM) and low-dose chemotherapy (LD: dox 0,1 µM + cp 2 µM), which after 4 days caused nearly 90% and 40% of cell death, respectively (**Figure 27**). Then, we matched low-dose chemotherapy with metformin in high glucose (hereafter referred as double combination) or in glucose starvation (hereafter referred as triple combination). We observed no significant differences between chemotherapy alone (irrespectively of glucose) and the double combination. Interestingly, the triple combination was the most impactful and caused nearly 90% of cell death, similar to high-dose chemotherapy (**Figure 27**).

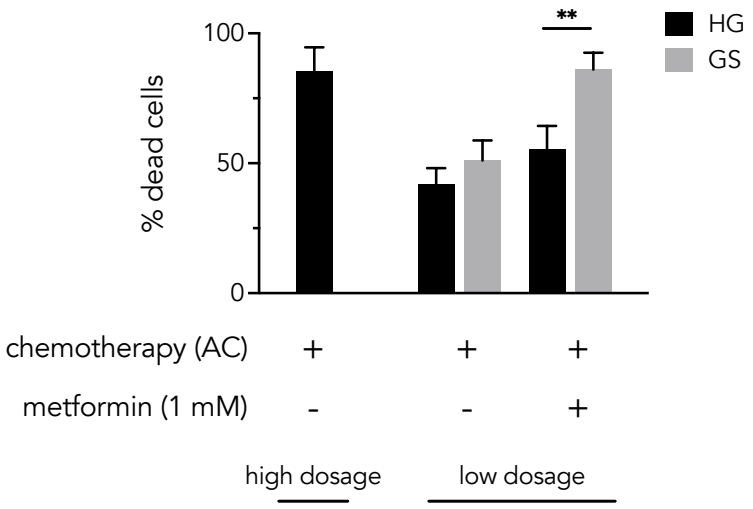

Figure 27: the triple combination induces cell death.

*Percentage of PI-positive MDA-MB-231 cells after 4 days of treatment with high-dose chemotherapy (HD: dox 1 µM + cp 20 µM) and low-dose chemotherapy (LD: dox 0,1 µM + cp 2 µM) in HG (1,8 g/L) or GS (0,45 g/L) ± metformin 1 mM. N = 3 replicates. Significances were calculated with one-way ANOVA. *p<0,05; **p<0,01; ***p<0,001; ****p<0,0001.*

Next, we performed colony forming assay to evaluate the clonogenic potential of the MDA-MB-231 cell line in the long run: cells that remained alive at the end of the experiment as described above were plated as single cell and grown without drugs nor glucose starvation up to 14 days. Cells previously subjected to the triple combination had the strongest clonogenic disadvantage (**Figure 28**), suggesting a long-term impact that remains even after drug removal.

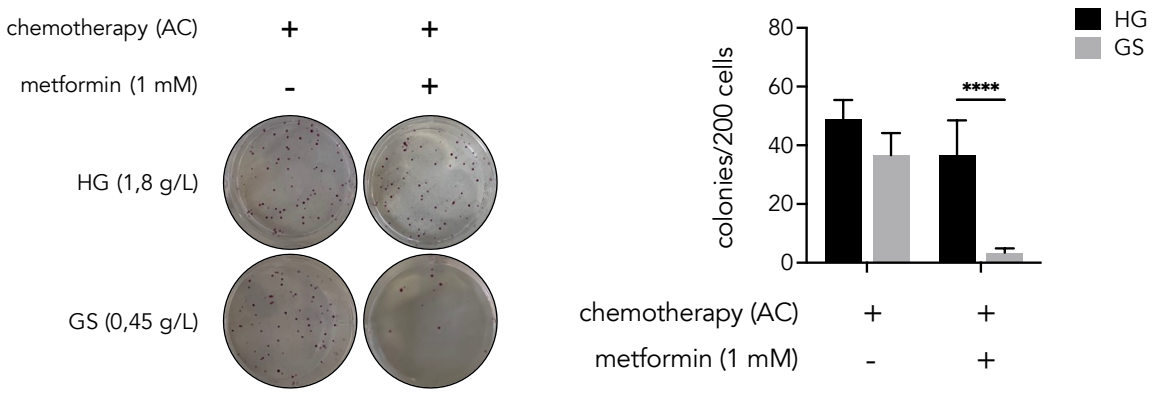

Figure 28: : the triple combination impairs clonogenic potential.

*Representative figures (left panel) and number of colonies (right panel) of colony forming assay. MDA-MB-231 cells were treated as previously indicated for 4 days. Then, cells that were still alive were plated as single cell at a concentration of 200 cells/well and grown for 14 days in standard culture medium. Medium was replaced every 3/4 days. N = 3 replicates. Significances were calculated with one-way ANOVA. *p<0,05; **p<0,01; ***p<0,001; ****p<0,0001.*

To verify that the results so far were not cell line-specific, we have screened a panel of TNBC cell lines as follows: metformin 1 mM, low-dose chemotherapy and the double or triple combination. As described for the MDA-MB-231 cells, the combination of metformin and glucose starvation had a modest impact, with most of the cell lines being resistant, and HCC1599, and, to a lesser extent, the MDA-MB-468, being the most sensitive cell lines (**Figure 29**). Again, the triple combination caused a marked cytotoxic effect (well described by the graphs above), while low-dose chemotherapy or the double combination were at most cytostatic (**Figure 29**). Among the more sensitive cell lines, HCC1599, MDA-MB-468 and MDA-MB-436 were characterized by a high number of mutations in the genes involved in the DDR and in DNA repair (Lehmann et al., 2011; Yin et al., 2020).

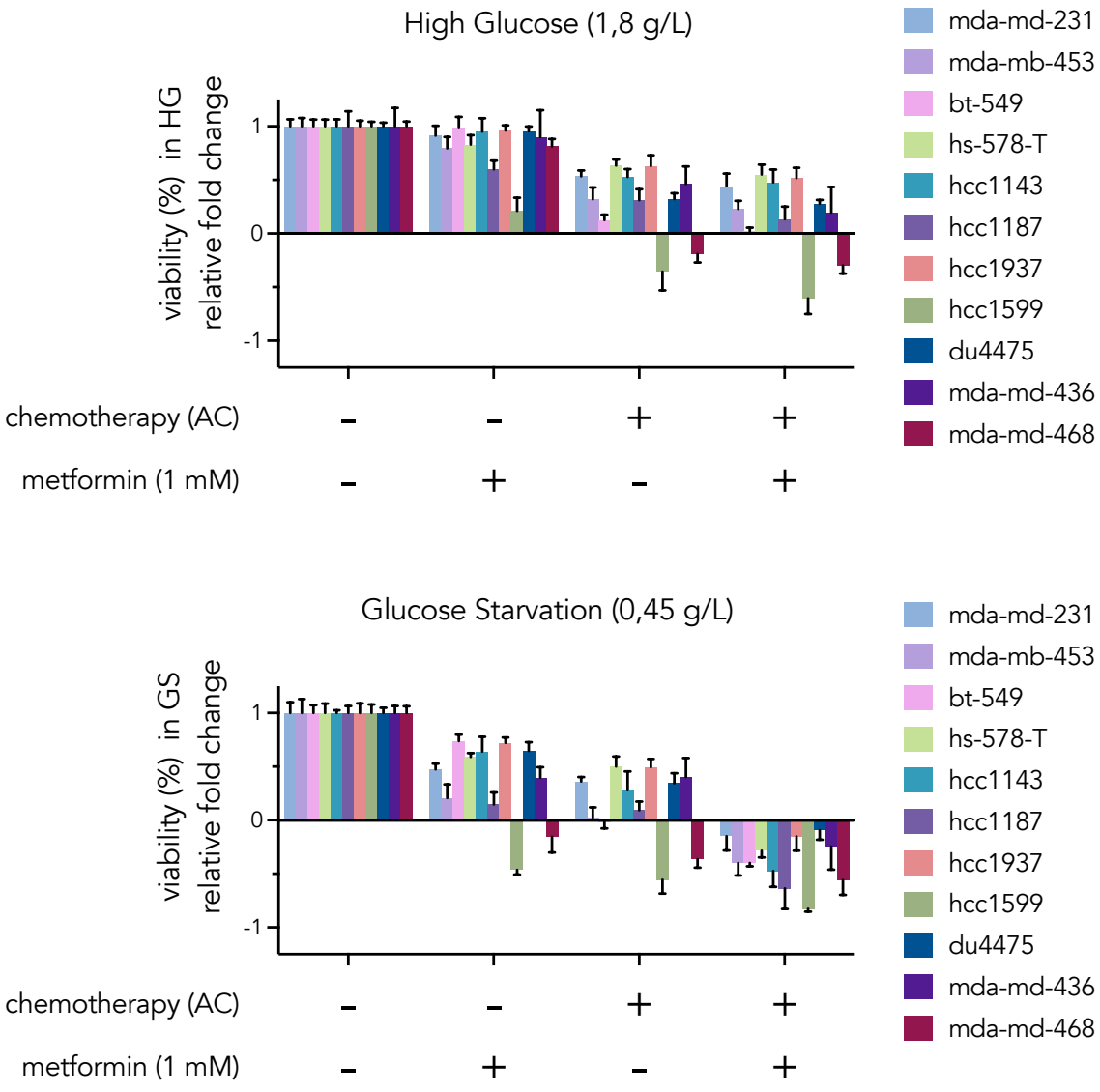

Figure 29: : the triple combination induces a cytotoxic effect in a panel of TNBC cell lines.

Viability of the indicated TNBC cell lines treated for 4 days as follows: HG (top panel, 1,8 g/L), GS (bottom panel, 0,45 g/L); metformin (1 mM); low-dose chemotherapy (dox 0,1 µM + cp 2 µM). Value of 1 indicate full viable cells (untreated, in HG and GS respectively). Value of 0 indicate no change compared to day 0 (cytostatic effect). Negative values indicate decrease in the number of cells (-1 indicate no cell remaining, cytotoxic effect). Each value in HG and in GS refers to its control (specific to each cell line) HG and GS, respectively. N = 3 replicates.

Standard culture media are far from being representative of the tumor metabolic environment (Vande Voorde et al., 2019). To improve the metabolic fidelity of our experimental setting and verify whether the synergism we observed is biased by an inadequate balance of nutrients, we took advantage of the Plasmax medium kindly provided by Saverio Tardito (Beatson Institute, Glasgow, Scotland). MDA-MB-231 cells have been adapted to the new medium and subjected the experimental protocol as described above. After 4 days, Plasmax medium rescued the (not significant) decrease in proliferation we have observed with standard DMEM upon the combination with metformin and glucose starvation, which could be caused by the simultaneous inhibition of glycolysis and OXPHOS, rather than the activation of a specific pathway (**Figure 30**). Nevertheless, the triple combination maintained the strongest anti-proliferative potential we have observed with DMEM, stressing the fact that the synergism is specifically mediated by the combination of metformin and glucose starvation and is not biased by metabolic catastrophe (**Figure 30**).

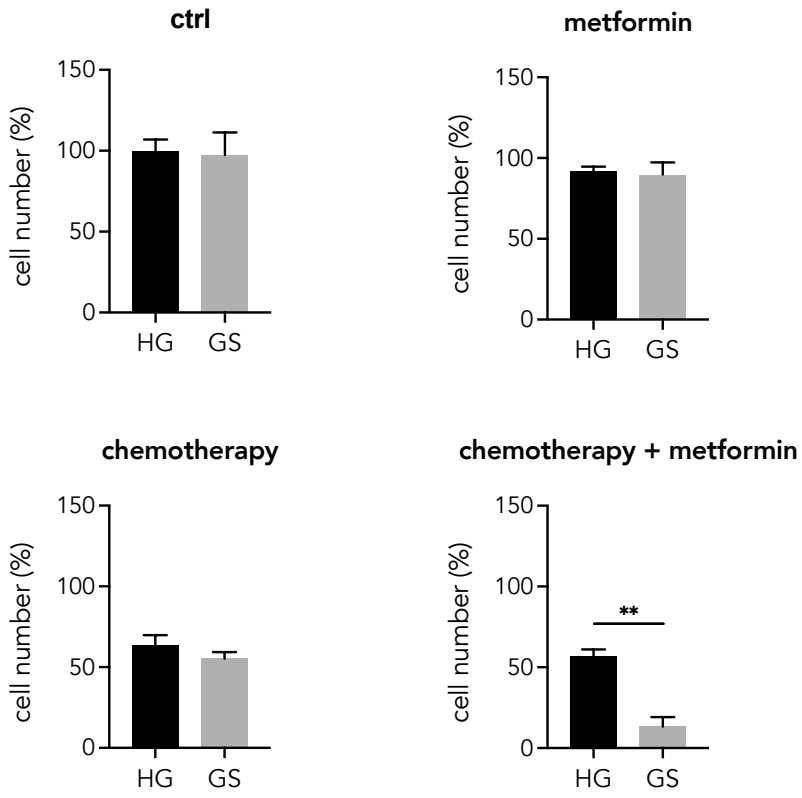

Figure 30: the triple combination is effective in a physiological culture medium.

*Viability of MDA-MB-231 cells cultured in Plasmax medium and treated for 4 days as follows: HG (1,8 g/L); GS (0,45 g/L); metformin (1 mM); low-dose chemotherapy (dox 0,1 µM + cp 2 µM). Values are relative to control samples (HG). N = 3 replicates. Significances were calculated with Student t-test. *p<0,05; **p<0,01; ***p<0,001; ****p<0,0001.*

3. Metformin and glucose starvation enhance the efficacy of chemotherapy in TNBC patient-derived tumors cells.

To further strengthen our observations *in vitro*, we took advantage of the patient-derived TNBC primary cells 197TX18 from our collaborators Dr. Pece and Tosoni. 197TX18 cells grow as aggregates in suspension and cannot be kept in culture for long; thus, we have adapted the treatment to the model, avoiding excessive manipulations such as changing the culture medium after 2 days. Even though 197TX18 cells were kept in culture for 4 days straight, glucose starvation did not

impact on cell viability (**Figure 31 left panel**). We raised metformin concentration to 2 mM, since the dose we previously used (1 mM) had no effect per se. The combination of metformin and glucose starvation reduced proliferation by 60% (**Figure 31 right panel**).

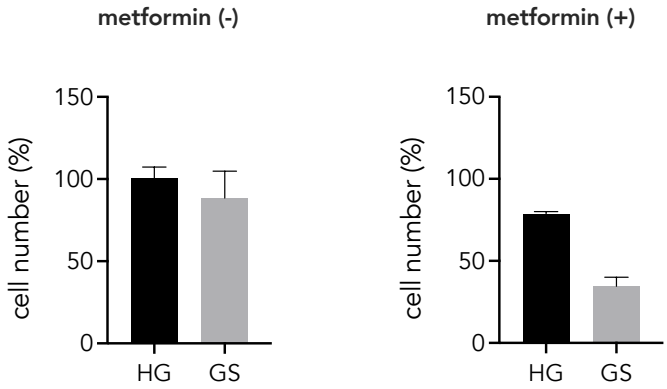

Figure 31: : impact of metformin and glucose starvation on patient-derived cells.

Viability of the patient-derived 197TX18 primary cells treated for 4 days as follows: HG (1,8 g/L); GS (0,45 g/L) ± metformin (2 mM). Values are relative to control sample (HG, left panel). N = 3 replicates.

Differently from the TNBC cell lines we used in the previous screening, 197TX18 cells were collected before the patient underwent any adjuvant/neo-adjuvant chemotherapy regimen; thus, 197TX18 cells were more sensitive to the combination of dox and cp and we halved the doses to investigate any synergistic effects. Chemotherapy and glucose starvation had an even more pronounced effect compared to MDA-MB-231 cell line (**Figure 32**). Again, the triple combination was the most powerful compared to chemotherapy alone or the double combination and almost abolished cell proliferation (**Figure 32**).

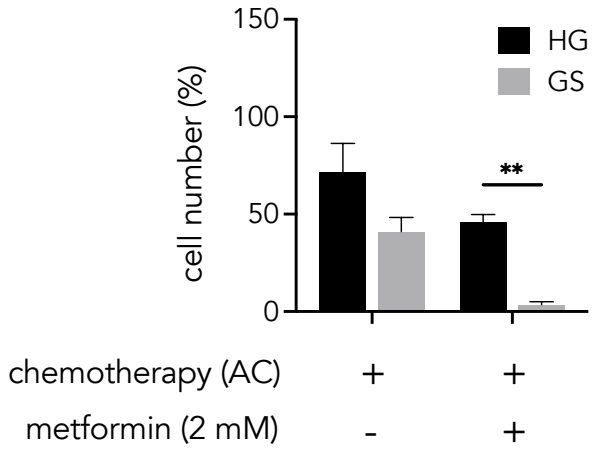

Figure 32: : the triple combination abolishes cell viability in patient-derived cells.

Viability of the patient-derived 197TX18 primary cells treated for 4 days as follows: HG (1,8 g/L); GS (0,45 g/L); metformin (2 mM); low-dose chemotherapy (dox 0,05 μM + cp 1 μM). Values are relative to control samples (HG, ***Figure 31****, left panel). N = 3 replicates. Significances were calculated with one-way ANOVA. *p<0,05; **p<0,01; ***p<0,001; ****p<0,0001.*

Since we observed almost the same trend in all models, we were confident that the synergism was not dependent of the specific features of the single cell line/patient-derived tumor but was strictly dependent on the combination of metformin and glucose starvation.

4. Metformin and intermittent fasting enhance the efficacy of chemotherapy and induce tumor regression in *vivo*.

We assessed whether the approach we propose here is safe and relevant also *in vivo*, and if it is advantageous compared to chemotherapy alone, which remains the standard of clinical care for TNBC patients and, in many cases, the only suitable option. To this purpose, we designed an experiment as shown in **Figure 33 top panel**;

we relied on the scheme of the BREAKFAST clinical trial, in which TNBC patients undergoing neo-adjuvant chemotherapy were subjected to a fasting mimicking diet (FMD) regimen with or without metformin. CD1-nude mice were injected with 250.000 MDA-MB-231 cells in the fourth mammary fat pad and subjected to different pharmacological treatments when the tumors were palpable. Each of the 4 weeks of treatment was organized as shown in **Figure 33 bottom panel**: low-dose chemotherapy (referred as AC from A = anthracycline, family to which doxorubicin belongs, and C = cyclophosphamide) was administered once per week while metformin (200 mg/Kg) was administered 3 times per week, alone or together with chemotherapy (referred as ACM = AC + metformin). Both chemotherapy and metformin were administered during the fasting period of a 24 hours feeding/fasting cycle - intermittent fasting (I.F.). I.F. involved the complete withdrawal of food but free access to water in the fasting days, while food was re-supplied *ad libitum* in the feeding days.

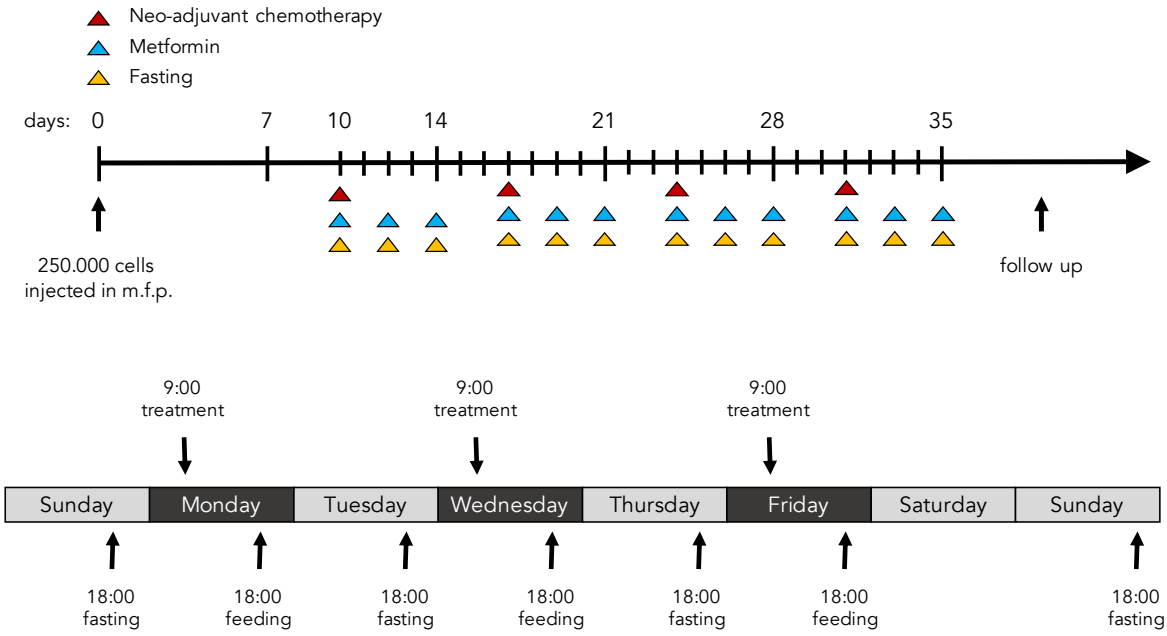

Figure 33: in vivo experiment setup.

Top panel: monthly organization. CD1-nude mice were injected with 250.000 MDA-MB-231 cells and subjected to different pharmacological treatments when the tumors were palpable (day 10) up to 4 weeks. Bottom panel: weekly organization with the timing of the different treatments and food withdrawal/addition.

In CD1-nude mice transplanted with MDA-MB-231 tumor cells, I.F. cycles lowered blood glucose to values similar to the ones used for the *in vitro* experiments (1,75 g/L during feeding and 0,44 g/L during fasting, respectively); metformin did not enhance the drop of blood glucose during fasting periods (**Figure 34**). This is in accordance with the effect of metformin which does not lower blood glucose in non-diabetic patients (Preiss et al., 2014). After each cycle, blood glucose returned to the same level and no dramatic drop was observed in the long-term (**Figure 34 – 35**).

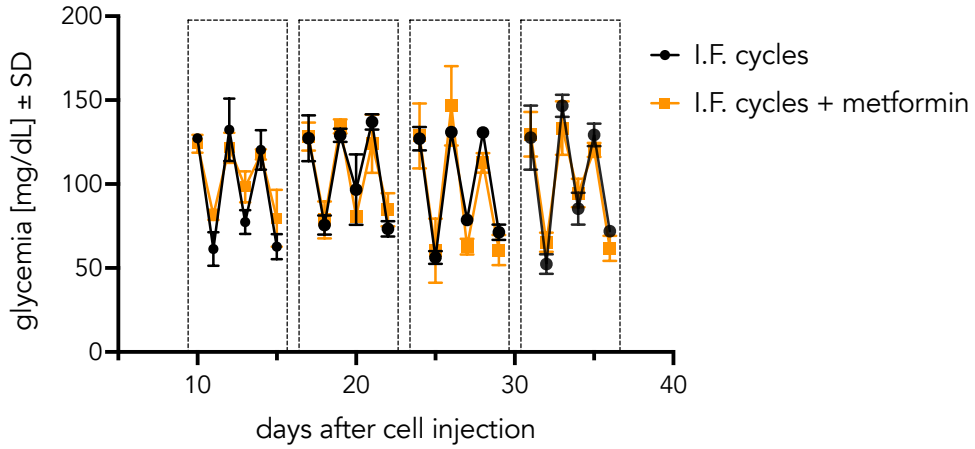

Figure 34: I.F. cycles lower blood glucose by 75% in CD-1 nude mice.

Blood glucose concentration (mg/dL) measured at the end of every feeding/fasting cycle in the I.F. and I.F. + metformin groups. Each point represents the mean of the measurements (either in feeding or in fasting) of every mouse for each group. Each dashed box represents one separate week. N = 3 mice/group.

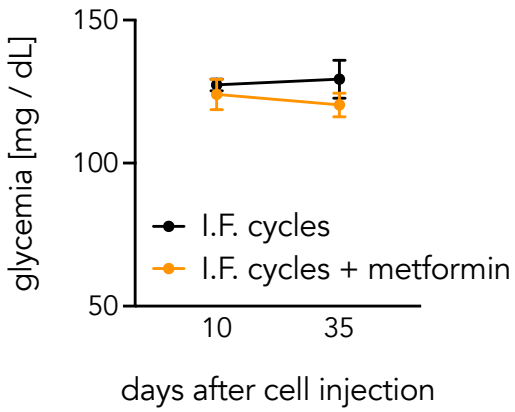

Figure 35: I.F. cycles do not decrease blood glucose over the long period in CD-1 nude mice.

Blood glucose concentration (mg/dL) measured at the beginning and at the end of the 4 weeks of feeding/fasting cycles in the I.F. and I.F. + metformin groups. Each point represents the mean of the measurements (in feeding) of every mouse for each group. N = 3 mice/group.

The weight of the animals dropped following one day on fasting and returned to normal after one day on feeding (**Figure 36**) and no significant weight loss was observed over the long period, thus excluding the toxicity of I.F. cycles (**Figure 37**).

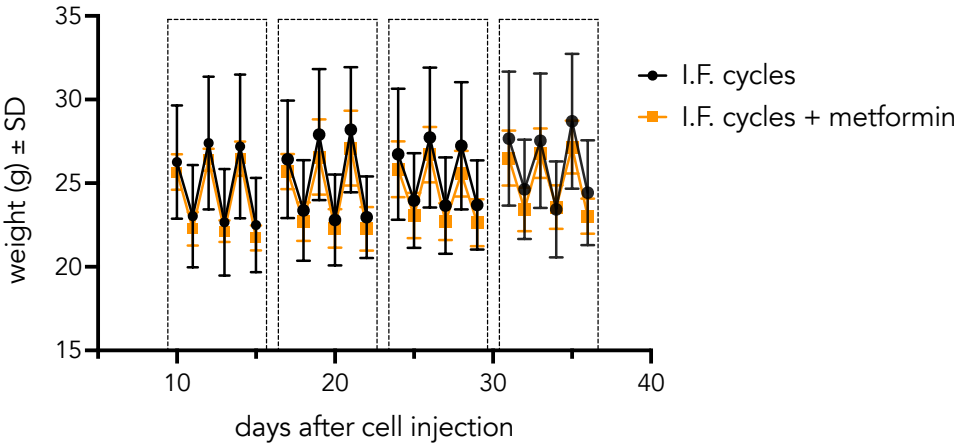

Figure 36: animal weight during the feeding and the fasting periods of the I.F. cycles.

Weight (g) measured at the end of every feeding/fasting cycle in the I.F. and I.F. + metformin groups. Each point represents the mean of the measurements (either in feeding or in fasting) of every mouse for each group. Each dashed box represents one separate week. N = 3 mice/group.

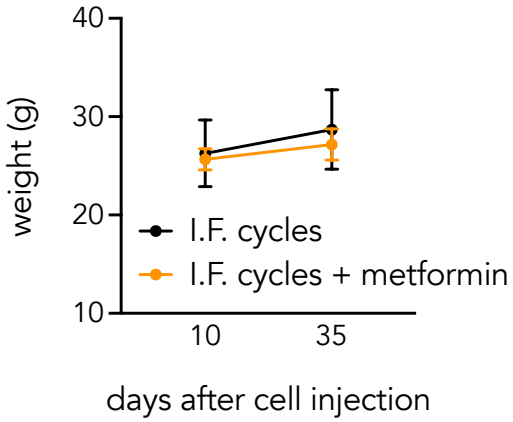

Figure 37: I.F. cycles does not reduce the weight over the long period in CD-1 nude mice.

Weight (g) measured at the beginning and at the end of the 4 weeks of feeding/fasting cycles in the I.F. and I.F. + metformin groups. Each point represents the mean of the measurements (in feeding) of every mouse for each group. N = 3 mice/group.

As for the in *vitro* experiments, also in the animal model we significantly lowered the dosage of chemotherapeutics to sub-optimal levels as a strategy to better study any cooperative effect. Low-dose chemotherapy was well tolerated both when administered during feeding and fasting, and no dramatic weight loss from chemotherapy, nor from chemotherapy and metformin, was observed after 4 weeks treatment (**Figure 38**). Mice were sacrificed when the major side of the tumor reached 15 mm.

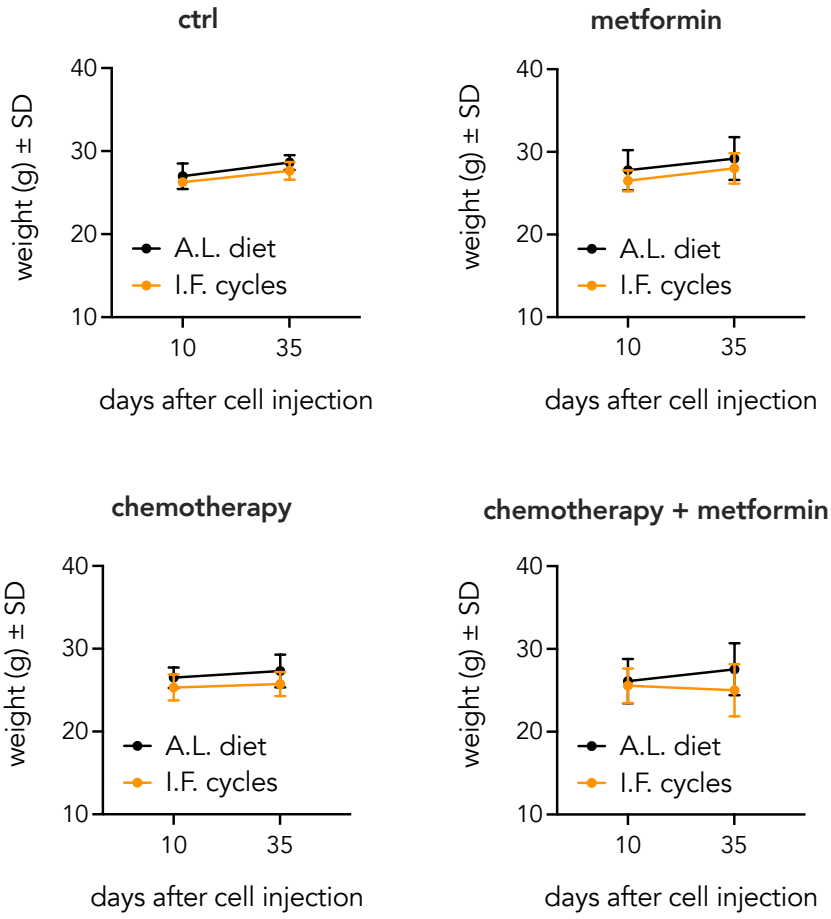

Figure 38: the combination of chemotherapy and metformin with I.F. is safe and tolerable in CD-1 nude mice.

Weight (g) of CD1-nude mice measured at the beginning and at the end of the 4 weeks of treatment as indicated. Each point represents the mean of the measurements (in feeding) of every mouse for each group. Number of animals: Ctrl = 13; Met = 11; AC = 13; ACM = 13; I.F. = 11; Met_I.F. = 14; AC_I.F. = 13; ACM_I.F. = 15.

Metformin had no appreciable effect and the growth curve was perfectly superimposable to that of controls, similarly to what we previously observed. Differently from the in *vitro* results, I.F. cycles reduced tumor growth. This discrepancy may be due to the fact that, while in *vitro* we artificially decrease only glucose in the culture medium, in *vivo* many nutrients drop during fasting and may contribute to

reduce tumor growth (Caffa et al., 2020). Compared to the I.F. regimen, metformin, administered in fasting, weakly impacted tumor growth, confirming the resistance of MDA-MB-231 cells to the metabolic combination. Low-dose chemotherapy decreased tumor growth and no significant differences were observed between the groups in feeding or fasting, nor with chemotherapy and metformin in feeding (double combination). Strikingly, the combination of metformin and low-dose chemotherapy in groups undergoing I.F. cycles (triple combination) produced the strongest anti-proliferative effect compared both to I.F. cycles (alone or with metformin) and chemotherapy, either in feeding or in fasting (**Figure 39, top panel**). At the ending point of the experiment (day 38), the difference in tumor size between the triple combination and other groups was statistically significant (**Figure 39, bottom panel**). Furthermore, and most importantly, the triple combination was the only condition to effectively induce tumor regression, while other treatments only reduced tumor growth; this was noticed by comparing tumor size at the beginning and at the ending point of the four weeks of treatment (**Figure 40**).

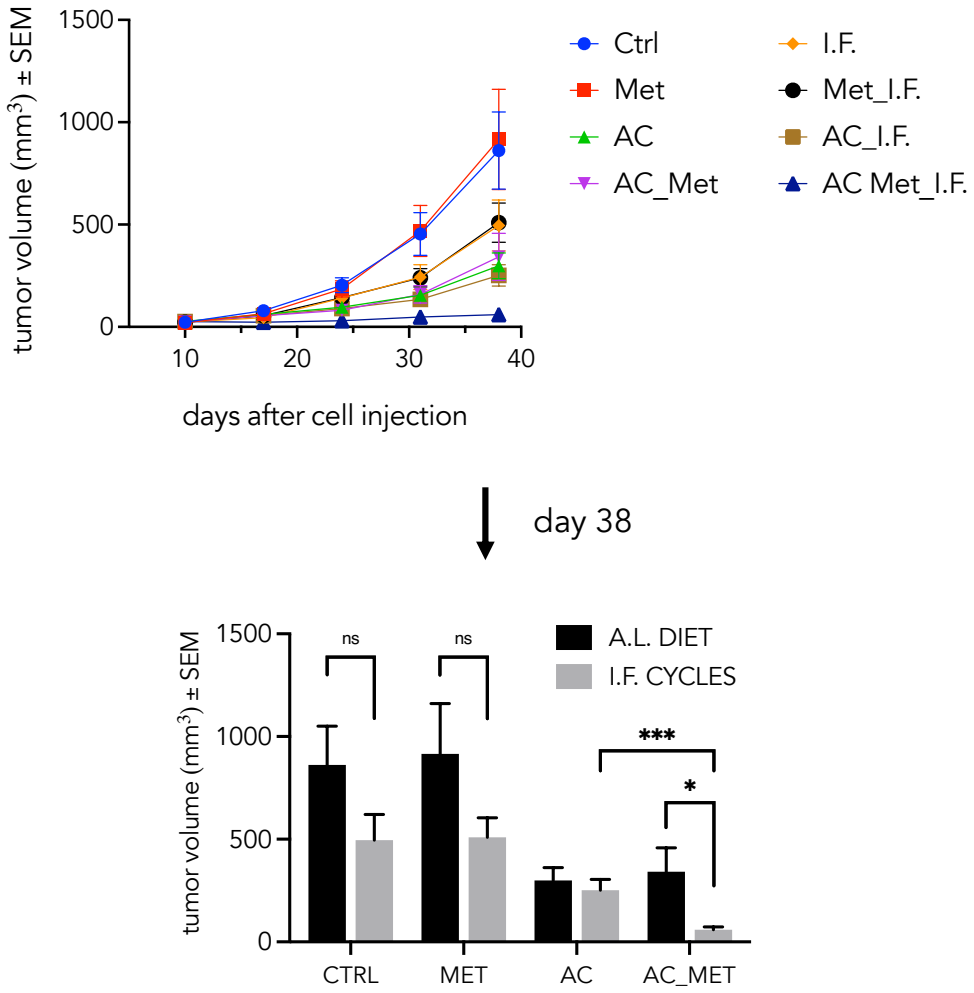

Figure 39: : the triple combination abolishes tumor growth in in CD-1 nude mice.

*Top panel: tumor growth measured by tumor volume in CD-1 nude mice injected with MDA-MB-231 cells and subjected to different treatments as described. Bars plots with error bars represent mean values and standard error of the mean. Bottom panel: tumor volume measured at the end of the treatment described (day 38). Bars plots with error bars represent mean values and standard error of the mean. Number of animals: Ctrl = 13; Met = 11; AC = 13; ACM = 13; I.F. = 11; Met I.F. = 14; AC I.F. = 13; ACM I.F. = 15. I.F., intermittent fasting cycles: met, metformin 200 mg/kg (dissolved in water); AC, doxorubicin 0,5 mg/kg (dissolved in saline solution) + cyclophosphamide 50 mg/kg (dissolved in saline solution); ACM, AC + metformin. Significances were calculated with two-tailed unpaired Student t test. *p<0,05; **p<0,01; ***p<0,001; ****p<0,0001.*

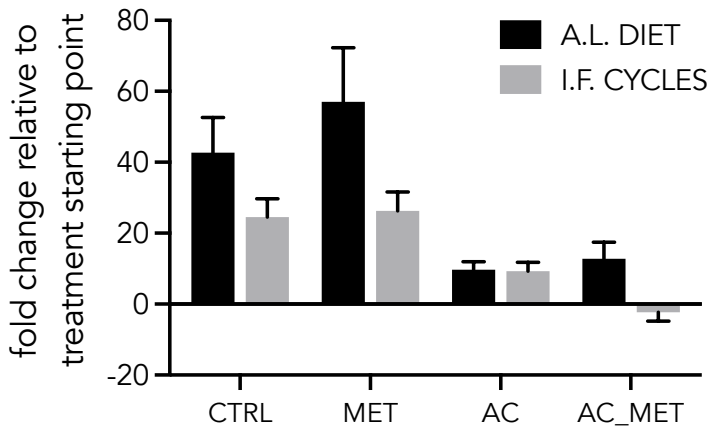

Figure 40: the triple combination induces tumor regression in vivo.

Fold change in tumor volume obtained by comparison of the tumor size at the beginning and at the ending point of the treatment as described. Bars plots with error bars represent mean values and standard error of the mean. Number of animals: Ctrl = 13; Met = 11; AC = 13; ACM = 13; I.F. = 11; Met I.F. = 14; AC I.F. = 13; ACM I.F. = 15. I.F., intermittent fasting cycles: met, metformin 200 mg/kg (dissolved in water); AC, doxorubicin 0,5 mg/kg (dissolved in saline solution) + cyclophosphamide 50 mg/kg (dissolved in saline solution); ACM, AC + metformin.

Together, these results support and encourage the use of metformin in association with chemotherapy and I.F. cycles or other strategies that lower blood glucose. The experimental setup we propose here could be well tolerated by patients and could provide an advantage over current therapies for TNBCs, mainly based on cytotoxic chemotherapy.

5. Metformin and glucose starvation attenuate the DDR and dampen DNA repair.

We investigated the molecular mechanism underlying the synergism between chemotherapy, metformin and glucose starvation. Firstly, we performed cell-cycle analysis of MDA-MB-231 cells after 1 day of treatment as described in **Figure 22**, before any evidence of cell death. Glucose starvation slightly increased the percentage of cells in G1 phase, while the combination with metformin increased the percentage of cells in S phase. As expected, cell cycle analysis revealed an important S-phase arrest upon treatment with low-dose chemotherapy, independently of glucose availability; we observed the same effect with the double combination. Surprisingly, the cell-cycle profile of cells subjected to the triple combination was more similar to the one of untreated samples and the percentage of halted cells was significantly lower compared to the other conditions (**Figure 41**).

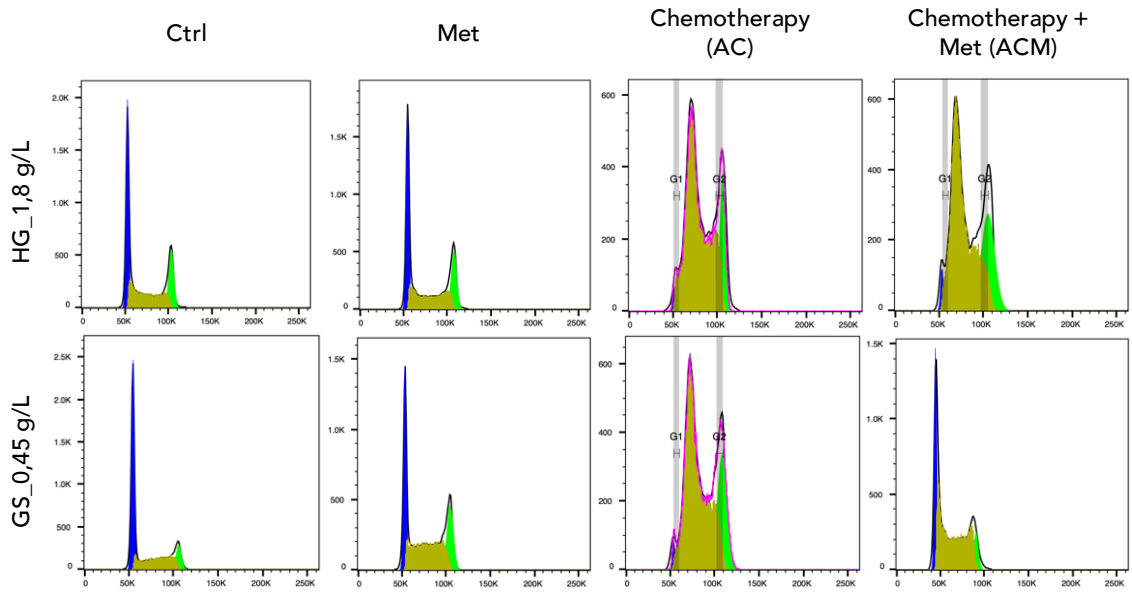

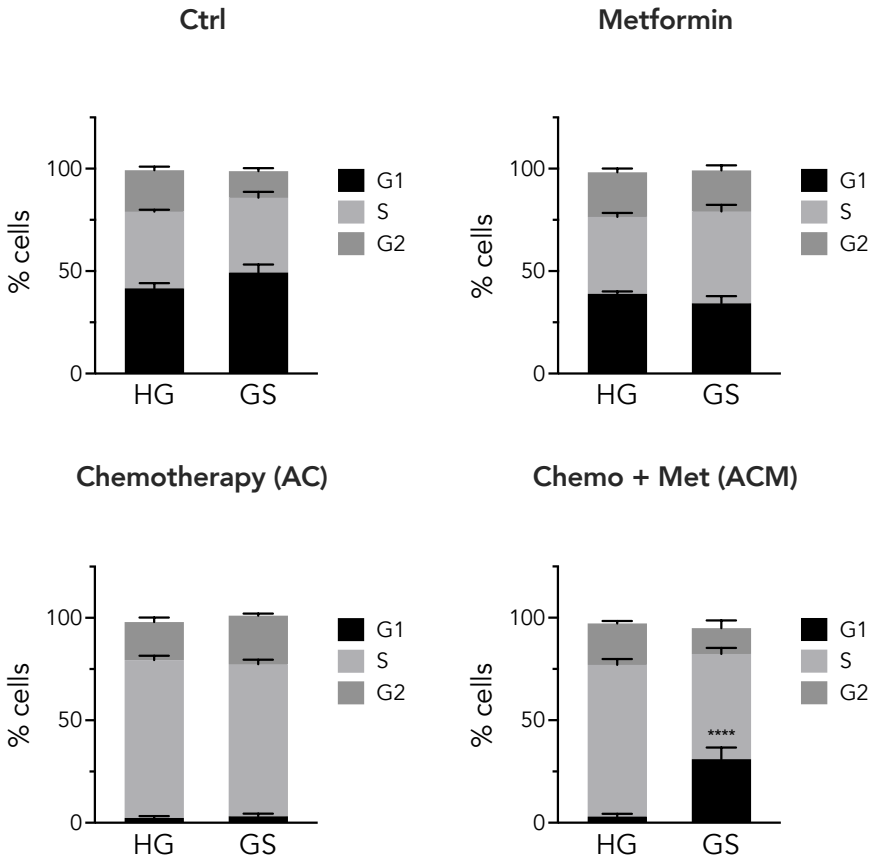

Figure 41: the triple combination abolishes the cell-cycle arrest imposed by chemotherapy.

*Top panel: cell cycle profile of MDA-MB-231 after 1 day of treatment as follows: HG (1,8 g/L); GS (0,45 g/L); metformin (1 mM); low-dose chemotherapy (dox 0,1 µM + cp 2 µM). Bottom panel: cell-cycle analysis of MDA-MB-231 cells after 1 day of treatment as in top panel. N = 3 replicates. Significances were calculated with one-way Anova. *p<0,05; **p<0,01; ***p<0,001; ****p<0,0001.*

Failure to arrest the cell cycle and increased cell death could be explained by a DDR checkpoint deficiency (Kerzendorfer & O'Driscoll, 2009). Thus, we investigated the status of the DDR in mammalian tumor cells upon the various treatments described above. We collected MDA-MB-231 cells for western blot after 1 day of treatment, in accordance with cell-cycle analysis results. Low-dose chemotherapy induced the phosphorylation and activation of both the ATR and the ATM pathways, which are the

apical kinases of the DDR, in line with the observed S-phase arrest (**Figure 42**). Surprisingly, the apical DDR kinases (ATR and ATM), together with the downstream kinases (CHK1 and CHK2, respectively) and histone H2Ax, which is phosphorylated around the site of DNA damage, exhibited reduced phosphorylation following the triple combination, suggesting a lower activation of the DDR during metabolic stress (**Figure 42**). The phosphorylation was lower only when metformin and glucose starvation were combined, suggesting they were both necessary to modulate the DDR. Interestingly, both the DDR kinases and histone H2Ax are known PP2A substrates (X. Li et al., 2015; Petersen et al., 2006); in this context, PP2A is required to maintain a low checkpoint activation in absence of DNA damage and to rapidly turn off the DDR when the lesion is solved (Freeman et al., 2010; Freeman & Monteiro, 2010; Ramos et al., 2019).

After phosphorylation by ATR and ATM, respectively, phosphorylated CHK1 and 2 (pCHK1 and pCHK2) are rapidly degraded to maintain the signaling cascade under control, with a consequent decrease in the total amount of protein (Bohgaki et al., 2013; García-Limones et al., 2016; C. Park et al., 2015). Accordingly, total CHK1 and CHK2 decreased upon treatment with chemotherapy alone or the double combination. In accordance with the reduced or nulled phosphorylation, CHK1 and CHK2 total protein levels remained unperturbed following the triple combination (**Figure 42**).

a

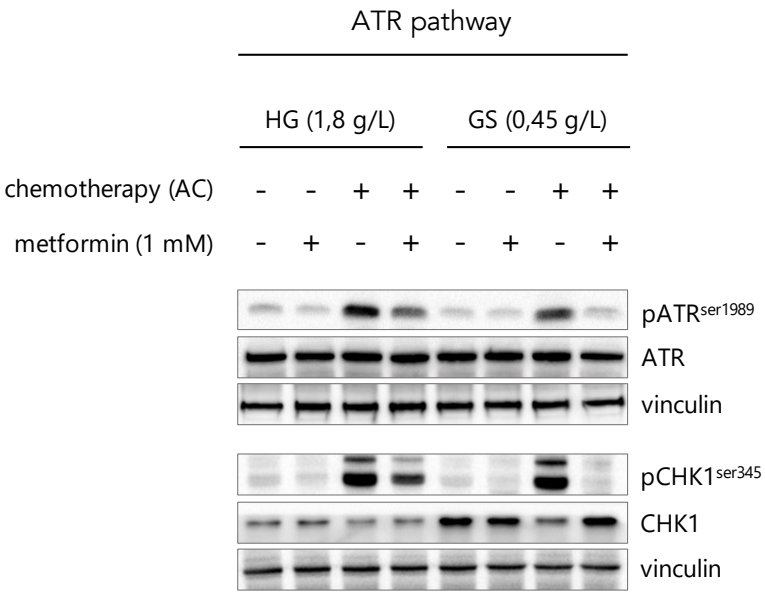
ATR pathway
HG (1,8 g/L)
GS (0,45 g/L)
chemotherapy (AC) - - + + - - + +
metformin (1 mM) - + - + - + - +
pATR ser1989
ATR
vinculin
pCHK1 ser345
CHK1
vinculin

b

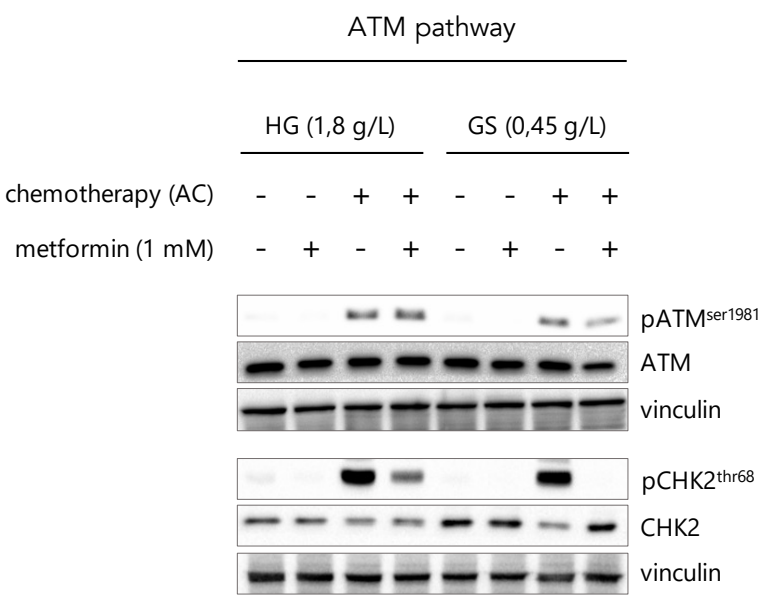
ATM pathway
HG (1,8 g/L)
GS (0,45 g/L)
chemotherapy (AC) - - + + - - + +
metformin (1 mM) - + - + - + - +
pATM ser1981
ATM
vinculin
pCHK2 thr68
CHK2
vinculin

c

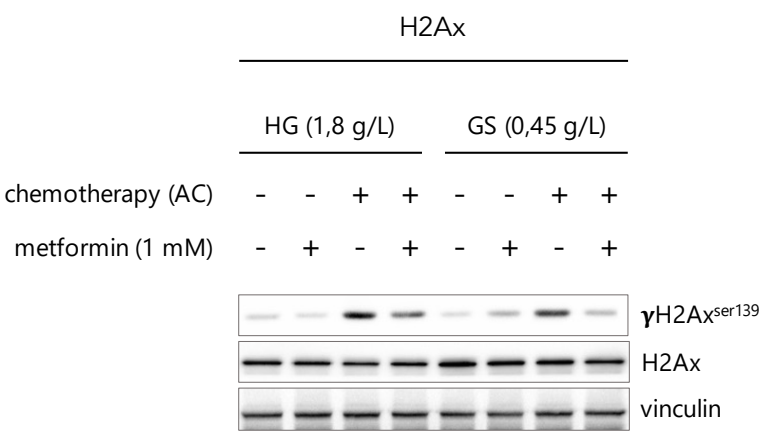
H2Ax
HG (1,8 g/L)
GS (0,45 g/L)
chemotherapy (AC) - - + + - - + +
metformin (1 mM) - + - + - + - +
γH2Ax ser139
H2Ax
vinculin

Figure 42: the triple combination reduces the activation of the DDR triggered by chemotherapy (I).

Western blot analysis showing the phosphorylation and the total levels of the indicated proteins after 1 day of treatment as follows: HG (1,8 g/L); GS (0,45 g/L); metformin (1 mM); low-dose chemotherapy (dox 0,1 μM + cp 2 μM). Vinculin was used as loading control. N = 3 replicates.

We observed the same pattern of phosphorylation by using the Plasmax culture medium as previously described, confirming once again that the combination of metformin and glucose starvation was strictly necessary for the observed effects, and that other nutrients did not affect (**Figure 43**).

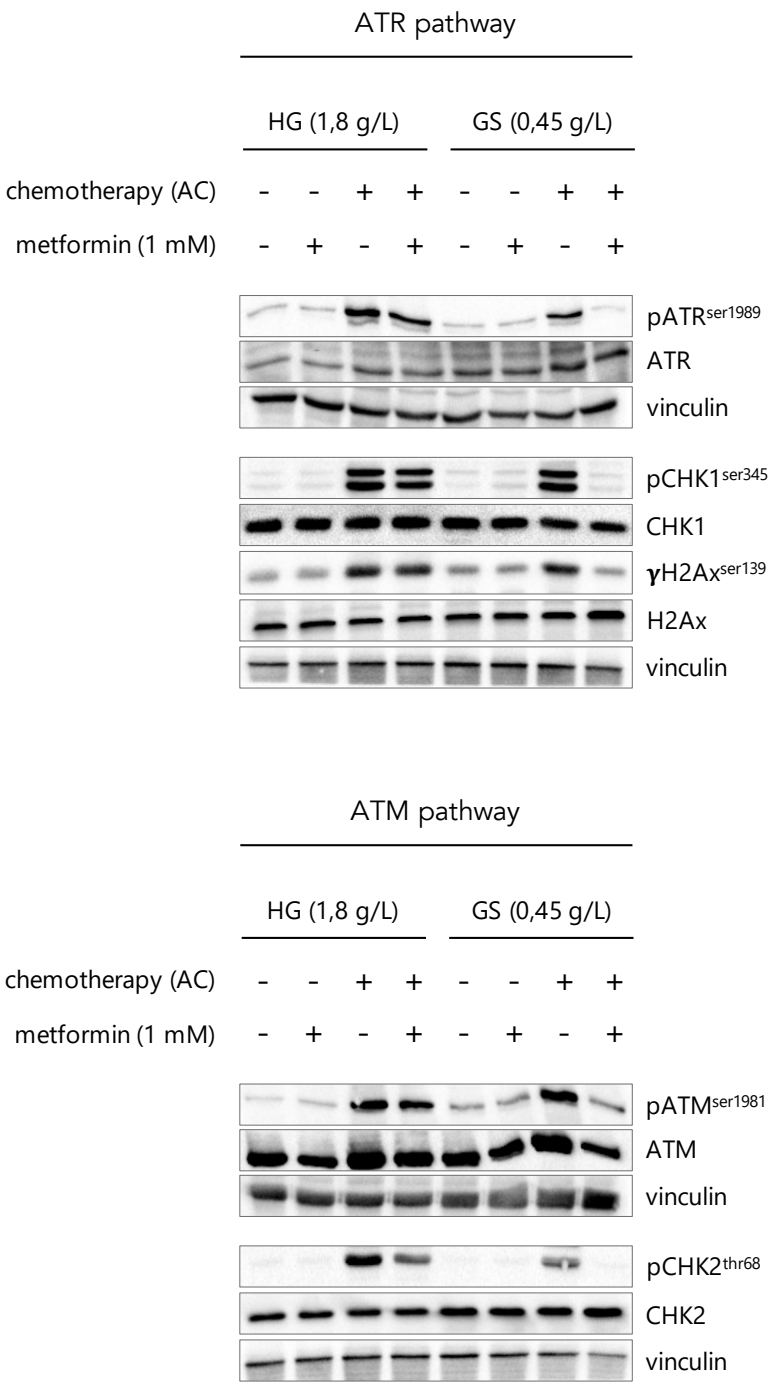

Figure 43: the triple combination reduces the activation of the DDR triggered by chemotherapy (II).

Western blot analysis showing the phosphorylation level of the indicated proteins after 1 day of treatment as follows: HG (1,8 g/L); GS (0,45 g/L); metformin (1 mM); low-dose chemotherapy (dox 0,1 μM + cp 2 μM). Top panel: ATR pathway. Bottom panel: ATM pathway. Vinculin was used as loading control. N = 3 replicates.

CDC25A is necessary for cell cycle progression and it is rapidly ubiquitinated and degraded following CHK1 and CHK2-dependent phosphorylation, thus resulting in cell cycle arrest. CDC25A protein levels decreased in accordance with the activation of CHK1 and the cell cycle arrest. On the contrary, the triple combination induced no decrease in CDC25A protein levels, in line with the failure to arrest the cell cycle and the DDR shutdown (**Figure 44**).

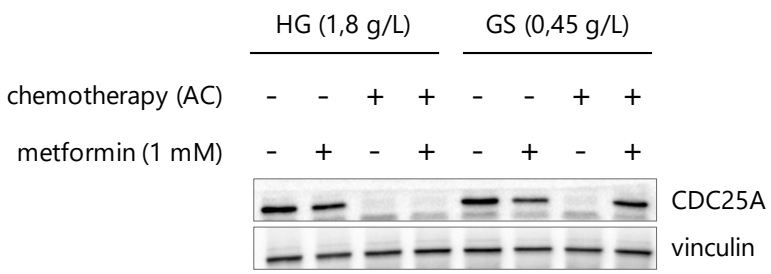

Figure 44: the triple combination does not reduce CDC25A protein levels.

Western blot analysis showing the levels of the indicated proteins after 1 day of treatment as follows: HG (1,8 g/L); GS (0,45 g/L); metformin (1 mM); low-dose chemotherapy (dox 0,1 μM + cp 2 μM). Vinculin was used as loading control.

We assessed whether the effect of the metabolic stress was an attenuation, rather than a failure to activate the DDR. CHK1 phosphorylation (which is an early event of the DDR and which we used as a parameter for DDR activation and progress) increased in a time-dependent manner in any condition that included chemotherapy, and no difference were observed in the first 12 hours of treatment; then, it decreased when metformin and glucose starvation were combined with chemotherapy at 24 hours (**Figure 45**). This suggested that the DDR initiated in presence of DNA-damaging chemotherapy, and was then attenuated due to metabolic stress.

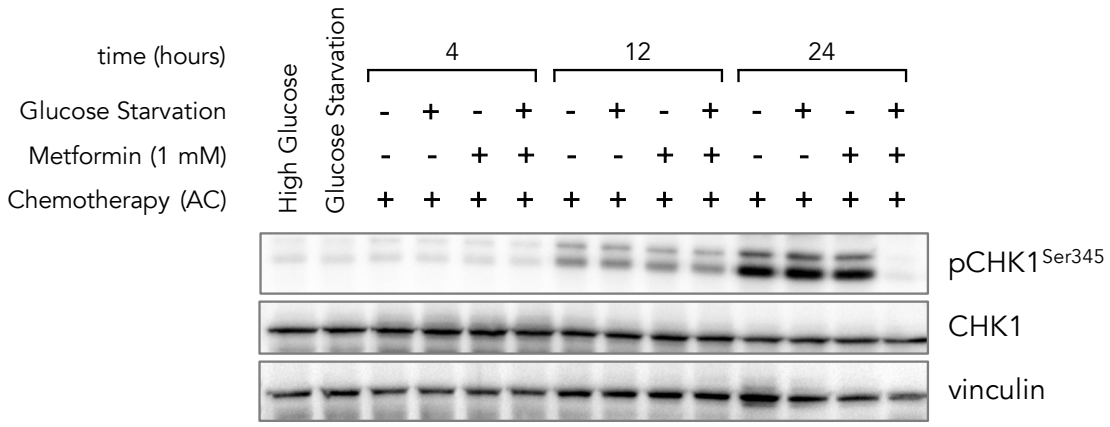

Figure 45: : the triple combination attenuates the DDR triggered by chemotherapy.

Western blot analysis showing the phosphorylation and the total levels of CHK1 in MDA-MB-231 treated as as follows for the indicated time points: HG (1,8 g/L); GS (0,45 g/L); metformin (1 mM); low-dose chemotherapy (dox 0,1 μM + cp 2 μM). Vinculin was used as loading control.

We observed a similar pattern of phosphorylation in the patient-derived primary tumor cells 197TX18, even though the phosphorylation level of DDR proteins was higher compared to MDA-MB-231 cells, suggesting that in *vitro* culture of primary tumor cells is a stressogenic condition (**Figure 46**).

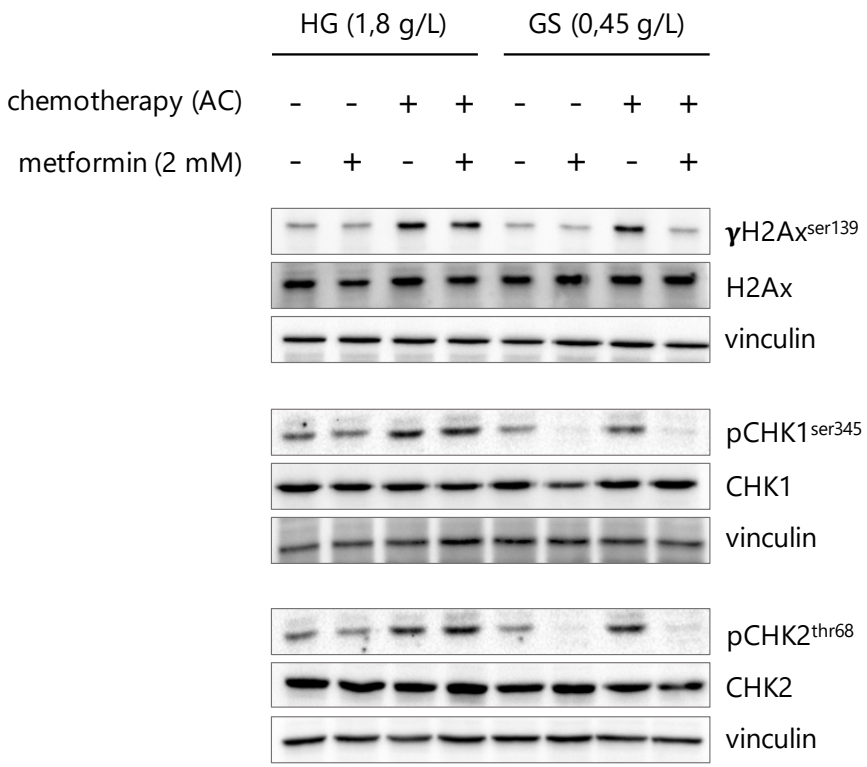

Figure 46: the triple combination reduces the activation of the DDR in patient-derived primary cells.

Western blot analysis showing the phosphorylation and the total levels of the indicated proteins after 1 day of treatment as follows: HG (1,8 g/L); GS (0,45 g/L); metformin (2 mM); low-dose chemotherapy (dox 0,05 μM + cp 1 μM). Vinculin was used as loading control. N = 2 replicates.

We hypothesized that the attenuation of the DDR prevented an appropriate signaling and repair of the DNA lesion, which accumulated in the continuous presence of chemotherapy to the point of becoming unbearable and incompatible with survival.

We performed neutral comet assay after 2 days of treatment to directly investigate DNA integrity: no major differences were observed upon chemotherapy treatments or the double combination. Intriguingly, cells subjected to the triple combination exhibited increased genomic fragmentation (**Figure 47 top panel**). The triple combination increased both the number of comets, namely the number of damaged

cells, and the tail moments, which are indicative of the number of DNA breaks per single cell, compared to chemotherapy alone (**Figure 47 bottom panel**). Of note, cells treated with chemotherapy and glucose starvation were characterized by a higher number of comets and increase tail moments, compared to the counterpart in high glucose, even though the difference was not statistically significant; this supported the observations from viability experiments. We also performed comet assay after 24 hours of treatment, that is, when we observed the peak of checkpoint dephosphorylation, but no comets were visible; this confirms that checkpoint shutdown is earlier and responsible for the failure of DNA repair resulting in genomic disruption (data not shown).

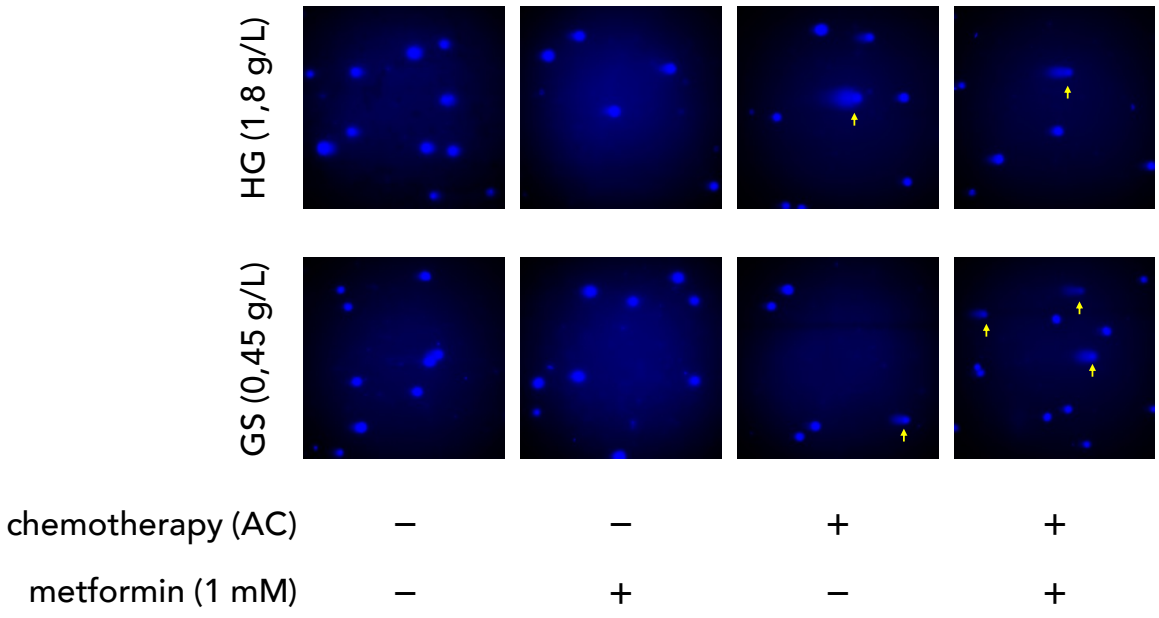

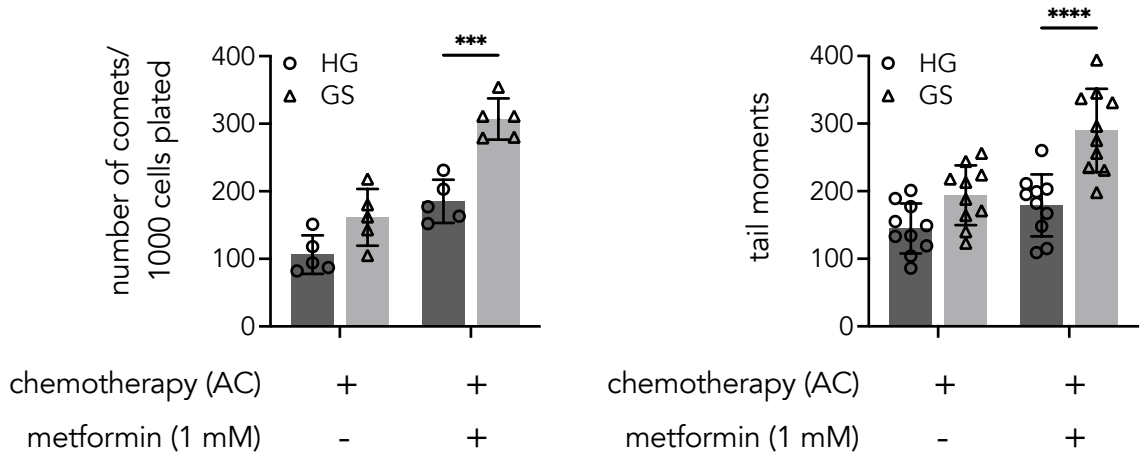

Figure 47: the triple combination dampens DNA repair.

*Neutral comet assay in MDA-MB-231 performed after 2 days of treatment as follows: HG (1,8 g/L); GS (0,45 g/L); metformin (1 mM); low-dose chemotherapy (dox 0,1 μM + cp 2 μM). Representative image (**top panel**); number of comets for 1000 plated cells (**bottom panel, left**); comet tail moments (**bottom panel, right**). N = 3 replicates. Significances were calculated with one-way ANOVA. *p<0,05; **p<0,01; ***p<0,001; ****p<0,0001.*

Lastly, to further confirm the impairment of DNA repair, we performed a competition assay as described in **Figure 48 left panel**: MDA-MB-231 were pulsed with high dose-chemotherapy for a short time (20 folds greater than low-dose chemotherapy for 8 hours) and then grown in different culture media up to 3 days. Cells grown in metformin-rich (1 mM), glucose-starved medium (0,45 g/L), had the strongest proliferative disadvantage compared to other conditions (**Figure 48 right panel**).

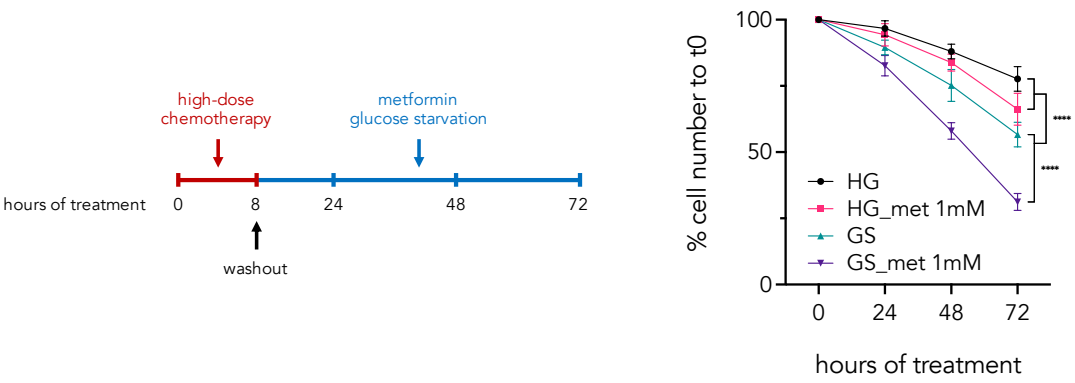

Figure 48: the triple combination confers proliferative disadvantage after a pulse with high-dose chemotherapy.

Competition assay performed as described in the left panel*; HG (1,8 g/L); GS (0,45 g/L); metformin (1 mM); high dose chemotherapy: doxo (2 µM), 4-hp-cpa (40 µM). Cell number is normalized to the starting point of the experiment. Bars plots with error bars represent mean values and standard deviation. Significances were calculated with one-way ANOVA. *p<0,05; **p<0,01; ***p<0,001; ****p<0,0001.*

6. PP2A is responsible for the attenuation of the DDR.

We assessed whether the effect of the triple combination was dependent on PP2A. PP2A is the major Ser/Thr phosphatase in eukaryotic cells and knock-out (KO) or knock-down (KD) of the catalytic C (PP2Ac) subunit is lethal. Therefore, to reduce *PPP2CA* (which is the gene encoding for PP2Acα, the most abundant C subunit) expression, we set up an inducible KD model based on the Tet-on system, that we could monitor and control over time. With this strategy, it was possible to reduce PP2Ac protein levels in MDA-MB-231 in a time-dependent manner (**Figure 49**) and carry out the viability experiments before the level of silencing was lethal, which happened after 8 days and a total of 3 inductions with doxycycline (**Figure 50 left panel**). We identified a time-window suitable for the treatment (day 2-6 from the first

doxycycline induction); indeed, at day 6 from the first induction, *PPP2CA* KD caused a 20-30% reduction in cell viability compared to scrambled-infected cells, which we have considered as acceptable for our experimental set-up (**Figure 50 right panel**).

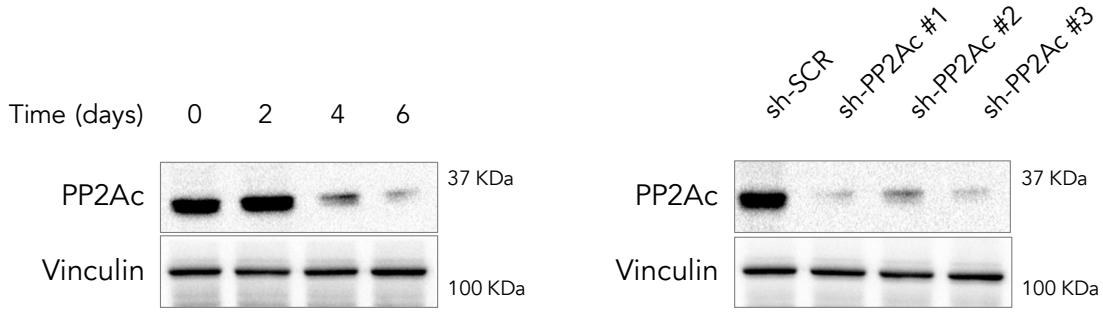

Figure 49: efficiency of the inducible KD of PPP2CA in MDA-MB-231 cells.

Left panel: western blot analysis showing PP2A protein level from day 0 to day 6. Day 8 was neglected because of excessive cell death. Vinculin was used as loading control. Right panel: western blot analysis performed at day 6 showing the efficiency of PPP2CA KD with 3 different shRNAs. Vinculin was used as loading control.

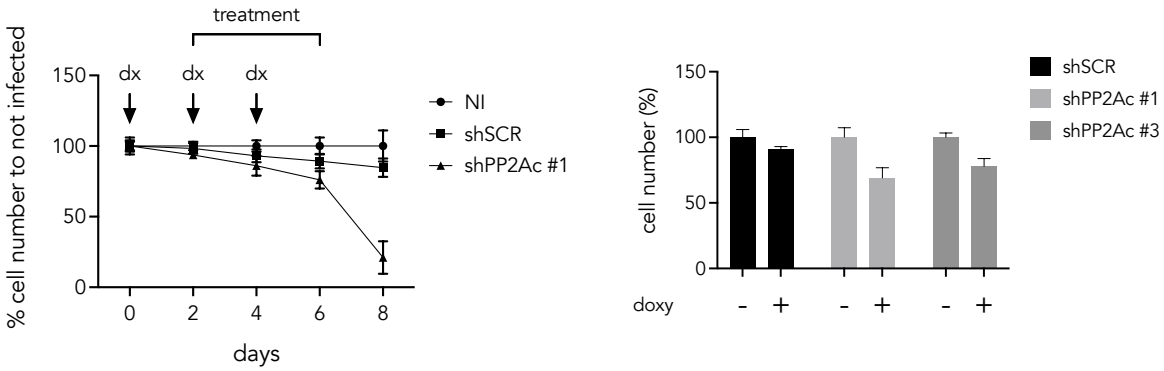

Figure 50: PP2Ac KD is lethal in MDA-MB-231 cells.

Left panel: experimental setup and growth curves of MDA-MB-231 not infected and infected with shSCR or shPP2Ac#1. Values are normalized against not infected samples. Doxycycline (2 µg/mL) inductions and time of treatment are listed. Right panel: viability of MDA-MB-231

cells infected with shSCR, shPP2Ac#1 and shPP2Ac#3, after 3 inductions of doxycycline (day 6). Each value is normalized against the non-induced sample.

The KD of *PPP2CA* reduced the cytotoxic effect of the triple combination both in terms of cell viability and cell death, which, following the 3 inductions of doxycycline, were no different from low-dose chemotherapy in glucose starvation, nor from the double combination (**Figure 51 – Figure 52**).

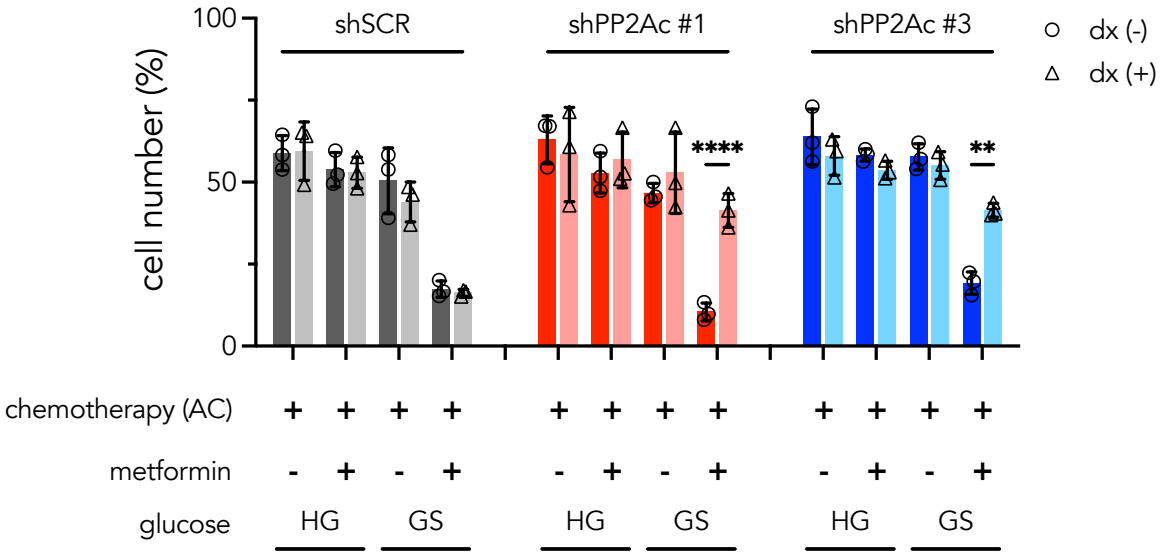

Figure 51: PPP2CA KD rescues the cytotoxic effect of the triple combination (I).

*Viability of MDA-MB-231 cells after 4 days of treatment (days 2-6) as follows: HG (1,8 g/L); GS (0,45 g/L); metformin (1 mM); low-dose chemotherapy (dox 0,1 µM + cp 2 µM). Different-colored bars indicate whether doxycycline was supplemented or not. Values are normalized against Ctrl_HG. N = 3 replicates. Significances were calculated with one-way ANOVA. *p<0,05; **p<0,01; ***p<0,001; ****p<0,0001.*

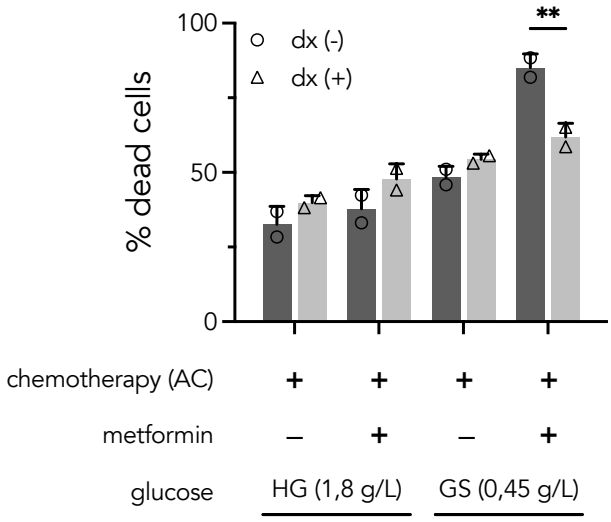

Figure 52: PP2Ac KD rescues the cytotoxic effect of the triple combination (II).

*Percentage of PI-positive MDA-MB-231 cells, infected with sh_PP2Ac #1 and induced with doxycycline, after 4 days of treatment (days 2-6) as follows HG (1,8 g/L); GS (0,45 g/L); metformin (1 mM); low-dose chemotherapy (dox 0,1 μM + cp 2 μM). Different-colored bars indicate whether doxycycline was supplemented or not. N = 2 replicates. Significances were calculated with one-way ANOVA. *p<0,05; **p<0,01; ***p<0,001; ****p<0,0001.*

Moreover, *PPP2CA* KD restored the phosphorylation of the DDR proteins even in presence of the triple combination, as assessed by western blot analysis at an early time point, which was 24 hours after the start of the treatments and 72 hours after the first doxycycline induction (**Figure 53**).

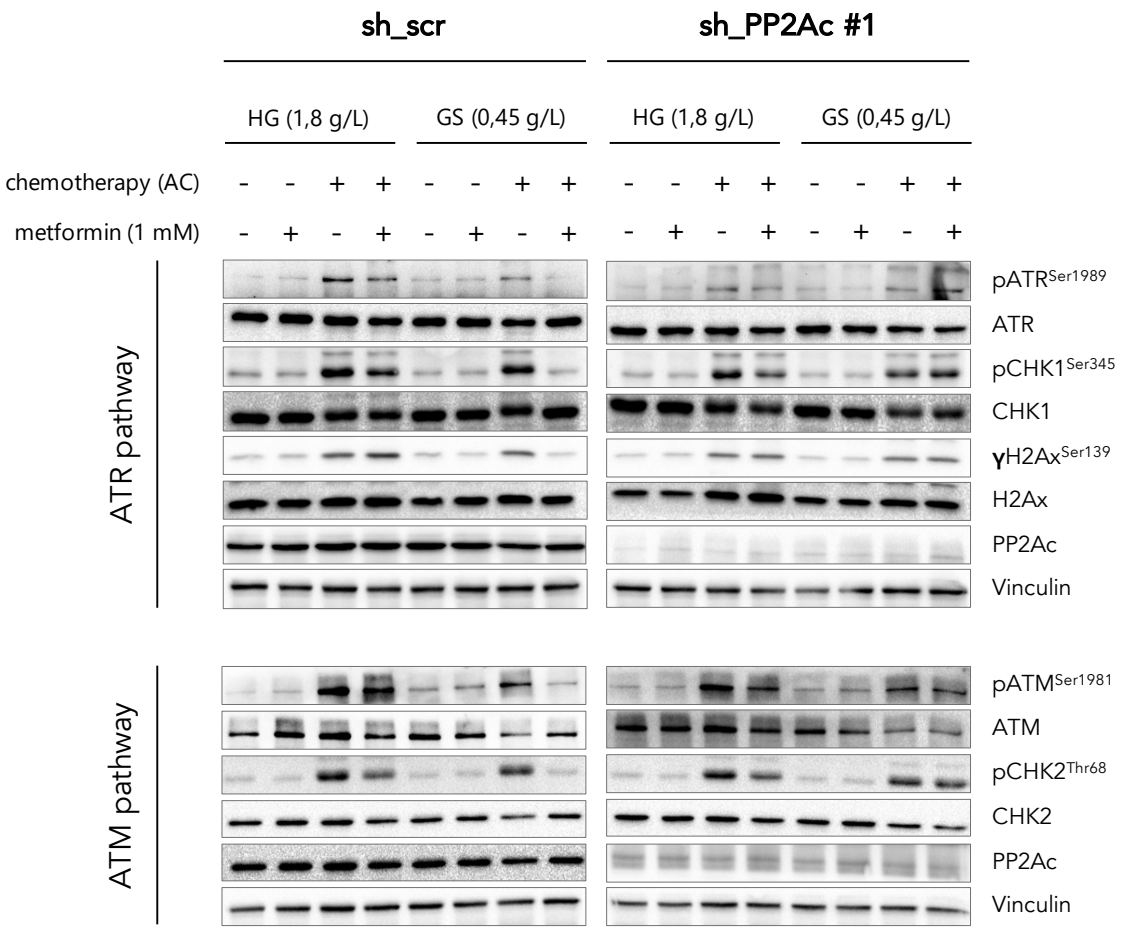

Figure 53: PPP2CA KD rescues the phosphorylation of the DDR checkpoints.

Western blot analysis of MDA-MB-231 cells, infected with sh_SCR or sh_PP2Ac #1 and induced with doxycycline, showing the phosphorylation and the total levels of the indicated proteins after 1 day of treatment as follows: HG (1,8 g/L); GS (0,45 g/L); metformin (1 mM); low-dose chemotherapy (dox 0,1 μM + cp 2 μM). Vinculin was used as loading control. N = 3 replicates.

Together with the increased activity measured with phosphatase assay (**Figure 21**), these results provided the second evidence about the involvement of PP2A in the synergism between chemotherapy, metformin and glucose starvation.

We pierced together these evidences and performed a time course experiment by measuring PP2A phosphatase activity at 4, 12 and 24 hours in MDA-MB-231 cells transiently transfected with the plasmid expressing flag tagged-PP2Ac. In particular,

we compared the double and the triple combination and observed a significant increase of PP2A activity over time in the latter. By bands quantification of CHK1 phosphorylation at the same time points (**Figure 45**) overlapped with PP2A phosphatase activity, we observed an inverse correlation between the phosphorylation of CHK1 and the increase of PP2A activity (**Figure 54**).

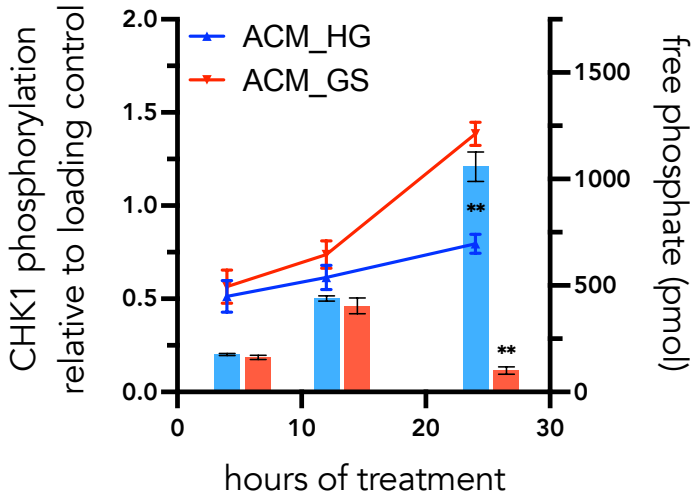

Figure 54: phosphorylation of CHK1 is inversely proportional to PP2A activation.

*Bands quantification of the western blot analysis described in **Figure 45** limited to the indicated samples (ACM_HG, or double combination, and ACM_GS, or triple combination) overlapped with PP2A phosphatase activity for the same samples. N = 3 replicates. Significances were calculated with one-way ANOVA. *p<0,05; **p<0,01; ***p<0,001; ****p<0,0001.*

7. The regulatory B56 family is involved in the synergism.

Since PP2A holoenzyme is "canonically" composed by the scaffold, the catalytic and one of many regulatory subunits, we inquired which specific regulatory B subunit/subunits was/were involved in the mechanism we described. We mainly focused on the two sub-families with tumor suppressor properties, namely the B55 (B or PR55) and B56 (B' or PR61) families (W. Chen et al., 2004; Fowle et al., 2019;

Westermarck & Neel, 2020). First of all, we measured by RT-qPCR the basal expression level of the different B55 and B56 subunits in the MDA-MB-231 cell line. We could not detect any expression of *PPP2R2B*, the gene encoding for the B55β subunit, thus ruling out its expression in MDA-MB-231 cells. The expression level of the B56 subunits was similar to that of *PPP2CA*, the gene encoding for PP2Ac, while the expression level of *PPP2R5B*, the gene encoding for B56β, was lower and similar to that of the B55 subunits (**Figure 55**).

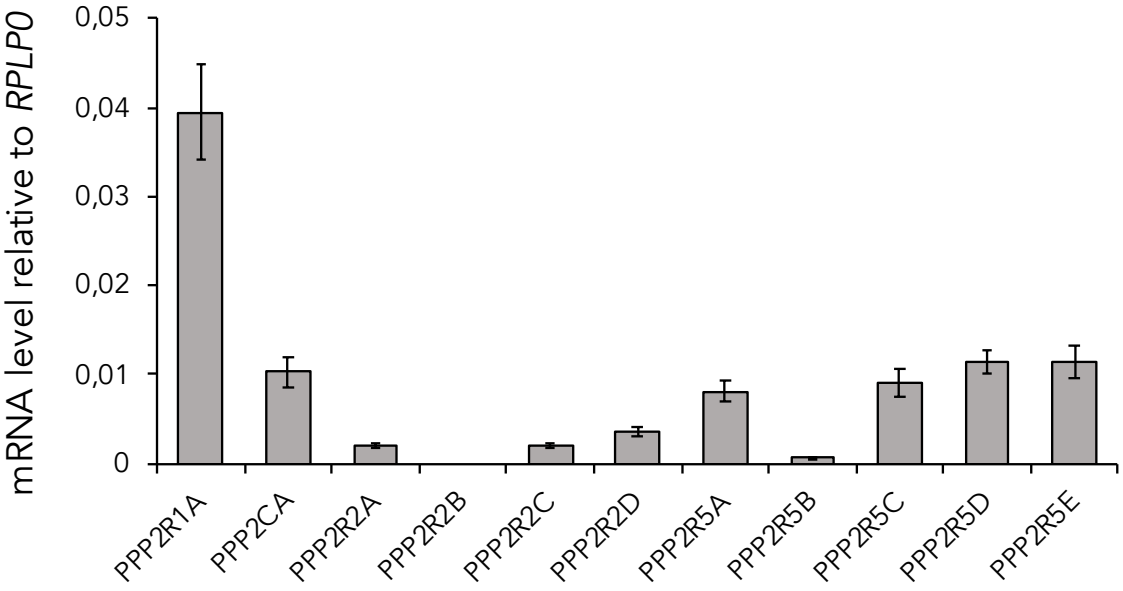

Figure 55: basal expression level of the B55 and B56 subunits in the MDA-MB-231 cell line.

Analysis of the mRNA levels of the B55 and B56 subunits in MDA-MB-231 cell line. Values are normalized against RPLP0. N = 3 replicates.

We also assessed the expression levels of the different B55 and B56 subunits upon one day of treatment with metformin (1 mM), glucose starvation, and the combination of the two, but we could not observe any significant difference, differently from what we

have previously observed in HeLa and HCT116 cell lines concerning the B56δ subunit (**Figure 56**).

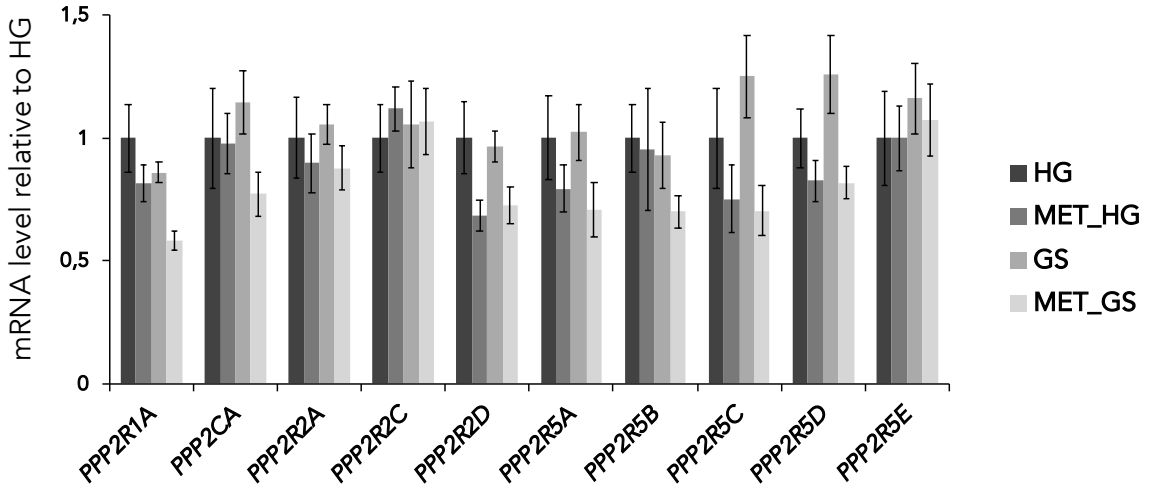

Figure 56: expression level of the B55 and B56 subunits in the MDA-MB-231 cell line upon metabolic stress.

Analysis of the mRNA levels of the B55 and B56 subunits in MDA-MB-231 cell cultured for 24 hours in HG (1,8 g/L) or GS (0,45 g/L) ± metformin 1 mM. Values are normalized against RPLP0. N = 3 replicates.

For the following experiments, we focused on the B56 family. We efficiently reduced the expression of all the B56 subunits through shRNA-mediated KD in MDA-MB-231 cells (**Figure 57**).

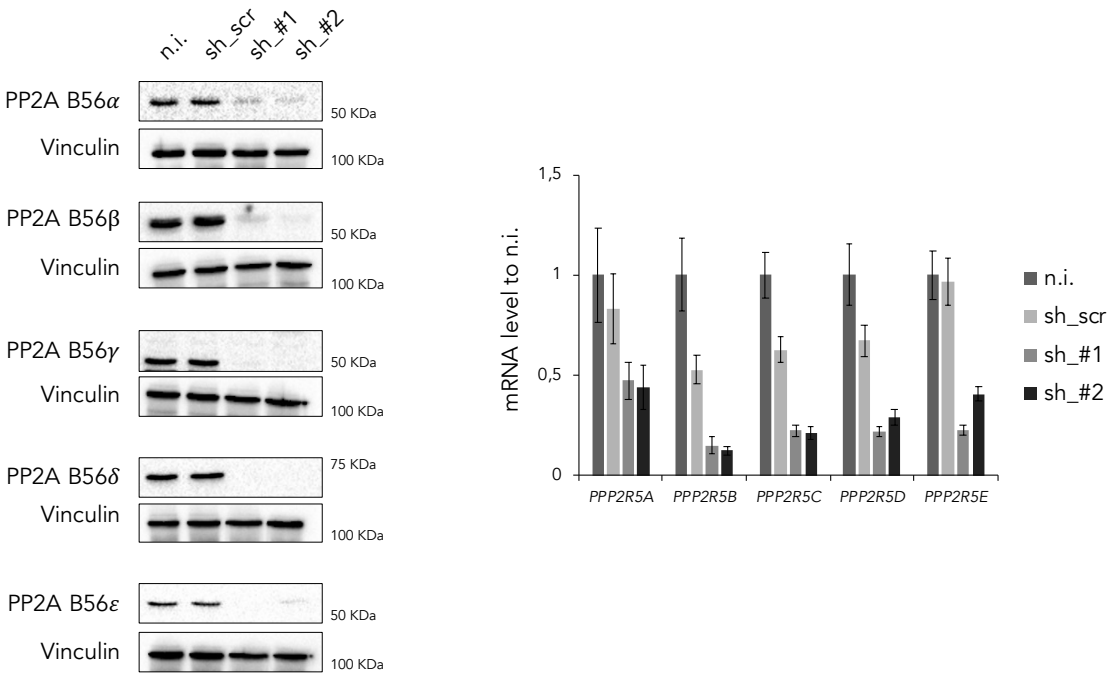

Figure 57: shRNA-mediated KD of the B56 subunits in MDA-MB-231 cells.

Western blot (left panel) and mRNA (right panel) analysis showing the efficiency of the depletion of the B56 subunits in MDA-MB-231 cells infected with two different shRNAs against each of the B56 subunits and one control shRNA. Protein levels are normalized against Vinculin. mRNA levels are normalized against RPLP0 and represented as fraction of the not infected sample (n.i.). N = 3 replicates.

Cells knocked-down for the single subunits did not present any significant growth defects, supporting a redundant function among subunits of the same family (data not shown). KD of B56 subunits (except for the B56β) reduced the cytotoxicity of the triple combination, both in terms of cells number and percentage of dead cells (**Figure 58**). As previously shown, B56β is the only B56 subunits to be expressed at very low levels in MDA-MB-231 cells; this could explain the lack of rescue effect. The rescue effect was lower compared to *PPP2CA* KD, which is in line with the hypothesized redundancy of B56 subunits.

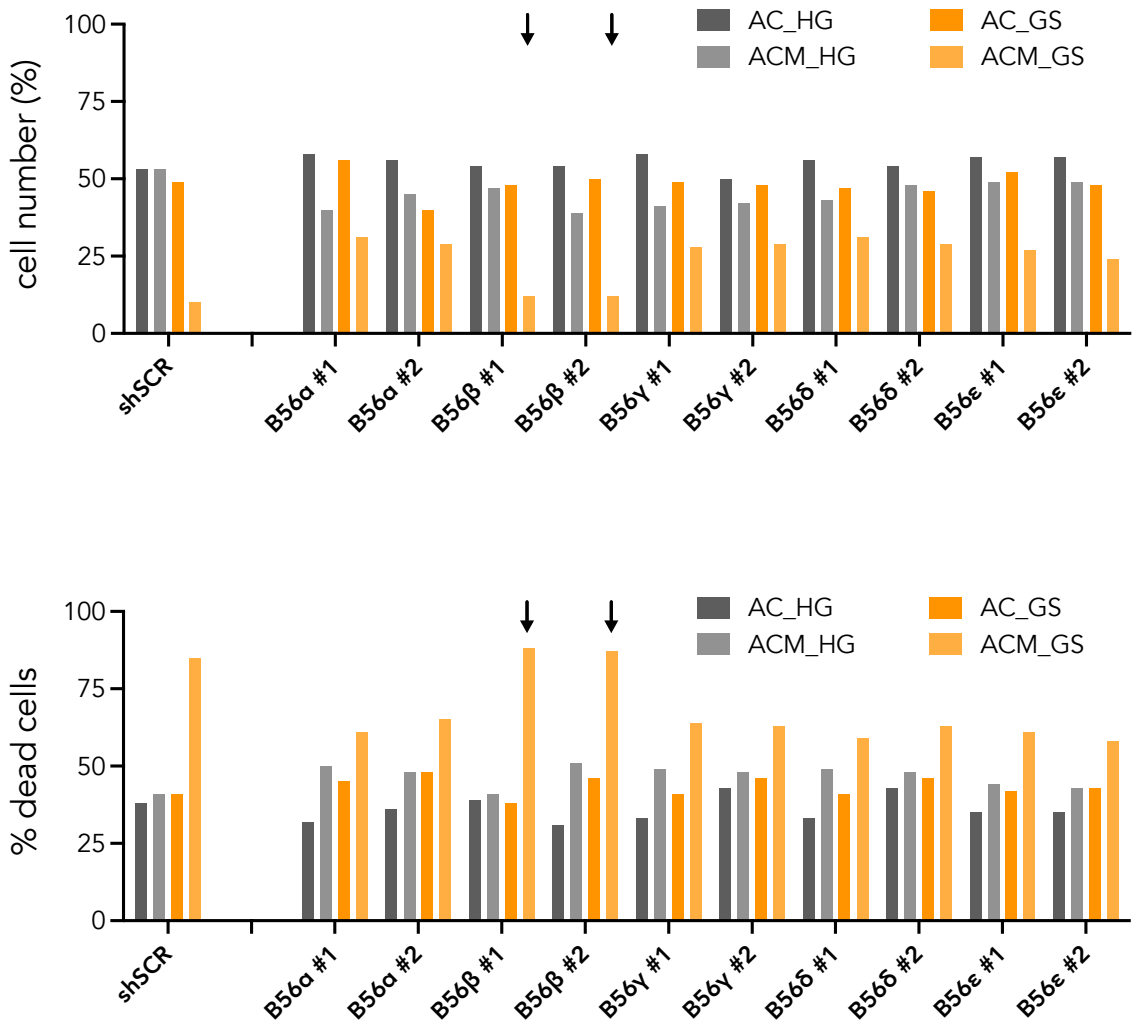

Figure 58: the KD of the B56 subunits partially rescues the cytotoxicity of the triple combination.

Viability (top panel) and percentage of PI-positive (bottom panel) MDA-MB-231 cells KD for the listed B56 subunits after 4 days of treatment as follows: HG (1,8 g/L); GS (0,45 g/L); metformin (1 mM); low-dose chemotherapy (dox 0,1 μM + cp 2 μM). In top panel each value is normalized against its control sample in HG.

We performed KD experiments of the B55 subunits as well (**Figure 59**), but we observed no rescue effect upon the triple combination (**Figure 60**).

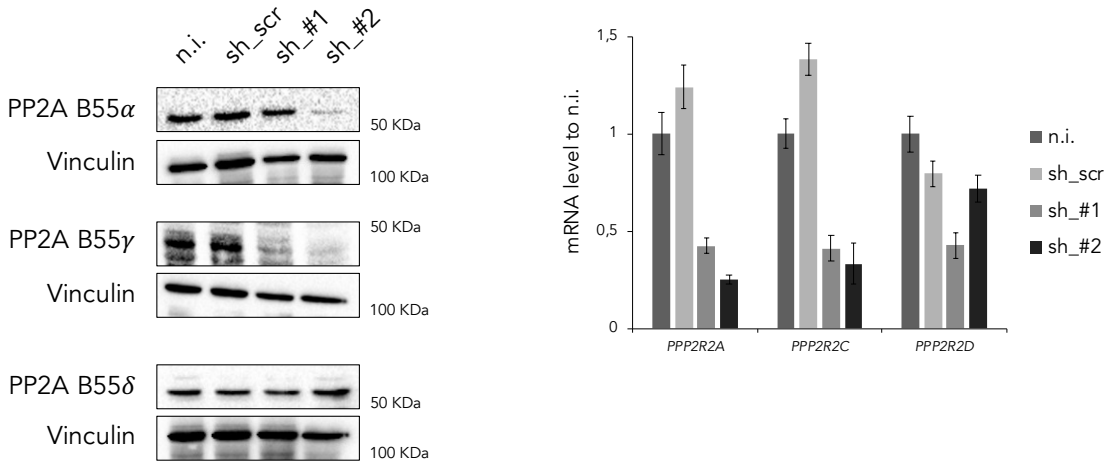

Figure 59: shRNA-mediated KD of the B55 subunits in MDA-MB-231.

Western blot (left panel) and mRNA (right panel) analysis showing the efficiency of the depletion of the B55 subunits in MDA-MB-231 cells infected with two different shRNAs against each of the B55 subunits and one control shRNA. Protein levels are normalized against Vinculin. mRNA levels are normalized against RPLP0 and represented as fraction of the not infected sample (n.i.). N = 3 replicates.

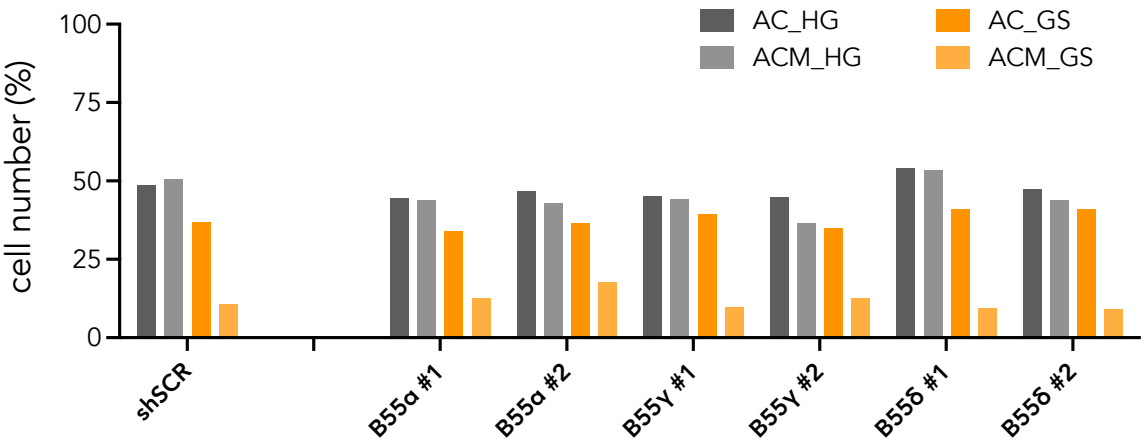

Figure 60: KD of the B55 subunits does not rescue the cytotoxicity of the triple combination.

Viability of MDA-MB-231 cells KD for the listed B55 subunits after 4 days of treatment as follows: HG (1,8 g/L); GS (0,45 g/L); metformin (1 mM); low-dose chemotherapy (dox 0,1 μM + cp 2 μM). Each value is normalized against its control sample in HG.

Our results suggested an involvement of all the B56 subunits which are expressed in the MDA-MB-231 cell line. Among different B56 subunits, B56γ and B56δ have been previously described as nuclear (Margolis et al., 2006; McCright et al., 1996) as they both contain a nuclear localization signal (KRTVETEAVQMLKDIKK). Also, B56α was described as CHK2-interacting protein (Freeman et al., 2010). B56ε subunit dephosphorylated γH2A and its translocation into the nucleus was described after camptothecin treatment (X. Li et al., 2015). It remains to be clarified whether all the B56 subunits contribute to the attenuation of the DDR, or if their loss leads to a destabilization of PP2A holoenzyme with consequent impairment of PP2A functions, in a similar way, albeit lower, to the KD of *PPP2CA*.

8. Investigation of PP2A activating pathways.

We investigated which metabolic pathway/pathways lead to PP2A over-activation upon the combination of metformin and glucose starvation. As previously shown, we could not confirm CIP2A down-regulation following metformin treatment, either with high or low-dose metformin (10 and 1 mM, respectively), probably due to high CIP2A content in several TNBC cell lines (**Figure 19 - 20** and **Figure 61**). As previously described for high-dose metformin, the combination of low-dose metformin with glucose starvation did not impact the phosphorylation of GSK3β, confirming that, at least in the MDA-MB-231 cell line, the pathway we previously described is not induced by the metabolic stress (**Figure 61**).

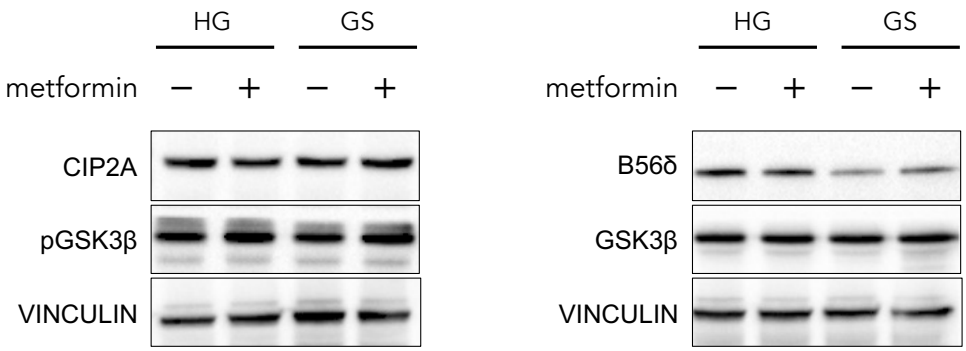

Figure 61: low-dose metformin and glucose starvation do not affect CIP2A and B56δ.

Western blot analysis showing the phosphorylation and the total levels of the indicated proteins after 1 day of treatment as follows: HG (1,8 g/L); GS (0,45 g/L) ± metformin (1 mM). Vinculin was used as loading control. N = 3 replicates.

Recently, CIP2A was described as a "hijacker" of the B56 subunits, preventing the holoenzyme assembly (J. Wang et al., 2017). Given the contribution of all the B56 subunits (those expressed in MDA-MB-231 cell line) in the synergistic effect of the triple combination, we hypothesized that the enormous amount of CIP2A may have masked the protein decrease following dissociation from PP2A holoenzyme upon metabolic stress. To address this question, we took advantage of the MDA-MB-231 cell line stably expressing CIP2A^{K21A} mutant (kindly provided by Jukka Westermarck, Turku, Finland); single point mutation in the *KIAA1524* gene (which encodes for CIP2A) was sufficient to strongly reduce the interaction between CIP2A and the B56 subunits. CIP2A^{K21A} clones proliferated slightly slower compared to the negative control (**Figure 62 left panel**). Furthermore, CIP2A^{K21A} clones were extremely sensitive to low-dose chemotherapy compared to the negative control, similarly to the effect of the triple combination; the negative control was affected by the triple combination as previously observed with the MDA-MB-231 WT (**Figure 62 right panel**).

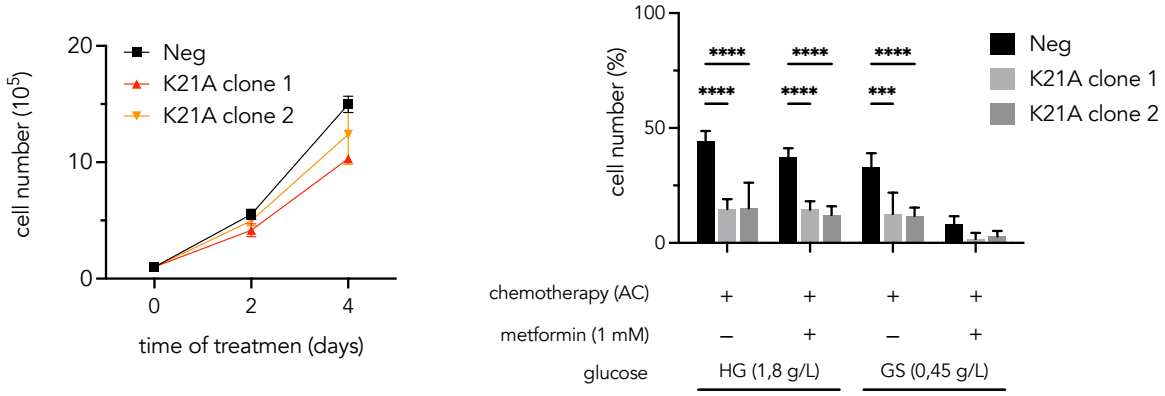

Figure 62: CIP2A mutants are hypersensitive to chemotherapy.

*Left panel: growth curves of MDA-MB-231 cells expressing the negative control (neg) or CIP2A^{K21A} mutants cultured for 4 days. Medium was replaced after two days. Right panel: viability of MDA-MB-231 cells expressing different CIP2A variants cultured for 4 days as follows: HG (1,8 g/L); GS (0,45 g/L); metformin (1 mM); low-dose chemotherapy (dox 0,1 μM + cp 2 μM). Values are normalized against Ctrl_HG. N = 3 replicates. Significances were calculated with one-way ANOVA. *p<0,05; **p<0,01; ***p<0,001; ****p<0,0001.*

The results so far are in line with the recently described function of CIP2A as a "hijacker" of the B56 subunits; at the same time, since CIP2A is highly expressed in MDA-MB-231 cell line, they do not exclude a more general role of CIP2A as a driver oncogene of TNBCs and supporter of tumor growth and survival under replicative stressors (as chemotherapy).

We investigated whether additional mechanisms were involved in PP2A activation in TNBC cells. mTORC1, which is a master regulator of cell metabolism and a well-known PP2A inhibitor, was a good candidate (Allen-Petersen et al., 2019; Ferrari et al., 2017; Laplante & Sabatini, 2012; Wong et al., 2015). The combination of low-dose metformin and glucose starvation reduced the phosphorylation of RPS6 and 4EBP1, which are downstream of mTORC1 and a *bona fide* indication of mTORC1

activity (**Figure 63**). Although this suggested a reduced mTORC1 signaling, we could not exclude that PP2A itself dephosphorylated pRPS6 and p4EBP1.

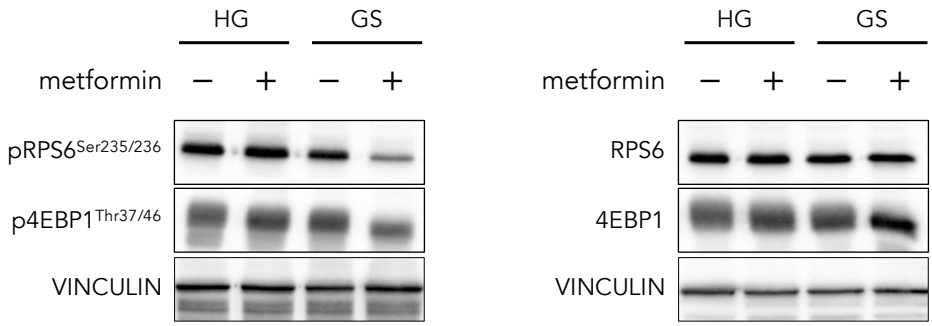

Figure 63: metformin and glucose starvation reduce mTORC1 activity.

Western blot analysis showing the phosphorylation and the total levels of the indicated proteins after 1 day of treatment as follows: HG (1,8 g/L); GS (0,45 g/L) ± metformin (1 mM). Vinculin was used as loading control. N = 3 replicates.

In line with these results, the mTORC1 inhibitor rapamycin synergized with chemotherapy similarly to the combination with metformin and glucose starvation, in accordance to what has been previously described in other work (J. Li et al., 2019; Mills et al., 2008; J. Zhang et al., 2016) (**Figure 64**).

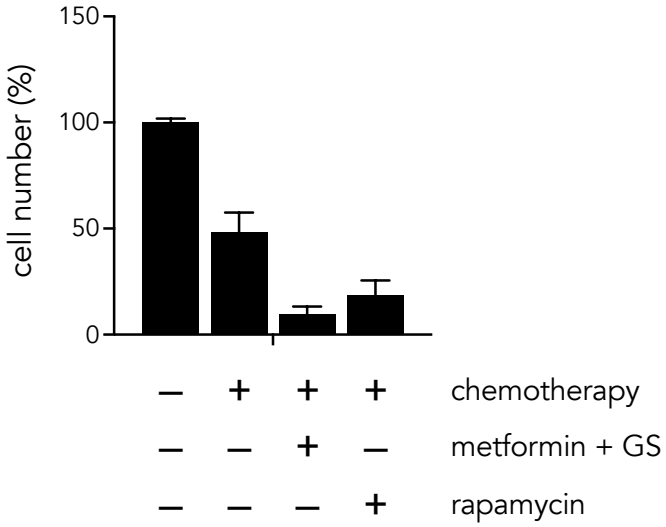

Figure 64: the mTORC1 inhibitor rapamycin synergizes with chemotherapy similarly to metformin and glucose starvation.

Viability of the MDA-MB-231 cells treated for 4 days as follows: HG (1,8 g/L); GS (0,45 g/L); metformin (1 mM); low-dose chemotherapy (dox 0,1 μM + cp 2 μM); rapamycin (1 μM). Values are relative to control samples (HG). N = 3 replicates.

mTORC1 and CIP2A are part of a positive circuit in which mTORC1 inhibits the autophagic degradation of CIP2A, while CIP2A maintains mTORC1 in a dephosphorylated, namely active, state through PP2A inhibition (Puustinen et al., 2014; Puustinen & Jäättelä, 2014). We hypothesized that both pathways may be involved in the activation of PP2A following metabolic stress.

9. Metformin and glucose starvation favor the accumulation of PP2A core enzyme on the chromatin.

Finally, we further investigate the molecular mechanism by which the metabolic stress attenuated the DDR through PP2A. First, we performed subcellular fractionation to investigate whether PP2A localization changes following different stimuli: cells were

harvested 24 hours after the beginning of the treatment (which corresponds the lowest peak of DDR checkpoint phosphorylation) and subjected to 3 subsequent fractionations to separate cytosol, nucleosol and chromatin fractions (for details refer to the appropriate section in Materials and Methods). We did not notice any considerable change in either the cytosolic or the nucleosolic distribution of PP2Aa (scaffold A subunit) and PP2Ac (catalytic C subunit) (**Figure 65 a, b**). As concerns the chromatin fraction, we observed a massive recruitment of both PP2Aa and PP2Ac on the chromatin fraction upon metabolic stress (**Figure 65 c**); for both the subunits, chromatin recruitment depended exclusively on the combination of metformin and glucose starvation, regardless of low-dose chemotherapy. Of note, glucose starvation itself increased the loading of PP2Ac on the chromatin, but not of PP2Aa. This was in line with the proposed role of PP2A in the attenuation of the DDR, which is a nuclear process, upon metabolic stress.

a

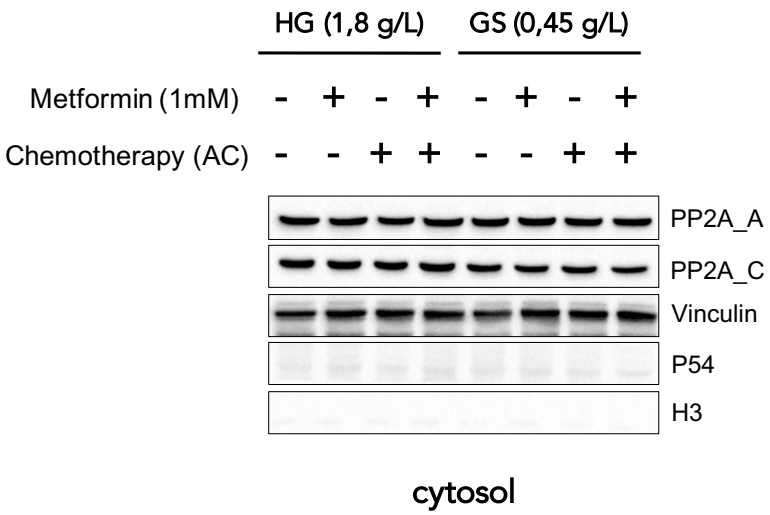

cytosol

b

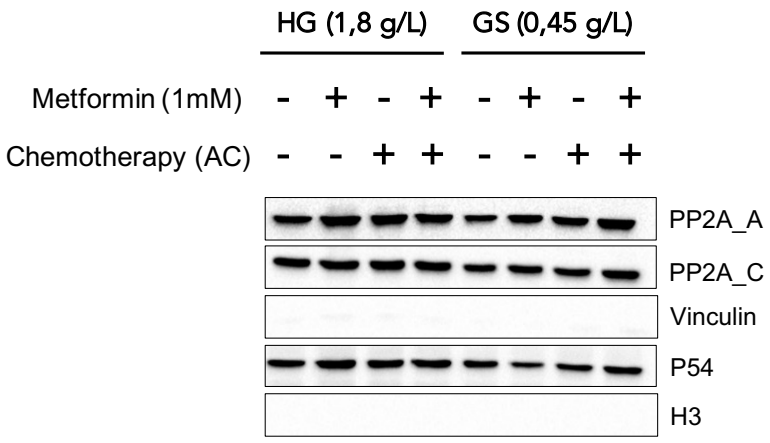

nucleosol

c

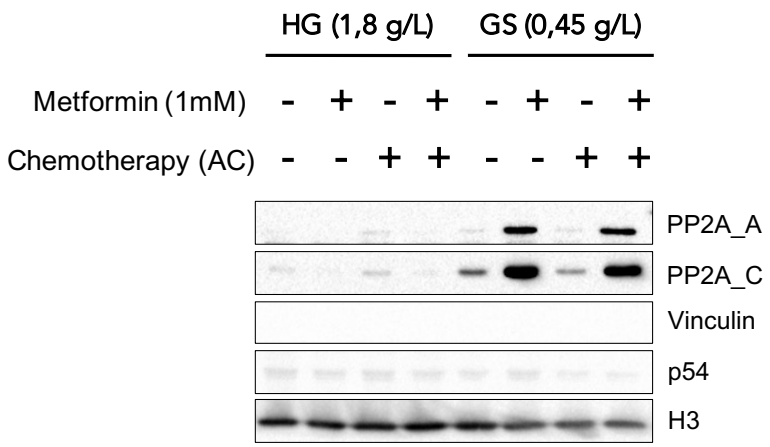

chromatin fraction

Figure 65: metformin and glucose starvation favor the accumulation of PP2A core enzyme on the chromatin (I).

*Western blot showing subcellular fractionation of MDA-MB-231 cells after 1 day of treatment as follows: HG (1,8 g/L); GS (0,45 g/L); metformin (1 mM); low-dose chemotherapy (dox 0,1 μM + cp 2 μM). Vinculin was used as loading control for the cytosol fraction (**a**); p54 was used as a loading control for the nucleosol fraction (**b**); H3 was used as a loading control for the chromatin fraction (**c**). Lack of visible loading control bands in specific cell fractions indicates the effectiveness of fractionation protocol. N = 3 replicates.*

We wanted to rule out that what we called the "chromatin fraction" excluded the nuclear lamina; through an already validated protocol (Myant et al., 2015) we efficiently separated the real chromatin fraction (marked by the presence of H3) and the nuclear lamina (marked by the presence of Lamin B). We confirmed what we observed with our protocol by adding an additional piece of information: under high glucose condition (first two samples on the left) PP2A remains mainly on the nuclear lamina, whereas under metabolic stress (combination of metformin and glucose starvation, sixth and eighth samples) there is a real translocation and PP2A core enzyme accumulates on chromatin. This is true for both scaffold and catalytic subunits (**Figure 66**).

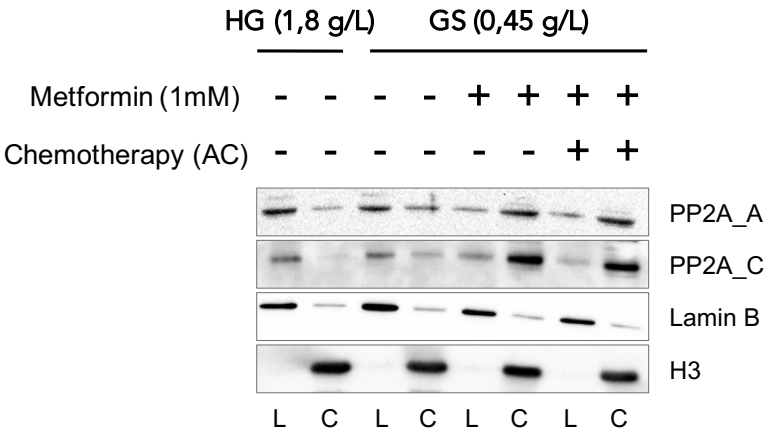

Figure 66: metformin and glucose starvation favor the accumulation of PP2A core enzyme on the chromatin (II).

Western blot showing subcellular fractionation of MDA-MB-231 cells after 1 day of treatment as follows: HG (1,8 g/L); GS (0,45 g/L); metformin (1 mM); low-dose chemotherapy (dox 0,1 μM + cp 2 μM). Lamin B1 was used as a loading control for the nuclear Lamin fraction (L); H3 was used as a loading control for the chromatin fraction (C). N = 2 replicates.

Upon metabolic stress, we observed an increase of PP2Ac protein level also in whole-cell lysate (**Figure 67**); given the huge cellular amount of PP2Ac protein, this was more readily detectable by loading a very low amount of protein (10 μg, which is one-third of what we originally used), so that the signal was not immediately saturated.

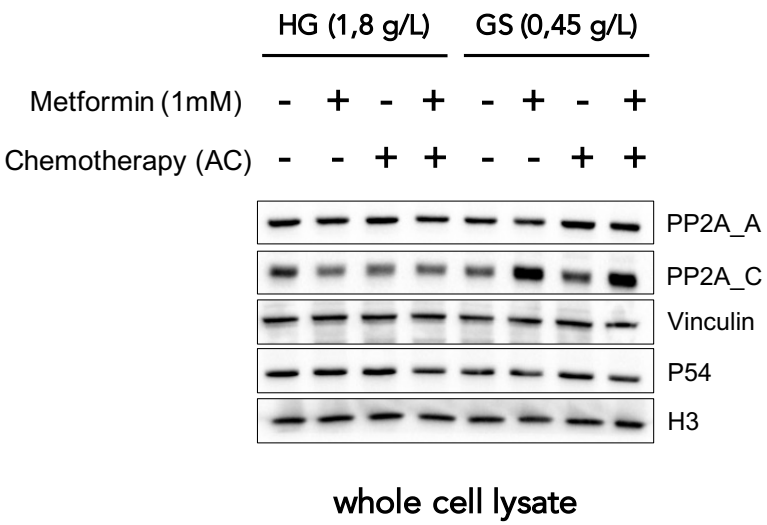

Figure 67: metformin and glucose starvation increase PP2Ac total amount.

Western blot showing whole cell lysate from MDA-MB-231 cells after 1 day of treatment as follows: HG (1,8 g/L); GS (0,45 g/L); metformin (1 mM); low-dose chemotherapy (dox 0,1 μM + cp 2 μM). Vinculin, p54 and H3 were used as loading control. N = 3 replicates.

We checked whether the higher protein amount of PP2Ac was caused by enhanced gene transcription but we could not detect any significant change in the mRNA expression of both *PPP2R1A* (which encodes for PP2Aa) and *PPP2CA* (which encodes for PP2Ac) following 24 hours of metabolic stress (**Figure 68**). Thus, we hypothesized that this phenomenon could be explained by reduced protein turn-over in the nucleus compared to the cytosol. Moreover, an increase in PP2Ac protein amount could also explain the enhanced phosphatase activity.

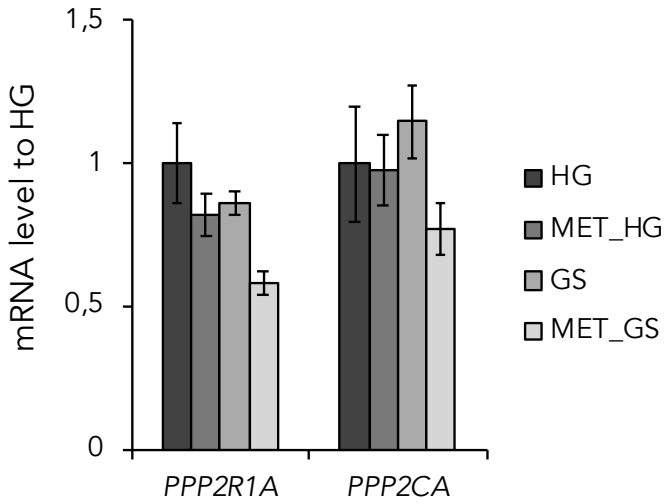

Figure 68: metformin and glucose starvation do not influence the expression of PPP2R1A and PPP2CA.

Analysis of PPP2R1A and PPP2CA mRNA levels in MDA-MB-231 cells cultured for 24 hours in HG (1,8 g/L) or GS (0,45 g/L) ± metformin 1 mM. Values are normalized against RPLP0 and referred as fraction of control (HG). N = 3 replicates.

This evidence opens another area of investigation for future studies. Since the DDR is a nuclear process, and the apical kinases ATM and ATR bind the DNA, the accumulation of PP2A on chromatin following metabolic stress strengthens the evidence that the attenuation of DDR is a PP2A-dependent process which is regulated directly by the enzyme. Further experiments are needed to understand whether or not the accumulation of PP2A on chromatin following metabolic stress is site-specific (ChIP-sequencing), and whether the localization changes when metabolic stress is combined with chemotherapy.

Discussion

PP2A is a critical tumor suppressor which counteracts the major oncogenic pathways (MEK, MYC and AKT) (Farrington et al., 2020; Kuo et al., 2008; Ugi et al., 2004), and acts as a brake on uncontrolled proliferative signals (Mumby, 2007) with its suppression accelerating tumor transformation (Junttila et al., 2007; Kauko et al., 2018; Neviani et al., 2005). Impairment of PP2A by endogenous inhibitors, which are often over-expressed in many cancer types, is far more common than genetic alterations, which have been found only in some types of cancer (Kauko & Westermarck, 2018). This has long undermined the identification of PP2A as tumor suppressor and the field of PP2A (and phosphatase in general) has not significantly benefited from the big *omics* era. At the moment, PP2A is experiencing renewed interest and many efforts are focused on awakening its anti-tumor potential and novel, orally-available, small molecules activator of PP2A (SMAPs) demonstrated robust anti-tumor activity (Chien et al., 2015; Kauko et al., 2018; Merisaari et al., 2020; C. M. O'Connor et al., 2018; Sachlos et al., 2012; Sangodkar et al., 2016; Vervoort et al., 2021). Other strategies have proven effective in bypassing endogenous inhibitors such as SET or CIP2A (Elgendy et al., 2019; Ferrari et al., 2017; Hu et al., 2022).

In the present work, we propose a model for enhancing PP2A activity through a metabolic approach consisting of the anti-diabetic drug metformin combined with glucose starvation. *In vitro*, the metabolic combination increased PP2A phosphatase activity without inducing profuse cell death; this allowed to investigate any synergistic effect with other drugs (in our case, DNA-damaging chemotherapy) without the latter being biased from the metabolic catastrophe that may arise from the simultaneous impairment of OXPHOS (with metformin) and glycolysis (with glucose starvation).

For decades, metformin has been the most widely used drug for type 2 diabetes, and it is currently undergoing intensive repositioning efforts for its putative anti-cancer properties on the basis of epidemiological studies and subsequent observations (Daugan et al., 2016). Here we have shown that metformin *per se* had poor beneficial effect, both in TNBC cell lines and in non-diabetic mouse models of TNBC. We observed the same even in combination with low-dose chemotherapy. This is in line with the results of a recent clinical trial: in breast-cancer patients (ER/PgR positive/negative) without diabetes, the addition of metformin to standard therapy did not significantly improve disease-free survival (Goodwin et al., 2022). Compared to what we have previously observed with other cell lines representative of other tumor types, in TNBC metformin had poor anti-cancer effect even if administered in condition of hypoglycemia, both in *vitro* and in *vivo*. This can be explained by the intrinsic resistance of several TNBC cell lines to the combination, possibly due to high protein levels of CIP2A (C.-Y. Liu et al., 2019; H. Liu et al., 2017; Tseng et al., 2012), which we had identified as the target of metformin.

We achieved the condition of hypoglycemia in *vitro* through a reduction of glucose in the culture medium (glucose starvation, which is 75% reduction compared to high glucose), and in *vivo* with intermittent fasting cycles of one-day duration (which means complete removal of food and free access to water). As for blood glucose, also the weight of the animals dropped during the fasting and rose again during the feeding days, and we observed no decrease over the long period (up to 4 weeks), supporting the feasibility and tolerability of an intermittent fasting regimen in CD1-nude mice. Intermittent fasting *per se* partially reduced tumor growth, similarly to what has been described by other groups (Caffa et al., 2020; di Biase et al., 2016; C. Lee et al., 2012). In *vitro*, glucose starvation did not exhibit the same anti-tumor effect. This discrepancy

may be due to the fact that, in *vivo*, intermittent fasting cycles (elsewhere referred as only-water diet) lower not only glucose but many other metabolites, some of which are fundamental for tumor maintenance and progression: these have been extensively described in other works and include C-peptide, insulin, insulin-like growth factor 1 (IGF1), insulin-like growth factor binding protein 3 (IGFBP3, which prevents circulating IGF1 from degradation) and leptin, while glucagon, ketone bodies and adiponectin increased upon fasting (Caffa et al., 2020; Nencioni et al., 2018).

We have demonstrated that the combination of metformin and glucose starvation (which we named metabolic stress) rapidly enhanced PP2A phosphatase activity in *vitro,* even with metformin doses as low as 0,1 mM. Mechanistically, the metabolic stress led to the accumulation of PP2A core enzyme (scaffold A and catalytic C subunits) on the chromatin. At the nuclear level, protein turnover may be slower, which could explain the net increase in PP2Ac protein levels and, consequently, the enhanced phosphatase activity. The accumulation of PP2A on the chromatin as a result of metabolic stress alone (i.e., without chemotherapy) had no significant consequences on proliferation, at least in our working model; here we have not investigated, and therefore do not rule out, that it may have an important impact on transcription, since chromatin-associated PP2A could influence RNA polymerase activity (K.-L. Huang et al., 2020; Vervoort et al., 2021; H. Zheng et al., 2020).

Since most TNBC cell lines were resistant to the metabolic stress alone, we considered more clinically-relevant experimental settings. The BREAKFAST clinical trial, based on our previous findings, provided us with an actual clinical protocol for TNBC patients that we translated first in *vitro* in cell lines and patient-derived cells, then in *vivo* in animal models. In order to provide pre-clinical and mechanistic evidences to support the trial, we combined the metabolic stress with DNA-damaging chemotherapy (a

condition we named triple combination), which corresponds to the first part of the BREAKFAST clinical trial. The consequences of the triple combination on tumor cells survival and cancer progression were dramatic and exceeded the effect of the single treatments; in particular, the triple combination was cytotoxic (while the single therapies were at most cytostatic), impaired colony formation and, lastly, induced tumor regression, regardless of how we obtained the hypoglycemia, whether it was glucose starvation in *vitro* or intermittent fasting in *vivo*. Thus, we concluded that the synergism was strictly dependent on metformin and hypoglycemia, and that other nutrients (which decrease in *vivo* as consequence of fasting) were less or not involved at all. The use of Plasmax medium, which better recapitulated nutrients in the tumor microenvironment (Vande Voorde et al., 2019), confirmed our conclusion: even with a culture medium richer in micronutrients, the combined effect still depended on metformin and glucose starvation. The triple combination was cytotoxic in all the TNBC cell lines we used, with some cell lines being more sensitive than others and with none being resistant. Noteworthy, the most sensitive cell lines were characterized by mutations in the DDR and DNA-repair genes (Lehmann et al., 2011; Yin et al., 2020). As already mentioned, we significantly lowered the dosage of chemotherapy compared to the standard; combined with the metabolic stress, low-dose chemotherapy maintained the clinical benefit.

We have shown that the synergistic effect of the triple combination was due to the attenuation of the DDR triggered by chemotherapy. The DDR detects the DNA-damage and arrests the cell cycle while allowing for DNA repair, and it is mainly a cascade of phosphorylation events by protein kinases (Harrison & Haber, 2006; J. H. Hoeijmakers, 2001; Huen & Chen, 2008; S. P. Jackson & Bartek, 2009; K. K. Khanna & Jackson, 2001; Matsuoka et al., 2007; Rouse & Jackson, 2002). PP2A, as other

phosphatase, antagonizes the DDR and maintains a proper signaling cascade in the absence of a DNA damage, or after it has been resolved (Freeman et al., 2010; Freeman & Monteiro, 2010; C. Y. Guo et al., 2002; Petersen et al., 2006; Ramos et al., 2019; Shimada & Nakanishi, 2013). Here we have shown that the DDR was efficiently primed by the DDR machinery after chemotherapy administration, and immediately switched-off by PP2A as a result of the metabolic stress. This had three early consequences: i) impaired recognition of the DNA-damage, as evidenced by the fact that the DNA-binding kinases ATM and ATR, their downstream effectors CHK2 and CHK1, and H2Ax, around the damage site, were all de-phosphorylated; ii) lack of cell cycle arrest, as evidenced by cell-cycle analysis and confirmed by CDC25A protein which did not decrease downstream of CHK1; iii) impaired DNA repair resulting in increased genomic fragmentation, as evidenced by comet assay.

Inhibiting the DDR is not a novel therapeutic approach; the approval of the PARP inhibitor Olaparib for BRCA-mutated advanced ovarian cancer is probably the best example translated into the clinic (Al-Ahmadie et al., 2014; Ashworth, 2008; Bartkova et al., 2005; M. J. O'Connor, 2015; Pilié et al., 2019; Robson, Goessl, et al., 2017; Robson, Im, et al., 2017; Tutt et al., 2010). Here we describe a metabolic approach to turn off the DDR, based on the use of metformin and lowering of (blood) glucose. Our strategy has many advantages: i) it proved to be safe and tolerable in animal models over the long period; ii) it attenuated the DDR at multiple levels (differently from yeast, in our model both the ATM and the ATR pathway were involved); iii) it allowed to lower the dosage of chemotherapy. From the perspective of clinical translation, what has been a technical requirement for us turns out to be a crucial point for patients, as lowering chemotherapy doses by combining them with drugs with very few side effects (as metformin) and diets can provide enormous benefit (J. Chang, 2000). This

is especially true for doxorubicin; in a previous work, fasting was shown to protect mice from doxorubicin-induced cardiomyopathy through expression of EGR1 (downstream of AMPK) and enhancement of autophagy (which removes malfunctioning mitochondria and toxic aggregates) (di Biase et al., 2017). Last but not least, our metabolic approach could overcome the problems associated SMAPs. Indeed, certain compounds derive from antipsychotic drugs such as phenothiazines and may maintain their effect on the central nervous system (Sachlos et al., 2012; Tsuji et al., 2021), while other PP2A activators are being criticized for their off-target effects on tubulin polymerization (Morita et al., 2022).

We also evaluated the effects of the triple combination on "healthy" cells in *vitro*; to this purpose, we took advantage of the MCF10A cell line, which are spontaneously immortalized normal breast cells (Qu et al., 2015). The triple combination was also effective on MCF10A cells, albeit to a lesser extent than on cancer cell lines, probably because they are more proficient in DDR and DNA-repair pathways. DDR checkpoints were also dephosphorylated, similarly to cancer cells (data not shown). Nevertheless, in *vivo*, the triple combination affected only the tumors while preserving healthy tissues, as reflected by the small toxicity (evaluated as weight loss over the long period). Several mechanisms may preserve the healthy and not the tumor cells, including lower ROS production, better antioxidant defenses, and, a more efficient DDR and DNA-repair machinery which is not compromised by mutations.

Worth mentioning, the present work mainly focuses on DNA-damaging chemotherapy as harmful stimulus which activates the DDR, in accordance to the first part of the BREAKFAST clinical trial. Since PP2A is involved in countless cellular processes, including microtubules organization, in future works it will be interesting to evaluate the impact of PP2A over-activation on other chemotherapeutic agents that do not

interfere with the DNA, such as taxanes, which are also first-line therapy for TNBC patients (Boudreau et al., 2019; Jang et al., 2021; Keshri et al., 2020; Khondker et al., 2020; Y. Liu et al., 2017; Varadkar et al., 2017). Other drugs which modulate the DDR machinery, could also be affected by PP2A. For example, a PP2A-B56-BRCA2 complex has been shown to be necessary for DNA repair by homologous recombination. In this context, the inhibition, not the activation, of PP2A impaired homologous recombination and synergized with PARP inhibitors (Ambjørn et al., 2021; Kalev et al., 2012). Making reference to the immunotherapy, the inhibition of PP2A, again, enhanced the cytotoxic functions of tumor-infiltrating lymphocytes (P. Zhou et al., 2014) and increased the efficacy of immunotherapy by PD-1 blockade (Ho, Wang, et al., 2018). This may be explained by the fact that PP2A is a negative regulator of effector T cells, and a positive regulator of regulatory T cells (Apostolidis et al., 2016; Delgoffe, 2016; Eil et al., 2016; Taffs et al., 1991).

We can confidently state that what we described was strictly dependent on PP2A based on the following evidences: i) the knock-down of the catalytic subunit recovered the phosphorylation of the DDR checkpoints and reduced the cytotoxicity of the triple combination; ii) the increased PP2A phosphatase activity (measured by immuno-precipitation of flag-tagged PP2Ac followed by phosphatase assay) inversely correlated with phosphorylation, i.e., activation, of the DDR checkpoints; iii) the localization of PP2A core enzyme on the chromatin following metabolic stress.

The role of PP2A (and phosphatases in general) on the chromatin is a novel topic of considerable interest. Although PP2A has been repeatedly associated with transcription and the DDR machinery, direct evidence about its localization and action on the DNA was lacking (Martina & Puertollano, 2018; Myant et al., 2015; Rice et al., 2014). In the case of PP2A, this may be due to the difficult designing of the

appropriate experimental setting. Given the abundance of the two constant subunits (scaffold A and catalytic C subunits), immunofluorescence experiments failed to distinguish nucleosolic PP2A from chromatin-bound PP2A (data not shown). Here we have optimized the fractionation protocol to achieve an accurate separation of the different compartments. In the past two years, Chromatin Immuno-Precipitation and sequencing (ChIP-seq) proved to be a powerful method to analyze chromatin-bound PP2A; by ChIP-seq it was shown that the interaction between PP2A and RNA pol II occurs within the Integrator complex, which is involved in processing nascent RNA (K.-L. Huang et al., 2020; Vervoort et al., 2021; H. Zheng et al., 2020). We cannot exclude that, even in our model, the recruitment of PP2A on the chromatin was Integrator-dependent, since depletion of INTS6 and INTS8 (necessary for PP2A recruitment) abolished PP2A loading on the chromatin (Vervoort et al., 2021; H. Zheng et al., 2020). It must be stressed, however, that the increased recruitment of PP2A on chromatin observed upon metabolic stress may also hint to a completely different mechanism of recruitment.

The systematic knock-down of all the regulatory B subunits expressed in our model system (in particular, the B56 family, which are predominant in MDA-MB-231 cells) failed to identify a single, specific responsible and all of them participated to the synergism. The fact that all the B subunits were apparently involved led us to reason that, as a result of individual knock-down, the functionality of the entire holoenzyme could be impaired, similarly, though less impactful, to the knock-down of the catalytic subunit. Moreover, the involvement of all the B56 subunits directed our attention to CIP2A, which we had previously identified as the target of metformin. In TNBC cell lines, CIP2A was not appreciably affected by (high or low doses) metformin nor by its combination with glucose starvation; but given the high protein levels, metformin

might be insufficient to induce an appreciable decrease. In cancer cell lines, CIP2A was shown to sequester the B56 subunits preventing the assembly of PP2A holoenzyme (J. Wang et al., 2017). In this regard, the use of the CIP2A^{K21A} mutant, with a point mutation that abolishes the ability to sequester the B56 subunits, yielded results similar to the triple combination. Still, this result does not exclude a more general role of CIP2A as an oncogenic driver of TNBC necessary to survive adverse conditions such as chemotherapy (Chao et al., 2015; Côme et al., 2009; A. Khanna et al., 2011; Laine et al., 2013, 2021). Other evidences support the idea that CIP2A may be involved in maintaining genomic integrity following DSBs occurring in mitosis (de Marco Zompit et al., 2022). In this context, cells expressing the CIP2A mutant might be more sensitive to chemotherapy; the same applies to cells in which metabolic stress could decrease the interaction between CIP2A and PP2A-B56 without lowering the net protein levels. In yeast, other metabolic circuits influenced PP2A: in detail, IRC21 and PPM1 counteract the DDR by activating PP2A, while the TORC1-Tap42 axis sustains the DDR by inhibiting PP2A (Ferrari et al., 2017). We found that mTORC1 pathway was strongly attenuated by the combination of metformin and glucose starvation, as evidenced by decreased phosphorylation of both RPS6 and 4EBP1, supporting the idea that, also in mammals, mTORC1 inhibition contributed to PP2A activation. RPS6 and 4EBP1 are themselves targets of PP2A (Gardner et al., 2015; K. Hahn et al., 2010; R. T. Peterson et al., 1999); thus, we cannot exclude that it was over-activated PP2A that attenuated the mTORC1downstream signaling. The mTORC1 inhibitor rapamycin synergized with low-dose chemotherapy similarly to the combination of metformin and glucose starvation, supporting the idea that it was mTORC1 that inhibited PP2A (in absence of metabolic stress) and not vice versa, at least in our experimental model. As useful as it is for the in *vitro* experiments, rapamycin has been shown to cause

hyperglycemia in mouse models (di Biase et al., 2017; Raffaghello et al., 2008), making its use counterproductive in our experimental setting; this further reinforces the use of metformin and hypoglycemia-producing strategies.

Since mTORC1 and CIP2A are part of a positive circuit in which mTORC1 inhibits the autophagic degradation of CIP2A, while CIP2A maintains mTORC1 in a dephosphorylated, namely active, state through PP2A inhibition (Lei et al., 2014; Puustinen et al., 2014; Puustinen & Jäättelä, 2014), we postulated that they both negatively regulated PP2A and they both were affected by the metabolic stress. While the role of mTORC1 as a master regulator of cell metabolism is well established, the link between CIP2A and cell metabolism remains elusive. Recently, our group proposed a model whereby inhibition of mitochondrial complex I, either with metformin or the more selective IACS-010759, led to the (ROS-dependent) dissociation of CIP2A from PP2A, resulting in the destabilization and degradation of CIP2A via proteosome and chaperone-mediated autophagy. Again, this mechanism was described mainly in HeLa and HCT116 cell lines, which express low levels of CIP2A compared with TNBC cell lines, and could be in line with other observations linking oxidative stress to the DDR through PP2A (Guillonneau et al., 2016).

Here we have mainly discussed about PP2A over-activation, but it is worth mentioning PP2A inhibition as a therapeutic strategy as well. In several tumor models, PP2A inhibition yielded significant results in combination with chemotherapy or radiotherapy (Lu et al., 2009; Martiniova et al., 2011; Zhu et al., 2015). In details, PP2A inhibition with LB100 resulted in aberrant cell cycle regulation characterized by constitutive CDK1 activation, probably due to over-activated PLK-1 and CDC25C, and mitotic catastrophe (D. Wei et al., 2013). Other works described a persistence of DDR following treatment with LB100 (K.-E. Chang et al., 2015; Ho, Sizdahkhani, et al.,

2018). In 2016, a clinical trial evaluated the toxicity, adverse events, and efficacy of LB100, and concluded that it deserved further study alone or in combination with existing therapies (Chung et al., 2017). It remains unclear, though not unprecedented, how the activation or the inhibition of the same protein can lead to similar effects. In our experimental setting, low-dose chemotherapy, which *per se* has a cytostatic rather than cytotoxic effect, is sufficient to trigger the DDR. In this context, PP2A activation attenuated the DDR machinery and rendered cancer cells unable to detect and repair the DNA damage, until the multiple lesions become incompatible with cell survival. With high-dose chemotherapy, which *per se* has a much stronger cytotoxic effect, the inhibition rather than the activation of PP2A might provide benefit: if the DNA damage is too extended and difficult to repair (such as that from high-dose chemotherapy), the DDR itself decides the cell's fate toward death. In this context, inhibition of PP2A "takes the brakes off" the running car.

Taken together, our results provide encouraging evidences and the molecular rationale to support trials such as the BRAKFAST clinical trial which is ongoing, and justify the use of metformin in combination with (low-dose) chemotherapy and (blood) glucose-lowering strategies, regardless of whether it was glucose starvation in *vitro* or intermittent fasting or fasting-mimicking diets in *vivo* (Vernieri et al., 2022). Mechanistically, we have shown that PP2A core enzyme, upon the metabolic stress as previously described, translocates onto the chromatin where it attenuates the DDR triggered by DNA-damaging chemotherapy. PP2A accumulation on the chromatin may prevent its proteolytic degradation, thus increasing the net amount of PP2Ac and, finally, PP2A phosphatase activity. The attenuation of the DDR in the continued presence of low-dose chemotherapy had important consequences on cell survival and tumor progression, as evidenced by survival and clonogenic assays, and resembled

high-dose chemotherapy, but without the side effects. Our work extends to mammalian cells observations previously described in yeast, and, following our latest published study, provides mechanistic details about PP2A over-activation upon the combination of metformin and glucose starvation. Transcriptional regulation by PP2A (and phosphatases in general) is gaining enormous interest; here, we describe an additional, metabolic mechanism that accumulates PP2A onto the chromatin. We have focused on the effects of PP2A on the DDR triggered by chemotherapy, but the function(s) of PP2A on chromatin, and whether these functions change as a consequence of metabolic dynamics, represent an undiscovered field that offers numerous possibilities and clinical implications.

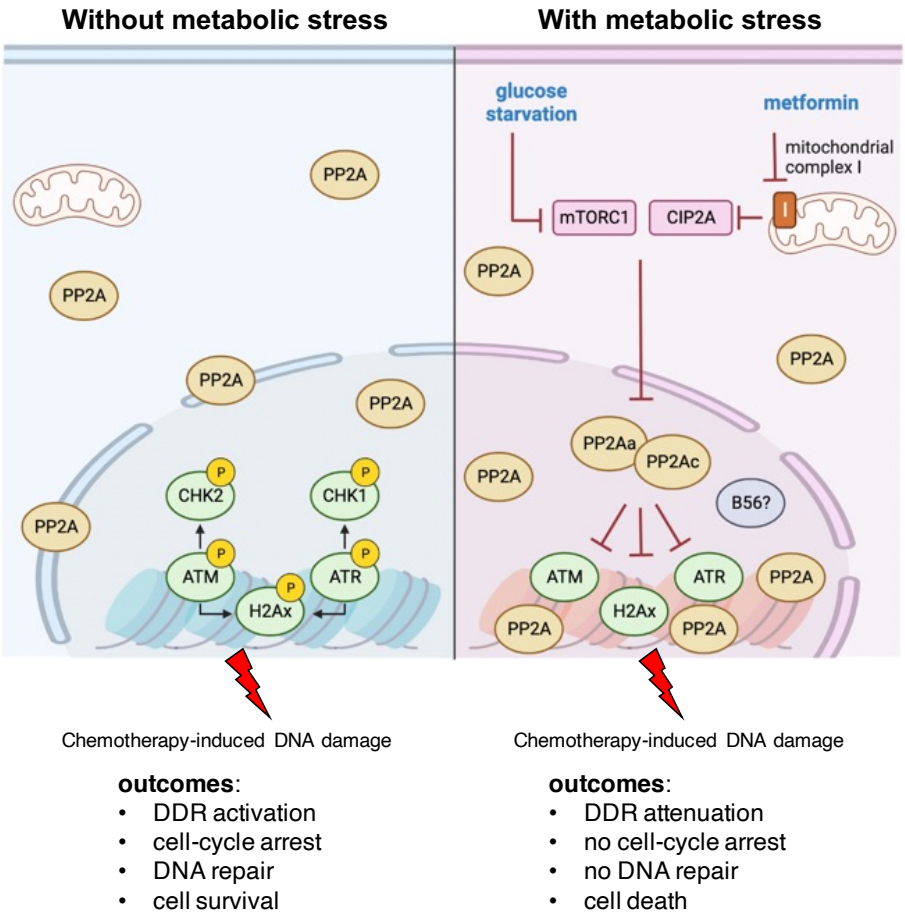

Figure 69: schematic representation of the proposed model.

Tumor cells activate the DDR in presence of low-dose chemotherapy; the DDR activation leads to the cell-cycle arrest, which is necessary for DNA repair, and cell survival. In presence of the metabolic stress (which is the combination of metformin, which is a mitochondrial complex I inhibitor, and glucose starvation), PP2A accumulates on the chromatin, where it attenuates the DDR, leading to lack of cell-cycle arrest and, consequently, impaired DNA repair and increased genetic lesions, inducing cell death. We are currently investigating which metabolic pathways lead to the accumulation of PP2A core enzyme onto the chromatin. Preliminary data obtained so far point to a role for mTORC1 and CIP2A, both inhibitors of PP2A, which interact with each other. As expected, mTORC1 was strongly modulated by the metabolic stress; on the contrary, the contribution of CIP2A - downstream of mitochondrial complex I inhibition - requires further investigation. Since they are known to interact with each other, we do not exclude that their simultaneous inhibition leads to activation of PP2A and its accumulation on the chromatin.

Bibliography

Aarts, M., Sharpe, R., Garcia-Murillas, I., Gevensleben, H., Hurd, M. S., Shumway, S. D., Toniatti, C., Ashworth, A., & Turner, N. C. (2012). Forced mitotic entry of S-phase cells as a therapeutic strategy induced by inhibition of WEE1. *Cancer Discovery*, *2*(6), 524–539. https://doi.org/10.1158/2159-8290.CD-11-0320

Afonso, O., Matos, I., Pereira, A. J., Aguiar, P., Lampson, M. A., & Maiato, H. (2014). Feedback control of chromosome separation by a midzone Aurora B gradient. *Science*, *345*(6194), 332–336. https://doi.org/10.1126/science.1251121

Al-Ahmadie, H., Iyer, G., Hohl, M., Asthana, S., Inagaki, A., Schultz, N., Hanrahan, A. J., Scott, S. N., Brannon, A. R., McDermott, G. C., Pirun, M., Ostrovnaya, I., Kim, P., Socci, N. D., Viale, A., Schwartz, G. K., Reuter, V., Bochner, B. H., Rosenberg, J. E., … Taylor, B. S. (2014). Synthetic lethality in ATM-deficient RAD50-mutant tumors underlies outlier response to cancer therapy. *Cancer Discovery*, *4*(9), 1014–1021. https://doi.org/10.1158/2159-8290.CD-14-0380

Allen-Petersen, B. L., Risom, T., Feng, Z., Wang, Z., Jenny, Z. P., Thoma, M. C., Pelz, K. R., Morton, J. P., Sansom, O. J., Lopez, C. D., Sheppard, B., Christensen, D. J., Ohlmeyer, M., Narla, G., & Sears, R. C. (2019). Activation of PP2A and Inhibition of mTOR Synergistically Reduce MYC Signaling and Decrease Tumor Growth in Pancreatic Ductal Adenocarcinoma. *Cancer Research*, *79*(1), 209–219. https://doi.org/10.1158/0008-5472.CAN-18-0717

Ambjørn, S. M., Duxin, J. P., Hertz, E. P. T., Nasa, I., Duro, J., Kruse, T., Lopez-Mendez, B., Rymarczyk, B., Cressey, L. E., van Overeem Hansen, T., Kettenbach, A. N., Oestergaard, V. H., Lisby, M., & Nilsson, J. (2021). A complex of BRCA2 and PP2A-B56 is required for DNA repair by homologous recombination. *Nature Communications*, *12*(1), 5748. https://doi.org/10.1038/s41467-021-26079-0

Apostolidis, S. A., Rodríguez-Rodríguez, N., Suárez-Fueyo, A., Dioufa, N., Ozcan, E., Crispín, J. C., Tsokos, M. G., & Tsokos, G. C. (2016). Phosphatase PP2A is requisite for the function of regulatory T cells. *Nature Immunology*, *17*(5), 556–564. https://doi.org/10.1038/ni.3390

Arnold, H. K., & Sears, R. C. (2006). Protein phosphatase 2A regulatory subunit B56alpha associates with c-myc and negatively regulates c-myc accumulation. *Molecular and Cellular Biology*, *26*(7), 2832–2844. https://doi.org/10.1128/MCB.26.7.2832-2844.2006

Arumugam, A., Subramani, R., Nandy, S. B., Terreros, D., Dwivedi, A. K., Saltzstein, E., & Lakshmanaswamy, R. (2019). Silencing growth hormone receptor inhibits estrogen receptor negative breast cancer through ATP-binding cassette sub-family G member 2. *Experimental & Molecular Medicine*, *51*(1), 1–13. https://doi.org/10.1038/s12276-018-0197-8

Ashworth, A. (2008a). A synthetic lethal therapeutic approach: poly(ADP) ribose polymerase inhibitors for the treatment of cancers deficient in DNA double-strand break repair. *Journal of Clinical Oncology : Official Journal of the American Society of Clinical Oncology*, *26*(22), 3785–3790. https://doi.org/10.1200/JCO.2008.16.0812

Atezolizumab Extends Survival for Breast Cancer. (2017). *Cancer Discovery*, *7*(6), OF10. https://doi.org/10.1158/2159-8290.CD-NB2017-053

Bakkenist, C. J., & Kastan, M. B. (2003). DNA damage activates ATM through intermolecular autophosphorylation and dimer dissociation. *Nature*, *421*(6922), 499–506. https://doi.org/10.1038/nature01368

Bakkenist, C. J., & Kastan, M. B. (2004). Initiating cellular stress responses. *Cell*, *118*(1), 9–17. https://doi.org/10.1016/j.cell.2004.06.023

Bardia, A., Gucalp, A., DaCosta, N., Gabrail, N., Danso, M., Ali, H., Blackwell, K. L., Carey, L. A., Eisner, J. R., Baskin-Bey, E. S., & Traina, T. A. (2018). Phase 1 study of seviteronel, a selective CYP17 lyase and androgen receptor inhibitor, in women with estrogen receptor-positive or triple-negative breast cancer. *Breast Cancer Research and Treatment*, *171*(1), 111–120. https://doi.org/10.1007/s10549-018-4813-z

Bareche, Y., Venet, D., Ignatiadis, M., Aftimos, P., Piccart, M., Rothe, F., & Sotiriou, C. (2018). Unravelling triple-negative breast cancer molecular heterogeneity using an integrative multiomic analysis. *Annals of Oncology : Official Journal of the European Society for Medical Oncology*, *29*(4), 895–902. https://doi.org/10.1093/annonc/mdy024

Bartkova, J., Hamerlik, P., Stockhausen, M.-T., Ehrmann, J., Hlobilkova, A., Laursen, H., Kalita, O., Kolar, Z., Poulsen, H. S., Broholm, H., Lukas, J., & Bartek, J. (2010). Replication stress and oxidative damage contribute to aberrant constitutive activation of DNA damage signalling in human gliomas. *Oncogene*, *29*(36), 5095–5102. https://doi.org/10.1038/onc.2010.249

Bartkova, J., Horejsí, Z., Koed, K., Krämer, A., Tort, F., Zieger, K., Guldberg, P., Sehested, M., Nesland, J. M., Lukas, C., Ørntoft, T., Lukas, J., & Bartek, J. (2005). DNA damage response as a candidate anti-cancer barrier in early human tumorigenesis. *Nature*, *434*(7035), 864–870. https://doi.org/10.1038/nature03482

Bauer, J. A., Chakravarthy, A. B., Rosenbluth, J. M., Mi, D., Seeley, E. H., de Matos Granja-Ingram, N., Olivares, M. G., Kelley, M. C., Mayer, I. A., Meszoely, I. M., Means-Powell, J. A., Johnson, K. N., Tsai, C. J., Ayers, G. D., Sanders, M. E., Schneider, R. J., Formenti, S. C., Caprioli, R. M., & Pietenpol, J. A. (2010). Identification of markers of taxane sensitivity using proteomic and genomic analyses of breast tumors from patients receiving neoadjuvant paclitaxel and radiation. *Clinical Cancer Research : An Official Journal of the American Association for Cancer Research*, *16*(2), 681–690. https://doi.org/10.1158/1078-0432.CCR-09-1091

Beck, H., Nähse-Kumpf, V., Larsen, M. S. Y., O'Hanlon, K. A., Patzke, S., Holmberg, C., Mejlvang, J., Groth, A., Nielsen, O., Syljuåsen, R. G., & Sørensen, C. S. (2012). Cyclin-dependent kinase suppression by WEE1 kinase protects the genome through control of replication initiation and nucleotide consumption. *Molecular and Cellular Biology*, *32*(20), 4226–4236. https://doi.org/10.1128/MCB.00412-12

Ben-Sahra, I., Howell, J. J., Asara, J. M., & Manning, B. D. (2013). Stimulation of de novo pyrimidine synthesis by growth signaling through mTOR and S6K1. *Science (New York, N.Y.)*, *339*(6125), 1323–1328. https://doi.org/10.1126/science.1228792

Bermejo, R., Capra, T., Jossen, R., Colosio, A., Frattini, C., Carotenuto, W., Cocito, A., Doksani, Y., Klein, H., Gómez-González, B., Aguilera, A., Katou, Y., Shirahige, K., & Foiani, M. (2011). The replication checkpoint protects fork stability by releasing transcribed genes from nuclear pores. *Cell*, *146*(2), 233–246. https://doi.org/10.1016/j.cell.2011.06.033

Bernier, C., Soliman, A., Gravel, M., Dankner, M., Savage, P., Petrecca, K., Park, M., Siegel, P. M., Shore, G. C., & Roulston, A. (2018). DZ-2384 has a superior preclinical profile to taxanes for the treatment of triple-negative breast cancer and is synergistic with anti-CTLA-4 immunotherapy. *Anti-Cancer Drugs*, *29*(8), 774–785. https://doi.org/10.1097/CAD.0000000000000653

Birsoy, K., Possemato, R., Lorbeer, F. K., Bayraktar, E. C., Thiru, P., Yucel, B., Wang, T., Chen, W. W., Clish, C. B., & Sabatini, D. M. (2014). Metabolic determinants of cancer cell sensitivity to glucose limitation and biguanides. *Nature*, *508*(7494), 108–112. https://doi.org/10.1038/nature13110

Bohgaki, M., Hakem, A., Halaby, M. J., Bohgaki, T., Li, Q., Bissey, P. A., Shloush, J., Kislinger, T., Sanchez, O., Sheng, Y., & Hakem, R. (2013). The E3 ligase PIRH2 polyubiquitylates CHK2 and regulates its turnover. *Cell Death and Differentiation*, *20*(6), 812–822. https://doi.org/10.1038/cdd.2013.7

Bonotto, M., Gerratana, L., Poletto, E., Driol, P., Giangreco, M., Russo, S., Minisini, A. M., Andreetta, C., Mansutti, M., Pisa, F. E., Fasola, G., & Puglisi, F. (2014). Measures of outcome in metastatic breast cancer: insights from a real-world scenario. *The Oncologist*, *19*(6), 608–615. https://doi.org/10.1634/theoncologist.2014-0002

Boudreau, V., Chen, R., Edwards, A., Sulaimain, M., & Maddox, P. S. (2019). PP2A-B55/SUR-6 collaborates with the nuclear lamina for centrosome separation during mitotic entry. *Molecular Biology of the Cell*, *30*(7), 876–886. https://doi.org/10.1091/mbc.E18-10-0631

Bouwman, P., Aly, A., Escandell, J. M., Pieterse, M., Bartkova, J., van der Gulden, H., Hiddingh, S., Thanasoula, M., Kulkarni, A., Yang, Q., Haffty, B. G., Tommiska, J., Blomqvist, C., Drapkin, R., Adams, D. J., Nevanlinna, H., Bartek, J., Tarsounas, M., Ganesan, S., & Jonkers, J. (2010). 53BP1 loss rescues BRCA1 deficiency and is associated with triple-negative and BRCA-mutated breast cancers. *Nature Structural & Molecular Biology*, *17*(6), 688–695. https://doi.org/10.1038/nsmb.1831

Bridges, H. R., Jones, A. J. Y., Pollak, M. N., & Hirst, J. (2014). Effects of metformin and other biguanides on oxidative phosphorylation in mitochondria. *The Biochemical Journal*, *462*(3), 475–487. https://doi.org/10.1042/BJ20140620

Brown, E. J., & Baltimore, D. (2003). Essential and dispensable roles of ATR in cell cycle arrest and genome maintenance. *Genes & Development*, *17*(5), 615–628. https://doi.org/10.1101/gad.1067403

Buisson, R., Boisvert, J. L., Benes, C. H., & Zou, L. (2015). Distinct but Concerted Roles of ATR, DNA-PK, and Chk1 in Countering Replication Stress during S Phase. *Molecular Cell*, *59*(6), 1011–1024. https://doi.org/10.1016/j.molcel.2015.07.029

Burstein, M. D., Tsimelzon, A., Poage, G. M., Covington, K. R., Contreras, A., Fuqua, S. A. W., Savage, M. I., Osborne, C. K., Hilsenbeck, S. G., Chang, J. C., Mills, G. B., Lau, C. C., & Brown, P. H. (2015). Comprehensive genomic analysis identifies novel subtypes and targets of triple-

negative breast cancer. *Clinical Cancer Research : An Official Journal of the American Association for Cancer Research*, *21*(7), 1688–1698. https://doi.org/10.1158/1078-0432.CCR-14-0432

Byun, T. S., Pacek, M., Yee, M., Walter, J. C., & Cimprich, K. A. (2005). Functional uncoupling of MCM helicase and DNA polymerase activities activates the ATR-dependent checkpoint. *Genes & Development*, *19*(9), 1040–1052. https://doi.org/10.1101/gad.1301205

Caffa, I., Spagnolo, V., Vernieri, C., Valdemarin, F., Becherini, P., Wei, M., Brandhorst, S., Zucal, C., Driehuis, E., Ferrando, L., Piacente, F., Tagliafico, A., Cilli, M., Mastracci, L., Vellone, V. G., Piazza, S., Cremonini, A. L., Gradaschi, R., Mantero, C., … Nencioni, A. (2020). Fasting-mimicking diet and hormone therapy induce breast cancer regression. *Nature*, *583*(7817), 620–624. https://doi.org/10.1038/s41586-020-2502-7

Cai, Z., Chehab, N. H., & Pavletich, N. P. (2009). Structure and activation mechanism of the CHK2 DNA damage checkpoint kinase. *Molecular Cell*, *35*(6), 818–829. https://doi.org/10.1016/j.molcel.2009.09.007

Cairns, R. A., Harris, I. S., & Mak, T. W. (2011). Regulation of cancer cell metabolism. *Nature Reviews. Cancer*, *11*(2), 85–95. https://doi.org/10.1038/nrc2981

Caldecott, K. W. (2014). DNA single-strand break repair. *Experimental Cell Research*, *329*(1), 2–8. https://doi.org/10.1016/j.yexcr.2014.08.027

Calin, G. A., di Iasio, M. G., Caprini, E., Vorechovsky, I., Natali, P. G., Sozzi, G., Croce, C. M., Barbanti-Brodano, G., Russo, G., & Negrini, M. (2000). Low frequency of alterations of the alpha (PPP2R1A) and beta (PPP2R1B) isoforms of the subunit A of the serine-threonine phosphatase 2A in human neoplasms. *Oncogene*, *19*(9), 1191–1195. https://doi.org/10.1038/sj.onc.1203389

Carey, L. A., Dees, E. C., Sawyer, L., Gatti, L., Moore, D. T., Collichio, F., Ollila, D. W., Sartor, C. I., Graham, M. L., & Perou, C. M. (2007). The triple negative paradox: primary tumor chemosensitivity of breast cancer subtypes. *Clinical Cancer Research : An Official Journal of the American Association for Cancer Research*, *13*(8), 2329–2334. https://doi.org/10.1158/1078-0432.CCR-06-1109

Carey, L. A., Rugo, H. S., Marcom, P. K., Mayer, E. L., Esteva, F. J., Ma, C. X., Liu, M. C., Storniolo, A. M., Rimawi, M. F., Forero-Torres, A., Wolff, A. C., Hobday, T. J., Ivanova, A., Chiu, W.-K., Ferraro, M., Burrows, E., Bernard, P. S., Hoadley, K. A., Perou, C. M., & Winer, E. P. (2012). TBCRC 001: randomized phase II study of cetuximab in combination with carboplatin in stage IV triple-negative breast cancer. *Journal of Clinical Oncology : Official Journal of the American Society of Clinical Oncology*, *30*(21), 2615–2623. https://doi.org/10.1200/JCO.2010.34.5579

Castedo, M., Perfettini, J.-L., Roumier, T., Andreau, K., Medema, R., & Kroemer, G. (2004). Cell death by mitotic catastrophe: a molecular definition. *Oncogene*, *23*(16), 2825–2837. https://doi.org/10.1038/sj.onc.1207528

Castedo, M., Perfettini, J.-L., Roumier, T., Valent, A., Raslova, H., Yakushijin, K., Horne, D., Feunteun, J., Lenoir, G., Medema, R., Vainchenker, W., & Kroemer, G. (2004). Mitotic catastrophe constitutes a special case of apoptosis whose suppression entails aneuploidy. *Oncogene*, *23*(25), 4362–4370. https://doi.org/10.1038/sj.onc.1207572

Ceccaldi, R., Rondinelli, B., & D'Andrea, A. D. (2016). Repair Pathway Choices and Consequences at the Double-Strand Break. *Trends in Cell Biology*, *26*(1), 52–64. https://doi.org/10.1016/j.tcb.2015.07.009

Chang, J. (2000). Chemotherapy dose reduction and delay in clinical practice. evaluating the risk to patient outcome in adjuvant chemotherapy for breast cancer. *European Journal of Cancer (Oxford, England : 1990)*, *36 Suppl 1*, S11-4. https://doi.org/10.1016/s0959-8049(99)00259-2

Chang, K.-E., Wei, B.-R., Madigan, J. P., Hall, M. D., Simpson, R. M., Zhuang, Z., & Gottesman, M. M. (2015). The protein phosphatase 2A inhibitor LB100 sensitizes ovarian carcinoma cells to cisplatin-mediated cytotoxicity. *Molecular Cancer Therapeutics*, *14*(1), 90–100. https://doi.org/10.1158/1535-7163.MCT-14-0496

Chao, T.-T., Wang, C.-Y., Chen, Y.-L., Lai, C.-C., Chang, F.-Y., Tsai, Y.-T., Chao, C.-H. H., Shiau, C.-W., Huang, Y.-C. T., Yu, C.-J., & Chen, K.-F. (2015). Afatinib induces apoptosis in NSCLC without EGFR mutation through Elk-1-mediated suppression of CIP2A. *Oncotarget*, *6*(4), 2164–2179. https://doi.org/10.18632/oncotarget.2941

Cheang, M. C. U., Martin, M., Nielsen, T. O., Prat, A., Voduc, D., Rodriguez-Lescure, A., Ruiz, A., Chia, S., Shepherd, L., Ruiz-Borrego, M., Calvo, L., Alba, E., Carrasco, E., Caballero, R., Tu, D., Pritchard, K. I., Levine, M. N., Bramwell, V. H., Parker, J., … Carey, L. A. (2015). Defining breast cancer intrinsic subtypes by quantitative receptor expression. *The Oncologist*, *20*(5), 474–482. https://doi.org/10.1634/theoncologist.2014-0372

Chen, M. J., Dixon, J. E., & Manning, G. (2017). Genomics and evolution of protein phosphatases. *Science Signaling*, *10*(474). https://doi.org/10.1126/scisignal.aag1796
Chen, W., Possemato, R., Campbell, K. T., Plattner, C. A., Pallas, D. C., & Hahn, W. C. (2004a). Identification of specific PP2A complexes involved in human cell transformation. *Cancer Cell*, *5*(2), 127–136. https://doi.org/10.1016/S1535-6108(04)00026-1
Chen, W., Possemato, R., Campbell, K. T., Plattner, C. A., Pallas, D. C., & Hahn, W. C. (2004b). Identification of specific PP2A complexes involved in human cell transformation. *Cancer Cell*, *5*(2), 127–136. https://doi.org/10.1016/s1535-6108(04)00026-1
Chen, Y.-H., Jones, M. J. K., Yin, Y., Crist, S. B., Colnaghi, L., Sims, R. J., Rothenberg, E., Jallepalli, P. v, & Huang, T. T. (2015). ATR-mediated phosphorylation of FANCI regulates dormant origin firing in response to replication stress. *Molecular Cell*, *58*(2), 323–338. https://doi.org/10.1016/j.molcel.2015.02.031
Chiang, C. W., Harris, G., Ellig, C., Masters, S. C., Subramanian, R., Shenolikar, S., Wadzinski, B. E., & Yang, E. (2001). Protein phosphatase 2A activates the proapoptotic function of BAD in interleukin- 3-dependent lymphoid cells by a mechanism requiring 14-3-3 dissociation. *Blood*, *97*(5), 1289–1297. https://doi.org/10.1182/blood.v97.5.1289
Chien, W., Sun, Q.-Y., Lee, K. L., Ding, L.-W., Wuensche, P., Torres-Fernandez, L. A., Tan, S. Z., Tokatly, I., Zaiden, N., Poellinger, L., Mori, S., Yang, H., Tyner, J. W., & Koeffler, H. P. (2015). Activation of protein phosphatase 2A tumor suppressor as potential treatment of pancreatic cancer. *Molecular Oncology*, *9*(4), 889–905. https://doi.org/10.1016/j.molonc.2015.01.002
Cho, U. S., & Xu, W. (2007). Crystal structure of a protein phosphatase 2A heterotrimeric holoenzyme. *Nature*, *445*(7123), 53–57. https://doi.org/10.1038/nature05351
Choi, J.-H., Lindsey-Boltz, L. A., Kemp, M., Mason, A. C., Wold, M. S., & Sancar, A. (2010). Reconstitution of RPA-covered single-stranded DNA-activated ATR-Chk1 signaling. *Proceedings of the National Academy of Sciences of the United States of America*, *107*(31), 13660–13665. https://doi.org/10.1073/pnas.1007856107
Chung, V., Mansfield, A. S., Braiteh, F., Richards, D., Durivage, H., Ungerleider, R. S., Johnson, F., & Kovach, J. S. (2017). Safety, Tolerability, and Preliminary Activity of LB-100, an Inhibitor of Protein Phosphatase 2A, in Patients with Relapsed Solid Tumors: An Open-Label, Dose Escalation, First-in-Human, Phase I Trial. *Clinical Cancer Research : An Official Journal of the American Association for Cancer Research*, *23*(13), 3277–3284. https://doi.org/10.1158/1078-0432.CCR-16-2299
Cimprich, K. A., & Cortez, D. (2008). ATR: an essential regulator of genome integrity. *Nature Reviews. Molecular Cell Biology*, *9*(8), 616–627. https://doi.org/10.1038/nrm2450
Côme, C., Laine, A., Chanrion, M., Edgren, H., Mattila, E., Liu, X., Jonkers, J., Ivaska, J., Isola, J., Darbon, J.-M., Kallioniemi, O., Thézenas, S., & Westermarck, J. (2009). CIP2A Is Associated with Human Breast Cancer Aggressivity. *Clinical Cancer Research*, *15*(16), 5092–5100. https://doi.org/10.1158/1078-0432.CCR-08-3283
Cosse, J.-P., & Michiels, C. (2008). Tumour hypoxia affects the responsiveness of cancer cells to chemotherapy and promotes cancer progression. *Anti-Cancer Agents in Medicinal Chemistry*, *8*(7), 790–797. https://doi.org/10.2174/187152008785914798
Couch, F. B., Bansbach, C. E., Driscoll, R., Luzwick, J. W., Glick, G. G., Bétous, R., Carroll, C. M., Jung, S. Y., Qin, J., Cimprich, K. A., & Cortez, D. (2013). ATR phosphorylates SMARCAL1 to prevent replication fork collapse. *Genes & Development*, *27*(14), 1610–1623. https://doi.org/10.1101/gad.214080.113
Curtin, N. J. (2012). DNA repair dysregulation from cancer driver to therapeutic target. *Nature Reviews. Cancer*, *12*(12), 801–817. https://doi.org/10.1038/nrc3399
d'Adda di Fagagna, F., Reaper, P. M., Clay-Farrace, L., Fiegler, H., Carr, P., von Zglinicki, T., Saretzki, G., Carter, N. P., & Jackson, S. P. (2003). A DNA damage checkpoint response in telomere-initiated senescence. *Nature*, *426*(6963), 194–198. https://doi.org/10.1038/nature02118
D'Aronzo, M., Vinciguerra, M., Mazza, T., Panebianco, C., Saracino, C., Pereira, S. P., Graziano, P., & Pazienza, V. (2015). Fasting cycles potentiate the efficacy of gemcitabine treatment in in vitro and in vivo pancreatic cancer models. *Oncotarget*, *6*(21), 18545–18557. https://doi.org/10.18632/oncotarget.4186
Daugan, M., Dufaÿ Wojcicki, A., d'Hayer, B., & Boudy, V. (2016). Metformin: An anti-diabetic drug to fight cancer. *Pharmacological Research*, *113*(Pt A), 675–685. https://doi.org/10.1016/j.phrs.2016.10.006
de Marco Zompit, M., Esteban, M. T., Mooser, C., Adam, S., Rossi, S. E., Jeanrenaud, A., Leimbacher, P.-A., Fink, D., Shorrocks, A.-M. K., Blackford, A. N., Durocher, D., & Stucki, M. (2022). The

CIP2A-TOPBP1 complex safeguards chromosomal stability during mitosis. *Nature Communications*, *13*(1), 4143. https://doi.org/10.1038/s41467-022-31865-5

DeBerardinis, R. J., & Chandel, N. S. (2016). Fundamentals of cancer metabolism. *Science Advances*, *2*(5), e1600200. https://doi.org/10.1126/sciadv.1600200

DeBerardinis, R. J., Mancuso, A., Daikhin, E., Nissim, I., Yudkoff, M., Wehrli, S., & Thompson, C. B. (2007). Beyond aerobic glycolysis: transformed cells can engage in glutamine metabolism that exceeds the requirement for protein and nucleotide synthesis. *Proceedings of the National Academy of Sciences of the United States of America*, *104*(49), 19345–19350. https://doi.org/10.1073/pnas.0709747104

Delgoffe, G. M. (2016). PP2A's restraint of mTOR is critical for T(reg) cell activity. *Nature Immunology*, *17*(5), 478–479. https://doi.org/10.1038/ni.3442

DeNicola, G. M., Chen, P.-H., Mullarky, E., Sudderth, J. A., Hu, Z., Wu, D., Tang, H., Xie, Y., Asara, J. M., Huffman, K. E., Wistuba, I. I., Minna, J. D., DeBerardinis, R. J., & Cantley, L. C. (2015). NRF2 regulates serine biosynthesis in non-small cell lung cancer. *Nature Genetics*, *47*(12), 1475–1481. https://doi.org/10.1038/ng.3421

DeNicola, G. M., Karreth, F. A., Humpton, T. J., Gopinathan, A., Wei, C., Frese, K., Mangal, D., Yu, K. H., Yeo, C. J., Calhoun, E. S., Scrimieri, F., Winter, J. M., Hruban, R. H., Iacobuzio-Donahue, C., Kern, S. E., Blair, I. A., & Tuveson, D. A. (2011). Oncogene-induced Nrf2 transcription promotes ROS detoxification and tumorigenesis. *Nature*, *475*(7354), 106–109. https://doi.org/10.1038/nature10189

Dent, R., Trudeau, M., Pritchard, K. I., Hanna, W. M., Kahn, H. K., Sawka, C. A., Lickley, L. A., Rawlinson, E., Sun, P., & Narod, S. A. (2007). Triple-negative breast cancer: clinical features and patterns of recurrence. *Clinical Cancer Research : An Official Journal of the American Association for Cancer Research*, *13*(15 Pt 1), 4429–4434. https://doi.org/10.1158/1078-0432.CCR-06-3045

di Biase, S., Lee, C., Brandhorst, S., Manes, B., Buono, R., Cheng, C.-W., Cacciottolo, M., Martin-Montalvo, A., de Cabo, R., Wei, M., Morgan, T. E., & Longo, V. D. (2016). Fasting-Mimicking Diet Reduces HO-1 to Promote T Cell-Mediated Tumor Cytotoxicity. *Cancer Cell*, *30*(1), 136–146. https://doi.org/10.1016/j.ccell.2016.06.005

di Biase, S., Shim, H. S., Kim, K. H., Vinciguerra, M., Rappa, F., Wei, M., Brandhorst, S., Cappello, F., Mirzaei, H., Lee, C., & Longo, V. D. (2017). Fasting regulates EGR1 and protects from glucose- and dexamethasone-dependent sensitization to chemotherapy. *PLoS Biology*, *15*(3), e2001951. https://doi.org/10.1371/journal.pbio.2001951

Do, K., Doroshow, J. H., & Kummar, S. (2013). Wee1 kinase as a target for cancer therapy. *Cell Cycle (Georgetown, Tex.)*, *12*(19), 3159–3164. https://doi.org/10.4161/cc.26062

Doane, A. S., Danso, M., Lal, P., Donaton, M., Zhang, L., Hudis, C., & Gerald, W. L. (2006). An estrogen receptor-negative breast cancer subset characterized by a hormonally regulated transcriptional program and response to androgen. *Oncogene*, *25*(28), 3994–4008. https://doi.org/10.1038/sj.onc.1209415

Doherty, J. R., & Cleveland, J. L. (2013). Targeting lactate metabolism for cancer therapeutics. *The Journal of Clinical Investigation*, *123*(9), 3685–3692. https://doi.org/10.1172/JCI69741

Dupré, A., Daldello, E. M., Nairn, A. C., Jessus, C., & Haccard, O. (2014). Phosphorylation of ARPP19 by protein kinase A prevents meiosis resumption in Xenopus oocytes. *Nature Communications*, *5*, 3318. https://doi.org/10.1038/ncomms4318

Eil, R., Vodnala, S. K., Clever, D., Klebanoff, C. A., Sukumar, M., Pan, J. H., Palmer, D. C., Gros, A., Yamamoto, T. N., Patel, S. J., Guittard, G. C., Yu, Z., Carbonaro, V., Okkenhaug, K., Schrump, D. S., Linehan, W. M., Roychoudhuri, R., & Restifo, N. P. (2016). Ionic immune suppression within the tumour microenvironment limits T cell effector function. *Nature*, *537*(7621), 539–543. https://doi.org/10.1038/nature19364

Elgendy, M., Cirò, M., Hosseini, A., Weiszmann, J., Mazzarella, L., Ferrari, E., Cazzoli, R., Curigliano, G., DeCensi, A., Bonanni, B., Budillon, A., Pelicci, P. G., Janssens, V., Ogris, M., Baccarini, M., Lanfrancone, L., Weckwerth, W., Foiani, M., & Minucci, S. (2019). Combination of Hypoglycemia and Metformin Impairs Tumor Metabolic Plasticity and Growth by Modulating the PP2A-GSK3β-MCL-1 Axis. *Cancer Cell*, *35*(5), 798-815.e5. https://doi.org/10.1016/j.ccell.2019.03.007

El-Mir, M. Y., Nogueira, V., Fontaine, E., Avéret, N., Rigoulet, M., & Leverve, X. (2000). Dimethylbiguanide inhibits cell respiration via an indirect effect targeted on the respiratory chain complex I. *The Journal of Biological Chemistry*, *275*(1), 223–228. https://doi.org/10.1074/jbc.275.1.223

Emadi, A., Jones, R. J., & Brodsky, R. A. (2009). Cyclophosphamide and cancer: golden anniversary. *Nature Reviews. Clinical Oncology*, *6*(11), 638–647. https://doi.org/10.1038/nrclinonc.2009.146
Evans, J. M. M., Donnelly, L. A., Emslie-Smith, A. M., Alessi, D. R., & Morris, A. D. (2005). Metformin and reduced risk of cancer in diabetic patients. *BMJ (Clinical Research Ed.)*, *330*(7503), 1304–1305. https://doi.org/10.1136/bmj.38415.708634.F7
Ewald, B., Sampath, D., & Plunkett, W. (2008). Nucleoside analogs: molecular mechanisms signaling cell death. *Oncogene*, *27*(50), 6522–6537. https://doi.org/10.1038/onc.2008.316
Falck, J., Coates, J., & Jackson, S. P. (2005). Conserved modes of recruitment of ATM, ATR and DNA-PKcs to sites of DNA damage. *Nature*, *434*(7033), 605–611. https://doi.org/10.1038/nature03442
Fan, J., Kamphorst, J. J., Mathew, R., Chung, M. K., White, E., Shlomi, T., & Rabinowitz, J. D. (2013). Glutamine-driven oxidative phosphorylation is a major ATP source in transformed mammalian cells in both normoxia and hypoxia. *Molecular Systems Biology*, *9*, 712. https://doi.org/10.1038/msb.2013.65
Fan, J., Ye, J., Kamphorst, J. J., Shlomi, T., Thompson, C. B., & Rabinowitz, J. D. (2014). Quantitative flux analysis reveals folate-dependent NADPH production. *Nature*, *510*(7504), 298–302. https://doi.org/10.1038/nature13236
Fantin, V. R., St-Pierre, J., & Leder, P. (2006). Attenuation of LDH-A expression uncovers a link between glycolysis, mitochondrial physiology, and tumor maintenance. *Cancer Cell*, *9*(6), 425–434. https://doi.org/10.1016/j.ccr.2006.04.023
Farrington, C. C., Yuan, E., Mazhar, S., Izadmehr, S., Hurst, L., Allen-Petersen, B. L., Janghorban, M., Chung, E., Wolczanski, G., Galsky, M., Sears, R., Sangodkar, J., & Narla, G. (2020). Protein phosphatase 2A activation as a therapeutic strategy for managing MYC-driven cancers. *The Journal of Biological Chemistry*, *295*(3), 757–770. https://doi.org/10.1074/jbc.RA119.011443
Ferrari, E., Bruhn, C., Peretti, M., Cassani, C., Carotenuto, W. V., Elgendy, M., Shubassi, G., Lucca, C., Bermejo, R., Varasi, M., Minucci, S., Longhese, M. P., & Foiani, M. (2017). PP2A Controls Genome Integrity by Integrating Nutrient-Sensing and Metabolic Pathways with the DNA Damage Response. *Molecular Cell*, *67*(2), 266-281.e4. https://doi.org/10.1016/j.molcel.2017.05.027
Fischer, K., Hoffmann, P., Voelkl, S., Meidenbauer, N., Ammer, J., Edinger, M., Gottfried, E., Schwarz, S., Rothe, G., Hoves, S., Renner, K., Timischl, B., Mackensen, A., Kunz-Schughart, L., Andreesen, R., Krause, S. W., & Kreutz, M. (2007). Inhibitory effect of tumor cell-derived lactic acid on human T cells. *Blood*, *109*(9), 3812–3819. https://doi.org/10.1182/blood-2006-07-035972
Flynn, R. L., & Zou, L. (2011). ATR: a master conductor of cellular responses to DNA replication stress. *Trends in Biochemical Sciences*, *36*(3), 133–140. https://doi.org/10.1016/j.tibs.2010.09.005
Foley, E. A., Maldonado, M., & Kapoor, T. M. (2011). Formation of stable attachments between kinetochores and microtubules depends on the B56-PP2A phosphatase. *Nature Cell Biology*, *13*(10), 1265–1271. https://doi.org/10.1038/ncb2327
Foulkes, W. D., Smith, I. E., & Reis-Filho, J. S. (2010). Triple-negative breast cancer. *The New England Journal of Medicine*, *363*(20), 1938–1948. https://doi.org/10.1056/NEJMra1001389
Fowle, H., Zhao, Z., & Graña, X. (2019). PP2A holoenzymes, substrate specificity driving cellular functions and deregulation in cancer. *Advances in Cancer Research*, *144*, 55–93. https://doi.org/10.1016/bs.acr.2019.03.009
Freeman, A. K., Dapic, V., & Monteiro, A. N. A. (2010). Negative regulation of CHK2 activity by protein phosphatase 2A is modulated by DNA damage. *Cell Cycle (Georgetown, Tex.)*, *9*(4), 736–747. https://doi.org/10.4161/cc.9.4.10613
Freeman, A. K., & Monteiro, A. N. (2010). Phosphatases in the cellular response to DNA damage. *Cell Communication and Signaling : CCS*, *8*, 27. https://doi.org/10.1186/1478-811X-8-27
Friboulet, L., Soria, J.-C., & Olaussen, K. A. (2019). The "Guardian of the Genome"-An Old Key to Unlock the ERCC1 Issue. *Clinical Cancer Research : An Official Journal of the American Association for Cancer Research*, *25*(8), 2369–2371. https://doi.org/10.1158/1078-0432.CCR-18-4123
Frohner, I. E., Mudrak, I., Kronlachner, S., Schüchner, S., & Ogris, E. (2020). Antibodies recognizing the C terminus of PP2A catalytic subunit are unsuitable for evaluating PP2A activity and holoenzyme composition. *Science Signaling*, *13*(616). https://doi.org/10.1126/scisignal.aax6490
Fukumura, D., Xu, L., Chen, Y., Gohongi, T., Seed, B., & Jain, R. K. (2001). Hypoxia and acidosis independently up-regulate vascular endothelial growth factor transcription in brain tumors in vivo. *Cancer Research*, *61*(16), 6020–6024.

García-Limones, C., Lara-Chica, M., Jiménez-Jiménez, C., Pérez, M., Moreno, P., Muñoz, E., & Calzado, M. A. (2016). CHK2 stability is regulated by the E3 ubiquitin ligase SIAH2. *Oncogene*, *35*(33), 4289–4301. https://doi.org/10.1038/onc.2015.495

Gardner, T. W., Abcouwer, S. F., Losiewicz, M. K., & Fort, P. E. (2015). Phosphatase control of 4E-BP1 phosphorylation state is central for glycolytic regulation of retinal protein synthesis. *American Journal of Physiology. Endocrinology and Metabolism*, *309*(6), E546-56. https://doi.org/10.1152/ajpendo.00180.2015

Gelmon, K. A., Tischkowitz, M., Mackay, H., Swenerton, K., Robidoux, A., Tonkin, K., Hirte, H., Huntsman, D., Clemons, M., Gilks, B., Yerushalmi, R., Macpherson, E., Carmichael, J., & Oza, A. (2011). Olaparib in patients with recurrent high-grade serous or poorly differentiated ovarian carcinoma or triple-negative breast cancer: a phase 2, multicentre, open-label, non-randomised study. *The Lancet. Oncology*, *12*(9), 852–861. https://doi.org/10.1016/S1470-2045(11)70214-5

Gharbi-Ayachi, A., Labbé, J.-C., Burgess, A., Vigneron, S., Strub, J.-M., Brioudes, E., Van-Dorsselaer, A., Castro, A., & Lorca, T. (2010). The substrate of Greatwall kinase, Arpp19, controls mitosis by inhibiting protein phosphatase 2A. *Science (New York, N.Y.)*, *330*(6011), 1673–1677. https://doi.org/10.1126/science.1197048

Gluz, O., Liedtke, C., Gottschalk, N., Pusztai, L., Nitz, U., & Harbeck, N. (2009). Triple-negative breast cancer--current status and future directions. *Annals of Oncology : Official Journal of the European Society for Medical Oncology*, *20*(12), 1913–1927. https://doi.org/10.1093/annonc/mdp492

Gonzalez-Angulo, A. M., Timms, K. M., Liu, S., Chen, H., Litton, J. K., Potter, J., Lanchbury, J. S., Stemke-Hale, K., Hennessy, B. T., Arun, B. K., Hortobagyi, G. N., Do, K.-A., Mills, G. B., & Meric-Bernstam, F. (2011). Incidence and outcome of BRCA mutations in unselected patients with triple receptor-negative breast cancer. *Clinical Cancer Research : An Official Journal of the American Association for Cancer Research*, *17*(5), 1082–1089. https://doi.org/10.1158/1078-0432.CCR-10-2560

Goodwin, P. J., Chen, B. E., Gelmon, K. A., Whelan, T. J., Ennis, M., Lemieux, J., Ligibel, J. A., Hershman, D. L., Mayer, I. A., Hobday, T. J., Bliss, J. M., Rastogi, P., Rabaglio-Poretti, M., Mukherjee, S. D., Mackey, J. R., Abramson, V. G., Oja, C., Wesolowski, R., Thompson, A. M., … Parulekar, W. R. (2022). Effect of Metformin vs Placebo on Invasive Disease-Free Survival in Patients With Breast Cancer: The MA.32 Randomized Clinical Trial. *JAMA*, *327*(20), 1963–1973. https://doi.org/10.1001/jama.2022.6147

Gorgoulis, V. G., Vassiliou, L.-V. F., Karakaidos, P., Zacharatos, P., Kotsinas, A., Liloglou, T., Venere, M., Ditullio, R. A., Kastrinakis, N. G., Levy, B., Kletsas, D., Yoneta, A., Herlyn, M., Kittas, C., & Halazonetis, T. D. (2005). Activation of the DNA damage checkpoint and genomic instability in human precancerous lesions. *Nature*, *434*(7035), 907–913. https://doi.org/10.1038/nature03485

Griss, T., Vincent, E. E., Egnatchik, R., Chen, J., Ma, E. H., Faubert, B., Viollet, B., DeBerardinis, R. J., & Jones, R. G. (2015). Metformin Antagonizes Cancer Cell Proliferation by Suppressing Mitochondrial-Dependent Biosynthesis. *PLoS Biology*, *13*(12), e1002309. https://doi.org/10.1371/journal.pbio.1002309

Gucalp, A., Tolaney, S., Isakoff, S. J., Ingle, J. N., Liu, M. C., Carey, L. A., Blackwell, K., Rugo, H., Nabell, L., Forero, A., Stearns, V., Doane, A. S., Danso, M., Moynahan, M. E., Momen, L. F., Gonzalez, J. M., Akhtar, A., Giri, D. D., Patil, S., … Translational Breast Cancer Research Consortium (TBCRC 011). (2013). Phase II trial of bicalutamide in patients with androgen receptor-positive, estrogen receptor-negative metastatic Breast Cancer. *Clinical Cancer Research : An Official Journal of the American Association for Cancer Research*, *19*(19), 5505–5512. https://doi.org/10.1158/1078-0432.CCR-12-3327

Guillonneau, M., Paris, F., Dutoit, S., Estephan, H., Bénéteau, E., Huot, J., & Corre, I. (2016). Oxidative stress disassembles the p38/NPM/PP2A complex, which leads to modulation of nucleophosmin-mediated signaling to DNA damage response. *FASEB Journal : Official Publication of the Federation of American Societies for Experimental Biology*, *30*(8), 2899–2914. https://doi.org/10.1096/fj.201500194R

Guo, C. Y., Brautigan, D. L., & Larner, J. M. (2002). ATM-dependent dissociation of B55 regulatory subunit from nuclear PP2A in response to ionizing radiation. *The Journal of Biological Chemistry*, *277*(7), 4839–4844. https://doi.org/10.1074/jbc.M110092200

Guo, F., Stanevich, V., Wlodarchak, N., Sengupta, R., Jiang, L., Satyshur, K. A., & Xing, Y. (2014). Structural basis of PP2A activation by PTPA, an ATP-dependent activation chaperone. *Cell Research*, *24*(2), 190–203. https://doi.org/10.1038/cr.2013.138

Guo, J. Y., Chen, H.-Y., Mathew, R., Fan, J., Strohecker, A. M., Karsli-Uzunbas, G., Kamphorst, J. J., Chen, G., Lemons, J. M. S., Karantza, V., Coller, H. A., Dipaola, R. S., Gelinas, C., Rabinowitz,

J. D., & White, E. (2011). Activated Ras requires autophagy to maintain oxidative metabolism and tumorigenesis. *Genes & Development*, *25*(5), 460–470. https://doi.org/10.1101/gad.2016311

Gutierrez, A., Pan, L., Groen, R. W. J., Baleydier, F., Kentsis, A., Marineau, J., Grebliunaite, R., Kozakewich, E., Reed, C., Pflumio, F., Poglio, S., Uzan, B., Clemons, P., VerPlank, L., An, F., Burbank, J., Norton, S., Tolliday, N., Steen, H., … Aster, J. C. (2014). Phenothiazines induce PP2A-mediated apoptosis in T cell acute lymphoblastic leukemia. *The Journal of Clinical Investigation*, *124*(2), 644–655. https://doi.org/10.1172/JCI65093

Guzy, R. D., Sharma, B., Bell, E., Chandel, N. S., & Schumacker, P. T. (2008). Loss of the SdhB, but Not the SdhA, subunit of complex II triggers reactive oxygen species-dependent hypoxia-inducible factor activation and tumorigenesis. *Molecular and Cellular Biology*, *28*(2), 718–731. https://doi.org/10.1128/MCB.01338-07

Haesen, D., Sents, W., Lemaire, K., Hoorne, Y., & Janssens, V. (2014). The Basic Biology of PP2A in Hematologic Cells and Malignancies. *Frontiers in Oncology*, *4*, 347. https://doi.org/10.3389/fonc.2014.00347

Hahn, K., Miranda, M., Francis, V. A., Vendrell, J., Zorzano, A., & Teleman, A. A. (2010). PP2A regulatory subunit PP2A-B' counteracts S6K phosphorylation. *Cell Metabolism*, *11*(5), 438–444. https://doi.org/10.1016/j.cmet.2010.03.015

Hanahan, D., & Weinberg, R. A. (2000). The hallmarks of cancer. *Cell*, *100*(1), 57–70. https://doi.org/10.1016/s0092-8674(00)81683-9

Hanahan, D., & Weinberg, R. A. (2011). Hallmarks of cancer: the next generation. *Cell*, *144*(5), 646–674. https://doi.org/10.1016/j.cell.2011.02.013

Hardie, D. G., Schaffer, B. E., & Brunet, A. (2016). AMPK: An Energy-Sensing Pathway with Multiple Inputs and Outputs. *Trends in Cell Biology*, *26*(3), 190–201. https://doi.org/10.1016/j.tcb.2015.10.013

Harris, I. S., Treloar, A. E., Inoue, S., Sasaki, M., Gorrini, C., Lee, K. C., Yung, K. Y., Brenner, D., Knobbe-Thomsen, C. B., Cox, M. A., Elia, A., Berger, T., Cescon, D. W., Adeoye, A., Brüstle, A., Molyneux, S. D., Mason, J. M., Li, W. Y., Yamamoto, K., … Mak, T. W. (2015). Glutathione and thioredoxin antioxidant pathways synergize to drive cancer initiation and progression. *Cancer Cell*, *27*(2), 211–222. https://doi.org/10.1016/j.ccell.2014.11.019

Harrison, J. C., & Haber, J. E. (2006). Surviving the breakup: the DNA damage checkpoint. *Annual Review of Genetics*, *40*, 209–235. https://doi.org/10.1146/annurev.genet.40.051206.105231

Hartlerode, A. J., Morgan, M. J., Wu, Y., Buis, J., & Ferguson, D. O. (2015). Recruitment and activation of the ATM kinase in the absence of DNA-damage sensors. *Nature Structural & Molecular Biology*, *22*(9), 736–743. https://doi.org/10.1038/nsmb.3072

Hay, N. (2016). Reprogramming glucose metabolism in cancer: can it be exploited for cancer therapy? *Nature Reviews. Cancer*, *16*(10), 635–649. https://doi.org/10.1038/nrc.2016.77

Helleday, T. (2011). The underlying mechanism for the PARP and BRCA synthetic lethality: clearing up the misunderstandings. *Molecular Oncology*, *5*(4), 387–393. https://doi.org/10.1016/j.molonc.2011.07.001

Hensley, C. T., Wasti, A. T., & DeBerardinis, R. J. (2013). Glutamine and cancer: cell biology, physiology, and clinical opportunities. *The Journal of Clinical Investigation*, *123*(9), 3678–3684. https://doi.org/10.1172/JCI69600

Hertz, E. P. T., Kruse, T., Davey, N. E., López-Méndez, B., Sigurðsson, J. O., Montoya, G., Olsen, J. v, & Nilsson, J. (2016). A Conserved Motif Provides Binding Specificity to the PP2A-B56 Phosphatase. *Molecular Cell*, *63*(4), 686–695. https://doi.org/10.1016/j.molcel.2016.06.024

Ho, W. S., Sizdahkhani, S., Hao, S., Song, H., Seldomridge, A., Tandle, A., Maric, D., Kramp, T., Lu, R., Heiss, J. D., Camphausen, K., Gilbert, M. R., Zhuang, Z., & Park, D. M. (2018). LB-100, a novel Protein Phosphatase 2A (PP2A) inhibitor, sensitizes malignant meningioma cells to the therapeutic effects of radiation. *Cancer Letters*, *415*, 217–226. https://doi.org/10.1016/j.canlet.2017.11.035

Ho, W. S., Wang, H., Maggio, D., Kovach, J. S., Zhang, Q., Song, Q., Marincola, F. M., Heiss, J. D., Gilbert, M. R., Lu, R., & Zhuang, Z. (2018). Pharmacologic inhibition of protein phosphatase-2A achieves durable immune-mediated antitumor activity when combined with PD-1 blockade. *Nature Communications*, *9*(1), 2126. https://doi.org/10.1038/s41467-018-04425-z

Hoeijmakers, J. H. (2001). Genome maintenance mechanisms for preventing cancer. *Nature*, *411*(6835), 366–374. https://doi.org/10.1038/35077232

Hoeijmakers, J. H. J. (2009). DNA damage, aging, and cancer. *The New England Journal of Medicine*, *361*(15), 1475–1485. https://doi.org/10.1056/NEJMra0804615

Horton, J. D., Goldstein, J. L., & Brown, M. S. (2002). SREBPs: activators of the complete program of cholesterol and fatty acid synthesis in the liver. *The Journal of Clinical Investigation*, *109*(9), 1125–1131. https://doi.org/10.1172/JCI15593

Hu, W., Wang, Z., Zhang, H., Mahaman, Y. A. R., Huang, F., Meng, D., Zhou, Y., Wang, S., Jiang, N., Xiong, J., Westermarck, J., Lu, Y., Wang, J., Wang, X., Shentu, Y., & Liu, R. (2022). Chk1 Inhibition Ameliorates Alzheimer's Disease Pathogenesis and Cognitive Dysfunction Through CIP2A/PP2A Signaling. *Neurotherapeutics : The Journal of the American Society for Experimental NeuroTherapeutics*, *19*(2), 570–591. https://doi.org/10.1007/s13311-022-01204-z

Huang, K.-L., Jee, D., Stein, C. B., Elrod, N. D., Henriques, T., Mascibroda, L. G., Baillat, D., Russell, W. K., Adelman, K., & Wagner, E. J. (2020). Integrator Recruits Protein Phosphatase 2A to Prevent Pause Release and Facilitate Transcription Termination. *Molecular Cell*, *80*(2), 345-358.e9. https://doi.org/10.1016/j.molcel.2020.08.016

Huang, X., Halicka, H. D., & Darzynkiewicz, Z. (2004). Detection of histone H2AX phosphorylation on Ser-139 as an indicator of DNA damage (DNA double-strand breaks). *Current Protocols in Cytometry*, *Chapter 7*, Unit 7.27. https://doi.org/10.1002/0471142956.cy0727s30

Hudis, C. A., & Gianni, L. (2011). Triple-negative breast cancer: an unmet medical need. *The Oncologist*, *16 Suppl 1*, 1–11. https://doi.org/10.1634/theoncologist.2011-S1-01

Huen, M. S. Y., & Chen, J. (2008). The DNA damage response pathways: at the crossroad of protein modifications. *Cell Research*, *18*(1), 8–16. https://doi.org/10.1038/cr.2007.109

Ibrahim, Y. H., García-García, C., Serra, V., He, L., Torres-Lockhart, K., Prat, A., Anton, P., Cozar, P., Guzmán, M., Grueso, J., Rodríguez, O., Calvo, M. T., Aura, C., Díez, O., Rubio, I. T., Pérez, J., Rodón, J., Cortés, J., Ellisen, L. W., … Baselga, J. (2012). PI3K inhibition impairs BRCA1/2 expression and sensitizes BRCA-proficient triple-negative breast cancer to PARP inhibition. *Cancer Discovery*, *2*(11), 1036–1047. https://doi.org/10.1158/2159-8290.CD-11-0348

Irie, A., Harada, K., Araki, N., & Nishimura, Y. (2012). Phosphorylation of SET protein at Ser171 by protein kinase D2 diminishes its inhibitory effect on protein phosphatase 2A. *PloS One*, *7*(12), e51242. https://doi.org/10.1371/journal.pone.0051242

Israelsen, W. J., & vander Heiden, M. G. (2015). Pyruvate kinase: Function, regulation and role in cancer. *Seminars in Cell & Developmental Biology*, *43*, 43–51. https://doi.org/10.1016/j.semcdb.2015.08.004

Ito, A., Kataoka, T. R., Watanabe, M., Nishiyama, K., Mazaki, Y., Sabe, H., Kitamura, Y., & Nojima, H. (2000). A truncated isoform of the PP2A B56 subunit promotes cell motility through paxillin phosphorylation. *The EMBO Journal*, *19*(4), 562–571. https://doi.org/10.1093/emboj/19.4.562

Ito, K., & Suda, T. (2014). Metabolic requirements for the maintenance of self-renewing stem cells. *Nature Reviews. Molecular Cell Biology*, *15*(4), 243–256. https://doi.org/10.1038/nrm3772

Jackson, S. P., & Bartek, J. (2009). The DNA-damage response in human biology and disease. *Nature*, *461*(7267), 1071–1078. https://doi.org/10.1038/nature08467

Jang, J. K., Gladstein, A. C., Das, A., Shapiro, J. G., Sisco, Z. L., & McKim, K. S. (2021). Multiple pools of PP2A regulate spindle assembly, kinetochore attachments and cohesion in Drosophila oocytes. *Journal of Cell Science*, *134*(14). https://doi.org/10.1242/jcs.254037

Janssens, V., & Goris, J. (2001). Protein phosphatase 2A: a highly regulated family of serine/threonine phosphatases implicated in cell growth and signalling. *The Biochemical Journal*, *353*(Pt 3), 417–439. https://doi.org/10.1042/0264-6021:3530417

Janssens, V., Jordens, J., Stevens, I., van Hoof, C., Martens, E., de Smedt, H., Engelborghs, Y., Waelkens, E., & Goris, J. (2003). Identification and functional analysis of two Ca2+-binding EF-hand motifs in the B"/PR72 subunit of protein phosphatase 2A. *The Journal of Biological Chemistry*, *278*(12), 10697–10706. https://doi.org/10.1074/jbc.M211717200

Janzer, A., German, N. J., Gonzalez-Herrera, K. N., Asara, J. M., Haigis, M. C., & Struhl, K. (2014). Metformin and phenformin deplete tricarboxylic acid cycle and glycolytic intermediates during cell transformation and NTPs in cancer stem cells. *Proceedings of the National Academy of Sciences of the United States of America*, *111*(29), 10574–10579. https://doi.org/10.1073/pnas.1409844111

Jeon, S.-M., Chandel, N. S., & Hay, N. (2012). AMPK regulates NADPH homeostasis to promote tumour cell survival during energy stress. *Nature*, *485*(7400), 661–665. https://doi.org/10.1038/nature11066

Jia, D., Lu, M., Jung, K. H., Park, J. H., Yu, L., Onuchic, J. N., Kaipparettu, B. A., & Levine, H. (2019). Elucidating cancer metabolic plasticity by coupling gene regulation with metabolic pathways. *Proceedings of the National Academy of Sciences of the United States of America*, *116*(9), 3909–3918. https://doi.org/10.1073/pnas.1816391116

Jiang, L., Shestov, A. A., Swain, P., Yang, C., Parker, S. J., Wang, Q. A., Terada, L. S., Adams, N. D., McCabe, M. T., Pietrak, B., Schmidt, S., Metallo, C. M., Dranka, B. P., Schwartz, B., & DeBerardinis, R. J. (2016). Reductive carboxylation supports redox homeostasis during anchorage-independent growth. *Nature*, *532*(7598), 255–258. https://doi.org/10.1038/nature17393

Jiricny, J. (2006). The multifaceted mismatch-repair system. *Nature Reviews. Molecular Cell Biology*, *7*(5), 335–346. https://doi.org/10.1038/nrm1907

Jones, R. M., Mortusewicz, O., Afzal, I., Lorvellec, M., García, P., Helleday, T., & Petermann, E. (2013). Increased replication initiation and conflicts with transcription underlie Cyclin E-induced replication stress. *Oncogene*, *32*(32), 3744–3753. https://doi.org/10.1038/onc.2012.387

Jones, T. A., Barker, H. M., da Cruz e Silva, E. F., Mayer-Jaekel, R. E., Hemmings, B. A., Spurr, N. K., Sheer, D., & Cohen, P. T. (1993). Localization of the genes encoding the catalytic subunits of protein phosphatase 2A to human chromosome bands 5q23-->q31 and 8p12-->p11.2, respectively. *Cytogenetics and Cell Genetics*, *63*(1), 35–41. https://doi.org/10.1159/000133497

Jovanović, B., Mayer, I. A., Mayer, E. L., Abramson, V. G., Bardia, A., Sanders, M. E., Kuba, M. G., Estrada, M. v, Beeler, J. S., Shaver, T. M., Johnson, K. C., Sanchez, V., Rosenbluth, J. M., Dillon, P. M., Forero-Torres, A., Chang, J. C., Meszoely, I. M., Grau, A. M., Lehmann, B. D., … Pietenpol, J. A. (2017). A Randomized Phase II Neoadjuvant Study of Cisplatin, Paclitaxel With or Without Everolimus in Patients with Stage II/III Triple-Negative Breast Cancer (TNBC): Responses and Long-term Outcome Correlated with Increased Frequency of DNA Damage Response Gene Mutations, TNBC Subtype, AR Status, and Ki67. *Clinical Cancer Research : An Official Journal of the American Association for Cancer Research*, *23*(15), 4035–4045. https://doi.org/10.1158/1078-0432.CCR-16-3055

Junttila, M. R., Puustinen, P., Niemelä, M., Ahola, R., Arnold, H., Böttzauw, T., Ala-aho, R., Nielsen, C., Ivaska, J., Taya, Y., Lu, S.-L., Lin, S., Chan, E. K. L., Wang, X.-J., Grènman, R., Kast, J., Kallunki, T., Sears, R., Kähäri, V.-M., & Westermarck, J. (2007). CIP2A inhibits PP2A in human malignancies. *Cell*, *130*(1), 51–62. https://doi.org/10.1016/j.cell.2007.04.044

Kalev, P., Simicek, M., Vazquez, I., Munck, S., Chen, L., Soin, T., Danda, N., Chen, W., & Sablina, A. (2012). Loss of PPP2R2A inhibits homologous recombination DNA repair and predicts tumor sensitivity to PARP inhibition. *Cancer Research*, *72*(24), 6414–6424. https://doi.org/10.1158/0008-5472.CAN-12-1667

Kamphorst, J. J., Cross, J. R., Fan, J., de Stanchina, E., Mathew, R., White, E. P., Thompson, C. B., & Rabinowitz, J. D. (2013). Hypoxic and Ras-transformed cells support growth by scavenging unsaturated fatty acids from lysophospholipids. *Proceedings of the National Academy of Sciences of the United States of America*, *110*(22), 8882–8887. https://doi.org/10.1073/pnas.1307237110

Kauko, O., O'Connor, C. M., Kulesskiy, E., Sangodkar, J., Aakula, A., Izadmehr, S., Yetukuri, L., Yadav, B., Padzik, A., Laajala, T. D., Haapaniemi, P., Momeny, M., Varila, T., Ohlmeyer, M., Aittokallio, T., Wennerberg, K., Narla, G., & Westermarck, J. (2018). PP2A inhibition is a druggable MEK inhibitor resistance mechanism in KRAS-mutant lung cancer cells. *Science Translational Medicine*, *10*(450). https://doi.org/10.1126/scitranslmed.aaq1093

Kauko, O., & Westermarck, J. (2018). Non-genomic mechanisms of protein phosphatase 2A (PP2A) regulation in cancer. *The International Journal of Biochemistry & Cell Biology*, *96*, 157–164. https://doi.org/10.1016/j.biocel.2018.01.005

Kerzendorfer, C., & O'Driscoll, M. (2009). Human DNA damage response and repair deficiency syndromes: linking genomic instability and cell cycle checkpoint proficiency. *DNA Repair*, *8*(9), 1139–1152. https://doi.org/10.1016/j.dnarep.2009.04.018

Keshri, R., Rajeevan, A., & Kotak, S. (2020). PP2A--B55γ counteracts Cdk1 and regulates proper spindle orientation through the cortical dynein adaptor NuMA. *Journal of Cell Science*, *133*(14). https://doi.org/10.1242/jcs.243857

Khanna, A., Böckelman, C., Hemmes, A., Junttila, M. R., Wiksten, J.-P., Lundin, M., Junnila, S., Murphy, D. J., Evan, G. I., Haglund, C., Westermarck, J., & Ristimäki, A. (2009). MYC-dependent regulation and prognostic role of CIP2A in gastric cancer. *Journal of the National Cancer Institute*, *101*(11), 793–805. https://doi.org/10.1093/jnci/djp103

Khanna, A., Okkeri, J., Bilgen, T., Tiirikka, T., Vihinen, M., Visakorpi, T., & Westermarck, J. (2011). ETS1 mediates MEK1/2-dependent overexpression of cancerous inhibitor of protein phosphatase 2A (CIP2A) in human cancer cells. *PloS One*, *6*(3), e17979. https://doi.org/10.1371/journal.pone.0017979

Khanna, K. K., & Jackson, S. P. (2001). DNA double-strand breaks: signaling, repair and the cancer connection. *Nature Genetics*, *27*(3), 247–254. https://doi.org/10.1038/85798

Khondker, S., Kajjo, S., Chandler-Brown, D., Skotheim, J., Rudner, A., & Ikui, A. E. (2020). PP2ACdc55 dephosphorylates Pds1 and inhibits spindle elongation in S. cerevisiae. *Journal of Cell Science*, *133*(14). https://doi.org/10.1242/jcs.243766

Kim, D., Fiske, B. P., Birsoy, K., Freinkman, E., Kami, K., Possemato, R. L., Chudnovsky, Y., Pacold, M. E., Chen, W. W., Cantor, J. R., Shelton, L. M., Gui, D. Y., Kwon, M., Ramkissoon, S. H., Ligon, K. L., Kang, S. W., Snuderl, M., vander Heiden, M. G., & Sabatini, D. M. (2015). SHMT2 drives glioma cell survival in ischaemia but imposes a dependence on glycine clearance. *Nature*, *520*(7547), 363–367. https://doi.org/10.1038/nature14363

Kruse, T., Gnosa, S. P., Nasa, I., Garvanska, D. H., Hein, J. B., Nguyen, H., Samsøe-Petersen, J., Lopez-Mendez, B., Hertz, E. P. T., Schwarz, J., Pena, H. S., Nikodemus, D., Kveiborg, M., Kettenbach, A. N., & Nilsson, J. (2020). Mechanisms of site-specific dephosphorylation and kinase opposition imposed by PP2A regulatory subunits. *The EMBO Journal*, *39*(13), e103695. https://doi.org/10.15252/embj.2019103695

Kumar, A., Pandurangan, A. K., Lu, F., Fyrst, H., Zhang, M., Byun, H.-S., Bittman, R., & Saba, J. D. (2012). Chemopreventive sphingadienes downregulate Wnt signaling via a PP2A/Akt/GSK3β pathway in colon cancer. *Carcinogenesis*, *33*(9), 1726–1735. https://doi.org/10.1093/carcin/bgs174

Kuo, Y.-C., Huang, K.-Y., Yang, C.-H., Yang, Y.-S., Lee, W.-Y., & Chiang, C.-W. (2008). Regulation of phosphorylation of Thr-308 of Akt, cell proliferation, and survival by the B55alpha regulatory subunit targeting of the protein phosphatase 2A holoenzyme to Akt. *The Journal of Biological Chemistry*, *283*(4), 1882–1892. https://doi.org/10.1074/jbc.M709585200

Labuschagne, C. F., van den Broek, N. J. F., Mackay, G. M., Vousden, K. H., & Maddocks, O. D. K. (2014). Serine, but not glycine, supports one-carbon metabolism and proliferation of cancer cells. *Cell Reports*, *7*(4), 1248–1258. https://doi.org/10.1016/j.celrep.2014.04.045

Laine, A., Nagelli, S. G., Farrington, C., Butt, U., Cvrljevic, A. N., Vainonen, J. P., Feringa, F. M., Grönroos, T. J., Gautam, P., Khan, S., Sihto, H., Qiao, X., Pavic, K., Connolly, D. C., Kronqvist, P., Elo, L. L., Maurer, J., Wennerberg, K., Medema, R. H., … Westermarck, J. (2021). CIP2A Interacts with TopBP1 and Drives Basal-Like Breast Cancer Tumorigenesis. *Cancer Research*, *81*(16), 4319–4331. https://doi.org/10.1158/0008-5472.CAN-20-3651

Laine, A., Sihto, H., Come, C., Rosenfeldt, M. T., Zwolinska, A., Niemelä, M., Khanna, A., Chan, E. K., Kähäri, V.-M., Kellokumpu-Lehtinen, P.-L., Sansom, O. J., Evan, G. I., Junttila, M. R., Ryan, K. M., Marine, J.-C., Joensuu, H., & Westermarck, J. (2013). Senescence sensitivity of breast cancer cells is defined by positive feedback loop between CIP2A and E2F1. *Cancer Discovery*, *3*(2), 182–197. https://doi.org/10.1158/2159-8290.CD-12-0292

Lao, D.-H., Yusoff, P., Chandramouli, S., Philp, R. J., Fong, C. W., Jackson, R. A., Saw, T. Y., Yu, C. Y., & Guy, G. R. (2007). Direct binding of PP2A to Sprouty2 and phosphorylation changes are a prerequisite for ERK inhibition downstream of fibroblast growth factor receptor stimulation. *The Journal of Biological Chemistry*, *282*(12), 9117–9126. https://doi.org/10.1074/jbc.M607563200

Laplante, M., & Sabatini, D. M. (2012). mTOR signaling in growth control and disease. *Cell*, *149*(2), 274–293. https://doi.org/10.1016/j.cell.2012.03.017

Le, A., Cooper, C. R., Gouw, A. M., Dinavahi, R., Maitra, A., Deck, L. M., Royer, R. E., vander Jagt, D. L., Semenza, G. L., & Dang, C. v. (2010). Inhibition of lactate dehydrogenase A induces oxidative stress and inhibits tumor progression. *Proceedings of the National Academy of Sciences of the United States of America*, *107*(5), 2037–2042. https://doi.org/10.1073/pnas.0914433107

Lee, C., Raffaghello, L., Brandhorst, S., Safdie, F. M., Bianchi, G., Martin-Montalvo, A., Pistoia, V., Wei, M., Hwang, S., Merlino, A., Emionite, L., de Cabo, R., & Longo, V. D. (2012). Fasting cycles retard growth of tumors and sensitize a range of cancer cell types to chemotherapy. *Science Translational Medicine*, *4*(124), 124ra27. https://doi.org/10.1126/scitranslmed.3003293

Lee, H. E., Kim, J. H., Kim, Y. J., Choi, S. Y., Kim, S.-W., Kang, E., Chung, I. Y., Kim, I. A., Kim, E. J., Choi, Y., Ryu, H. S., & Park, S. Y. (2011). An increase in cancer stem cell population after primary systemic therapy is a poor prognostic factor in breast cancer. *British Journal of Cancer*, *104*(11), 1730–1738. https://doi.org/10.1038/bjc.2011.159

Lee, J.-H., & Paull, T. T. (2005). ATM activation by DNA double-strand breaks through the Mre11-Rad50-Nbs1 complex. *Science (New York, N.Y.)*, *308*(5721), 551–554. https://doi.org/10.1126/science.1108297

Lehmann, B. D., Bauer, J. A., Chen, X., Sanders, M. E., Chakravarthy, A. B., Shyr, Y., & Pietenpol, J. A. (2011). Identification of human triple-negative breast cancer subtypes and preclinical models for

selection of targeted therapies. *The Journal of Clinical Investigation*, *121*(7), 2750–2767. https://doi.org/10.1172/JCI45014
Lehmann, B. D., & Pietenpol, J. A. (2014). Identification and use of biomarkers in treatment strategies for triple-negative breast cancer subtypes. *The Journal of Pathology*, *232*(2), 142–150. https://doi.org/10.1002/path.4280
Lei, N., Peng, B., & Zhang, J.-Y. (2014). CIP2A regulates cell proliferation via the AKT signaling pathway in human lung cancer. *Oncology Reports*, *32*(4), 1689–1694. https://doi.org/10.3892/or.2014.3375
Leonard, D., Huang, W., Izadmehr, S., O'Connor, C. M., Wiredja, D. D., Wang, Z., Zaware, N., Chen, Y., Schlatzer, D. M., Kiselar, J., Vasireddi, N., Schüchner, S., Perl, A. L., Galsky, M. D., Xu, W., Brautigan, D. L., Ogris, E., Taylor, D. J., & Narla, G. (2020). Selective PP2A Enhancement through Biased Heterotrimer Stabilization. *Cell*, *181*(3), 688-701.e16. https://doi.org/10.1016/j.cell.2020.03.038
Letourneux, C., Rocher, G., & Porteu, F. (2006). B56-containing PP2A dephosphorylate ERK and their activity is controlled by the early gene IEX-1 and ERK. *The EMBO Journal*, *25*(4), 727–738. https://doi.org/10.1038/sj.emboj.7600980
Li, J., Liu, W., Hao, H., Wang, Q., & Xue, L. (2019). Rapamycin enhanced the antitumor effects of doxorubicin in myelogenous leukemia K562 cells by downregulating the mTOR/p70S6K pathway. *Oncology Letters*, *18*(3), 2694–2703. https://doi.org/10.3892/ol.2019.10589
Li, X., Nan, A., Xiao, Y., Chen, Y., & Lai, Y. (2015). PP2A-B56ϵ complex is involved in dephosphorylation of γ-H2AX in the repair process of CPT-induced DNA double-strand breaks. *Toxicology*, *331*, 57–65. https://doi.org/10.1016/j.tox.2015.03.007
Li, X., Scuderi, A., Letsou, A., & Virshup, D. M. (2002). B56-associated protein phosphatase 2A is required for survival and protects from apoptosis in Drosophila melanogaster. *Molecular and Cellular Biology*, *22*(11), 3674–3684. https://doi.org/10.1128/MCB.22.11.3674-3684.2002
Li, X., Wilmanns, M., Thornton, J., & Köhn, M. (2013). Elucidating human phosphatase-substrate networks. *Science Signaling*, *6*(275), rs10. https://doi.org/10.1126/scisignal.2003203
Li, X., Yost, H. J., Virshup, D. M., & Seeling, J. M. (2001). Protein phosphatase 2A and its B56 regulatory subunit inhibit Wnt signaling in Xenopus. *The EMBO Journal*, *20*(15), 4122–4131. https://doi.org/10.1093/emboj/20.15.4122
Lieber, M. R. (2010). The mechanism of double-strand DNA break repair by the nonhomologous DNA end-joining pathway. *Annual Review of Biochemistry*, *79*, 181–211. https://doi.org/10.1146/annurev.biochem.052308.093131
Liedtke, C., Mazouni, C., Hess, K. R., André, F., Tordai, A., Mejia, J. A., Symmans, W. F., Gonzalez-Angulo, A. M., Hennessy, B., Green, M., Cristofanilli, M., Hortobagyi, G. N., & Pusztai, L. (2008). Response to neoadjuvant therapy and long-term survival in patients with triple-negative breast cancer. *Journal of Clinical Oncology : Official Journal of the American Society of Clinical Oncology*, *26*(8), 1275–1281. https://doi.org/10.1200/JCO.2007.14.4147
Lin, N. U., Claus, E., Sohl, J., Razzak, A. R., Arnaout, A., & Winer, E. P. (2008). Sites of distant recurrence and clinical outcomes in patients with metastatic triple-negative breast cancer: high incidence of central nervous system metastases. *Cancer*, *113*(10), 2638–2645. https://doi.org/10.1002/cncr.23930
Lin, S. S., Bassik, M. C., Suh, H., Nishino, M., Arroyo, J. D., Hahn, W. C., Korsmeyer, S. J., & Roberts, T. M. (2006). PP2A regulates BCL-2 phosphorylation and proteasome-mediated degradation at the endoplasmic reticulum. *The Journal of Biological Chemistry*, *281*(32), 23003–23012. https://doi.org/10.1074/jbc.M602648200
Liu, C.-Y., Huang, T.-T., Chen, Y.-T., Chen, J.-L., Chu, P.-Y., Huang, C.-T., Wang, W.-L., Lau, K.-Y., Dai, M.-S., Shiau, C.-W., & Tseng, L.-M. (2019). Targeting SET to restore PP2A activity disrupts an oncogenic CIP2A-feedforward loop and impairs triple negative breast cancer progression. *EBioMedicine*, *40*, 263–275. https://doi.org/10.1016/j.ebiom.2018.12.032
Liu, H., Qiu, H., Song, Y., Liu, Y., Wang, H., Lu, M., Deng, M., Gu, Y., Yin, J., Luo, K., Zhang, Z., Jia, X., Zheng, G., & He, Z. (2017). Cip2a promotes cell cycle progression in triple-negative breast cancer cells by regulating the expression and nuclear export of p27Kip1. *Oncogene*, *36*(14), 1952–1964. https://doi.org/10.1038/onc.2016.355
Liu, L., Wang, Y., Miao, L., Liu, Q., Musetti, S., Li, J., & Huang, L. (2018). Combination Immunotherapy of MUC1 mRNA Nano-vaccine and CTLA-4 Blockade Effectively Inhibits Growth of Triple Negative Breast Cancer. *Molecular Therapy : The Journal of the American Society of Gene Therapy*, *26*(1), 45–55. https://doi.org/10.1016/j.ymthe.2017.10.020

Liu, Y., Zhang, Z., Liang, H., Zhao, X., Liang, L., Wang, G., Yang, J., Jin, Y., McNutt, M. A., & Yin, Y. (2017). Protein Phosphatase 2A (PP2A) Regulates EG5 to Control Mitotic Progression. *Scientific Reports*, *7*(1), 1630. https://doi.org/10.1038/s41598-017-01915-w

Liu, Y.-R., Jiang, Y.-Z., Xu, X.-E., Yu, K.-D., Jin, X., Hu, X., Zuo, W.-J., Hao, S., Wu, J., Liu, G.-Y., Di, G.-H., Li, D.-Q., He, X.-H., Hu, W.-G., & Shao, Z.-M. (2016). Comprehensive transcriptome analysis identifies novel molecular subtypes and subtype-specific RNAs of triple-negative breast cancer. *Breast Cancer Research : BCR*, *18*(1), 33. https://doi.org/10.1186/s13058-016-0690-8

Livasy, C. A., Karaca, G., Nanda, R., Tretiakova, M. S., Olopade, O. I., Moore, D. T., & Perou, C. M. (2006). Phenotypic evaluation of the basal-like subtype of invasive breast carcinoma. *Modern Pathology : An Official Journal of the United States and Canadian Academy of Pathology, Inc*, *19*(2), 264–271. https://doi.org/10.1038/modpathol.3800528

Lowe, M., Gonatas, N. K., & Warren, G. (2000). The mitotic phosphorylation cycle of the cis-Golgi matrix protein GM130. *The Journal of Cell Biology*, *149*(2), 341–356. https://doi.org/10.1083/jcb.149.2.341

Lu, J., Kovach, J. S., Johnson, F., Chiang, J., Hodes, R., Lonser, R., & Zhuang, Z. (2009). Inhibition of serine/threonine phosphatase PP2A enhances cancer chemotherapy by blocking DNA damage induced defense mechanisms. *Proceedings of the National Academy of Sciences*, *106*(28), 11697–11702. https://doi.org/10.1073/pnas.0905930106

Lussey-Lepoutre, C., Hollinshead, K. E. R., Ludwig, C., Menara, M., Morin, A., Castro-Vega, L.-J., Parker, S. J., Janin, M., Martinelli, C., Ottolenghi, C., Metallo, C., Gimenez-Roqueplo, A.-P., Favier, J., & Tennant, D. A. (2015). Loss of succinate dehydrogenase activity results in dependency on pyruvate carboxylation for cellular anabolism. *Nature Communications*, *6*, 8784. https://doi.org/10.1038/ncomms9784

Ma, F., Li, H., Wang, H., Shi, X., Fan, Y., Ding, X., Lin, C., Zhan, Q., Qian, H., & Xu, B. (2014). Enriched CD44(+)/CD24(-) population drives the aggressive phenotypes presented in triple-negative breast cancer (TNBC). *Cancer Letters*, *353*(2), 153–159. https://doi.org/10.1016/j.canlet.2014.06.022

Ma, Y., Chapman, J., Levine, M., Polireddy, K., Drisko, J., & Chen, Q. (2014). High-dose parenteral ascorbate enhanced chemosensitivity of ovarian cancer and reduced toxicity of chemotherapy. *Science Translational Medicine*, *6*(222), 222ra18. https://doi.org/10.1126/scitranslmed.3007154

Macheret, M., & Halazonetis, T. D. (2015). DNA replication stress as a hallmark of cancer. *Annual Review of Pathology*, *10*, 425–448. https://doi.org/10.1146/annurev-pathol-012414-040424

Manchado, E., Guillamot, M., de Cárcer, G., Eguren, M., Trickey, M., García-Higuera, I., Moreno, S., Yamano, H., Cañamero, M., & Malumbres, M. (2010). Targeting mitotic exit leads to tumor regression in vivo: Modulation by Cdk1, Mastl, and the PP2A/B55α,δ phosphatase. *Cancer Cell*, *18*(6), 641–654. https://doi.org/10.1016/j.ccr.2010.10.028

Margolis, S. S., Perry, J. A., Forester, C. M., Nutt, L. K., Guo, Y., Jardim, M. J., Thomenius, M. J., Freel, C. D., Darbandi, R., Ahn, J.-H., Arroyo, J. D., Wang, X.-F., Shenolikar, S., Nairn, A. C., Dunphy, W. G., Hahn, W. C., Virshup, D. M., & Kornbluth, S. (2006). Role for the PP2A/B56delta phosphatase in regulating 14-3-3 release from Cdc25 to control mitosis. *Cell*, *127*(4), 759–773. https://doi.org/10.1016/j.cell.2006.10.035

Martina, J. A., & Puertollano, R. (2018). Protein phosphatase 2A stimulates activation of TFEB and TFE3 transcription factors in response to oxidative stress. *Journal of Biological Chemistry*, *293*(32), 12525–12534. https://doi.org/10.1074/jbc.RA118.003471

Martiniova, L., Lu, J., Chiang, J., Bernardo, M., Lonser, R., Zhuang, Z., & Pacak, K. (2011). Pharmacologic modulation of serine/threonine phosphorylation highly sensitizes PHEO in a MPC cell and mouse model to conventional chemotherapy. *PloS One*, *6*(2), e14678. https://doi.org/10.1371/journal.pone.0014678

Mathupala, S. P., Rempel, A., & Pedersen, P. L. (2001). Glucose catabolism in cancer cells: identification and characterization of a marked activation response of the type II hexokinase gene to hypoxic conditions. *The Journal of Biological Chemistry*, *276*(46), 43407–43412. https://doi.org/10.1074/jbc.M108181200

Matsuoka, S., Ballif, B. A., Smogorzewska, A., McDonald, E. R., Hurov, K. E., Luo, J., Bakalarski, C. E., Zhao, Z., Solimini, N., Lerenthal, Y., Shiloh, Y., Gygi, S. P., & Elledge, S. J. (2007). ATM and ATR substrate analysis reveals extensive protein networks responsive to DNA damage. *Science (New York, N.Y.)*, *316*(5828), 1160–1166. https://doi.org/10.1126/science.1140321

Maya-Mendoza, A., Petermann, E., Gillespie, D. A. F., Caldecott, K. W., & Jackson, D. A. (2007). Chk1 regulates the density of active replication origins during the vertebrate S phase. *The EMBO Journal*, *26*(11), 2719–2731. https://doi.org/10.1038/sj.emboj.7601714

Mayers, J. R., Wu, C., Clish, C. B., Kraft, P., Torrence, M. E., Fiske, B. P., Yuan, C., Bao, Y., Townsend, M. K., Tworoger, S. S., Davidson, S. M., Papagiannakopoulos, T., Yang, A., Dayton, T. L., Ogino, S., Stampfer, M. J., Giovannucci, E. L., Qian, Z. R., Rubinson, D. A., … Wolpin, B. M. (2014). Elevation of circulating branched-chain amino acids is an early event in human pancreatic adenocarcinoma development. *Nature Medicine*, *20*(10), 1193–1198. https://doi.org/10.1038/nm.3686

McConnell, J. L., Gomez, R. J., McCorvey, L. R. A., Law, B. K., & Wadzinski, B. E. (2007). Identification of a PP2A-interacting protein that functions as a negative regulator of phosphatase activity in the ATM/ATR signaling pathway. *Oncogene*, *26*(41), 6021–6030. https://doi.org/10.1038/sj.onc.1210406

McCright, B., Rivers, A. M., Audlin, S., & Virshup, D. M. (1996). The B56 family of protein phosphatase 2A (PP2A) regulatory subunits encodes differentiation-induced phosphoproteins that target PP2A to both nucleus and cytoplasm. *The Journal of Biological Chemistry*, *271*(36), 22081–22089. https://doi.org/10.1074/jbc.271.36.22081

Memmott, R. M., Mercado, J. R., Maier, C. R., Kawabata, S., Fox, S. D., & Dennis, P. A. (2010). Metformin prevents tobacco carcinogen--induced lung tumorigenesis. *Cancer Prevention Research (Philadelphia, Pa.)*, *3*(9), 1066–1076. https://doi.org/10.1158/1940-6207.CAPR-10-0055

Merisaari, J., Denisova, O. v, Doroszko, M., le Joncour, V., Johansson, P., Leenders, W. P. J., Kastrinsky, D. B., Zaware, N., Narla, G., Laakkonen, P., Nelander, S., Ohlmeyer, M., & Westermarck, J. (2020). Monotherapy efficacy of blood-brain barrier permeable small molecule reactivators of protein phosphatase 2A in glioblastoma. *Brain Communications*, *2*(1), fcaa002. https://doi.org/10.1093/braincomms/fcaa002

Miller, K., Wang, M., Gralow, J., Dickler, M., Cobleigh, M., Perez, E. A., Shenkier, T., Cella, D., & Davidson, N. E. (2007). Paclitaxel plus Bevacizumab versus Paclitaxel Alone for Metastatic Breast Cancer. *New England Journal of Medicine*, *357*(26), 2666–2676. https://doi.org/10.1056/NEJMoa072113

Mills, J. R., Hippo, Y., Robert, F., Chen, S. M. H., Malina, A., Lin, C.-J., Trojahn, U., Wendel, H.-G., Charest, A., Bronson, R. T., Kogan, S. C., Nadon, R., Housman, D. E., Lowe, S. W., & Pelletier, J. (2008). mTORC1 promotes survival through translational control of Mcl-1. *Proceedings of the National Academy of Sciences of the United States of America*, *105*(31), 10853–10858. https://doi.org/10.1073/pnas.0804821105

Mitra, A., Menezes, M. E., Pannell, L. K., Mulekar, M. S., Honkanen, R. E., Shevde, L. A., & Samant, R. S. (2012). DNAJB6 chaperones PP2A mediated dephosphorylation of GSK3β to downregulate β-catenin transcription target, osteopontin. *Oncogene*, *31*(41), 4472–4483. https://doi.org/10.1038/onc.2011.623

Mochida, S., Ikeo, S., Gannon, J., & Hunt, T. (2009). Regulated activity of PP2A-B55 delta is crucial for controlling entry into and exit from mitosis in Xenopus egg extracts. *The EMBO Journal*, *28*(18), 2777–2785. https://doi.org/10.1038/emboj.2009.238

Mochida, S., Maslen, S. L., Skehel, M., & Hunt, T. (2010). Greatwall phosphorylates an inhibitor of protein phosphatase 2A that is essential for mitosis. *Science (New York, N.Y.)*, *330*(6011), 1670–1673. https://doi.org/10.1126/science.1195689

Morita, K., He, S., Nowak, R. P., Wang, J., Zimmerman, M. W., Fu, C., Durbin, A. D., Martel, M. W., Prutsch, N., Gray, N. S., Fischer, E. S., & Look, A. T. (2022). Retraction Notice to: Allosteric Activators of Protein Phosphatase 2A Display Broad Antitumor Activity Mediated by Dephosphorylation of MYBL2. *Cell*, *185*(16), 3058. https://doi.org/10.1016/j.cell.2022.07.008

Moynahan, M. E., & Jasin, M. (2010). Mitotic homologous recombination maintains genomic stability and suppresses tumorigenesis. *Nature Reviews. Molecular Cell Biology*, *11*(3), 196–207. https://doi.org/10.1038/nrm2851

Mukhopadhyay, A., Saddoughi, S. A., Song, P., Sultan, I., Ponnusamy, S., Senkal, C. E., Snook, C. F., Arnold, H. K., Sears, R. C., Hannun, Y. A., & Ogretmen, B. (2009). Direct interaction between the inhibitor 2 and ceramide via sphingolipid-protein binding is involved in the regulation of protein phosphatase 2A activity and signaling. *FASEB Journal : Official Publication of the Federation of American Societies for Experimental Biology*, *23*(3), 751–763. https://doi.org/10.1096/fj.08-120550

Mullen, A. R., Wheaton, W. W., Jin, E. S., Chen, P.-H., Sullivan, L. B., Cheng, T., Yang, Y., Linehan, W. M., Chandel, N. S., & DeBerardinis, R. J. (2012). Reductive carboxylation supports growth in tumour cells with defective mitochondria. *Nature*, *481*(7381), 385–388. https://doi.org/10.1038/nature10642

Mumby, M. (2007). PP2A: unveiling a reluctant tumor suppressor. *Cell*, *130*(1), 21–24. https://doi.org/10.1016/j.cell.2007.06.034

Murai, J., Huang, S. N., Das, B. B., Renaud, A., Zhang, Y., Doroshow, J. H., Ji, J., Takeda, S., & Pommier, Y. (2012). Trapping of PARP1 and PARP2 by Clinical PARP Inhibitors. *Cancer Research*, *72*(21), 5588–5599. https://doi.org/10.1158/0008-5472.CAN-12-2753

Myant, K., Qiao, X., Halonen, T., Come, C., Laine, A., Janghorban, M., Partanen, J. I., Cassidy, J., Ogg, E.-L., Cammareri, P., Laiterä, T., Okkeri, J., Klefström, J., Sears, R. C., Sansom, O. J., & Westermarck, J. (2015). Serine 62-Phosphorylated MYC Associates with Nuclear Lamins and Its Regulation by CIP2A Is Essential for Regenerative Proliferation. *Cell Reports*, *12*(6), 1019–1031. https://doi.org/10.1016/j.celrep.2015.07.003

Nakashima, A., Tanimura-Ito, K., Oshiro, N., Eguchi, S., Miyamoto, T., Momonami, A., Kamada, S., Yonezawa, K., & Kikkawa, U. (2013). A positive role of mammalian Tip41-like protein, TIPRL, in the amino-acid dependent mTORC1-signaling pathway through interaction with PP2A. *FEBS Letters*, *587*(18), 2924–2929. https://doi.org/10.1016/j.febslet.2013.07.027

Nanda, R., Chow, L. Q. M., Dees, E. C., Berger, R., Gupta, S., Geva, R., Pusztai, L., Pathiraja, K., Aktan, G., Cheng, J. D., Karantza, V., & Buisseret, L. (2016). Pembrolizumab in Patients With Advanced Triple-Negative Breast Cancer: Phase Ib KEYNOTE-012 Study. *Journal of Clinical Oncology : Official Journal of the American Society of Clinical Oncology*, *34*(21), 2460–2467. https://doi.org/10.1200/JCO.2015.64.8931

Nencioni, A., Caffa, I., Cortellino, S., & Longo, V. D. (2018). Fasting and cancer: molecular mechanisms and clinical application. *Nature Reviews. Cancer*, *18*(11), 707–719. https://doi.org/10.1038/s41568-018-0061-0

Neviani, P., Santhanam, R., Trotta, R., Notari, M., Blaser, B. W., Liu, S., Mao, H., Chang, J. S., Galietta, A., Uttam, A., Roy, D. C., Valtieri, M., Bruner-Klisovic, R., Caligiuri, M. A., Bloomfield, C. D., Marcucci, G., & Perrotti, D. (2005). The tumor suppressor PP2A is functionally inactivated in blast crisis CML through the inhibitory activity of the BCR/ABL-regulated SET protein. *Cancer Cell*, *8*(5), 355–368. https://doi.org/10.1016/j.ccr.2005.10.015

Nghiem, P., Park, P. K., Kim, Y., Vaziri, C., & Schreiber, S. L. (2001). ATR inhibition selectively sensitizes G1 checkpoint-deficient cells to lethal premature chromatin condensation. *Proceedings of the National Academy of Sciences of the United States of America*, *98*(16), 9092–9097. https://doi.org/10.1073/pnas.161281798

Nieman, K. M., Kenny, H. A., Penicka, C. v, Ladanyi, A., Buell-Gutbrod, R., Zillhardt, M. R., Romero, I. L., Carey, M. S., Mills, G. B., Hotamisligil, G. S., Yamada, S. D., Peter, M. E., Gwin, K., & Lengyel, E. (2011). Adipocytes promote ovarian cancer metastasis and provide energy for rapid tumor growth. *Nature Medicine*, *17*(11), 1498–1503. https://doi.org/10.1038/nm.2492

O'Connor, C. M., Perl, A., Leonard, D., Sangodkar, J., & Narla, G. (2018). Therapeutic targeting of PP2A. *The International Journal of Biochemistry & Cell Biology*, *96*, 182–193. https://doi.org/10.1016/j.biocel.2017.10.008

O'Connor, M. J. (2015). Targeting the DNA Damage Response in Cancer. *Molecular Cell*, *60*(4), 547–560. https://doi.org/10.1016/j.molcel.2015.10.040

Owen, M. R., Doran, E., & Halestrap, A. P. (2000). Evidence that metformin exerts its anti-diabetic effects through inhibition of complex 1 of the mitochondrial respiratory chain. *The Biochemical Journal*, *348 Pt 3*, 607–614.

Park, C., Suh, Y., & Cuervo, A. M. (2015). Regulated degradation of Chk1 by chaperone-mediated autophagy in response to DNA damage. *Nature Communications*, *6*, 6823. https://doi.org/10.1038/ncomms7823

Park, S. Y., Lee, H. E., Li, H., Shipitsin, M., Gelman, R., & Polyak, K. (2010). Heterogeneity for stem cell-related markers according to tumor subtype and histologic stage in breast cancer. *Clinical Cancer Research : An Official Journal of the American Association for Cancer Research*, *16*(3), 876–887. https://doi.org/10.1158/1078-0432.CCR-09-1532

Parker, J. S., Mullins, M., Cheang, M. C. U., Leung, S., Voduc, D., Vickery, T., Davies, S., Fauron, C., He, X., Hu, Z., Quackenbush, J. F., Stijleman, I. J., Palazzo, J., Marron, J. S., Nobel, A. B., Mardis, E., Nielsen, T. O., Ellis, M. J., Perou, C. M., & Bernard, P. S. (2009). Supervised risk predictor of breast cancer based on intrinsic subtypes. *Journal of Clinical Oncology : Official Journal of the American Society of Clinical Oncology*, *27*(8), 1160–1167. https://doi.org/10.1200/JCO.2008.18.1370

Pastan, I., & Hassan, R. (2014). Discovery of mesothelin and exploiting it as a target for immunotherapy. *Cancer Research*, *74*(11), 2907–2912. https://doi.org/10.1158/0008-5472.CAN-14-0337

Patel, A. G., Sarkaria, J. N., & Kaufmann, S. H. (2011). Nonhomologous end joining drives poly(ADP-ribose) polymerase (PARP) inhibitor lethality in homologous recombination-deficient cells. *Proceedings of the National Academy of Sciences of the United States of America*, *108*(8), 3406–3411. https://doi.org/10.1073/pnas.1013715108

Paull, T. T. (2015). Mechanisms of ATM Activation. *Annual Review of Biochemistry*, *84*, 711–738. https://doi.org/10.1146/annurev-biochem-060614-034335

Paulsen, R. D., & Cimprich, K. A. (2007). The ATR pathway: fine-tuning the fork. *DNA Repair*, *6*(7), 953–966. https://doi.org/10.1016/j.dnarep.2007.02.015

Pavlova, N. N., & Thompson, C. B. (2016). The Emerging Hallmarks of Cancer Metabolism. *Cell Metabolism*, *23*(1), 27–47. https://doi.org/10.1016/j.cmet.2015.12.006

Pearce, E. L., Poffenberger, M. C., Chang, C.-H., & Jones, R. G. (2013). Fueling immunity: insights into metabolism and lymphocyte function. *Science (New York, N.Y.)*, *342*(6155), 1242454. https://doi.org/10.1126/science.1242454

Perou, C. M., Sørlie, T., Eisen, M. B., van de Rijn, M., Jeffrey, S. S., Rees, C. A., Pollack, J. R., Ross, D. T., Johnsen, H., Akslen, L. A., Fluge, O., Pergamenschikov, A., Williams, C., Zhu, S. X., Lønning, P. E., Børresen-Dale, A. L., Brown, P. O., & Botstein, D. (2000). Molecular portraits of human breast tumours. *Nature*, *406*(6797), 747–752. https://doi.org/10.1038/35021093

Perry, D. M., Kitatani, K., Roddy, P., El-Osta, M., & Hannun, Y. A. (2012). Identification and characterization of protein phosphatase 2C activation by ceramide. *Journal of Lipid Research*, *53*(8), 1513–1521. https://doi.org/10.1194/jlr.M025395

Petermann, E., Maya-Mendoza, A., Zachos, G., Gillespie, D. A. F., Jackson, D. A., & Caldecott, K. W. (2006). Chk1 requirement for high global rates of replication fork progression during normal vertebrate S phase. *Molecular and Cellular Biology*, *26*(8), 3319–3326. https://doi.org/10.1128/MCB.26.8.3319-3326.2006

Petermann, E., Woodcock, M., & Helleday, T. (2010). Chk1 promotes replication fork progression by controlling replication initiation. *Proceedings of the National Academy of Sciences of the United States of America*, *107*(37), 16090–16095. https://doi.org/10.1073/pnas.1005031107

Petersen, P., Chou, D. M., You, Z., Hunter, T., Walter, J. C., & Walter, G. (2006). Protein phosphatase 2A antagonizes ATM and ATR in a Cdk2- and Cdc7-independent DNA damage checkpoint. *Molecular and Cellular Biology*, *26*(5), 1997–2011. https://doi.org/10.1128/MCB.26.5.1997-2011.2006

Peterson, R. T., Desai, B. N., Hardwick, J. S., & Schreiber, S. L. (1999). Protein phosphatase 2A interacts with the 70-kDa S6 kinase and is activated by inhibition of FKBP12-rapamycinassociated protein. *Proceedings of the National Academy of Sciences of the United States of America*, *96*(8), 4438–4442. https://doi.org/10.1073/pnas.96.8.4438

Peterson, T. R., Sengupta, S. S., Harris, T. E., Carmack, A. E., Kang, S. A., Balderas, E., Guertin, D. A., Madden, K. L., Carpenter, A. E., Finck, B. N., & Sabatini, D. M. (2011). mTOR complex 1 regulates lipin 1 localization to control the SREBP pathway. *Cell*, *146*(3), 408–420. https://doi.org/10.1016/j.cell.2011.06.034

Pilié, P. G., Tang, C., Mills, G. B., & Yap, T. A. (2019). State-of-the-art strategies for targeting the DNA damage response in cancer. *Nature Reviews. Clinical Oncology*, *16*(2), 81–104. https://doi.org/10.1038/s41571-018-0114-z

Pollak, M. (2014). Overcoming Drug Development Bottlenecks With Repurposing: Repurposing biguanides to target energy metabolism for cancer treatment. *Nature Medicine*, *20*(6), 591–593. https://doi.org/10.1038/nm.3596

Pommier, Y., Leo, E., Zhang, H., & Marchand, C. (2010). DNA topoisomerases and their poisoning by anticancer and antibacterial drugs. *Chemistry & Biology*, *17*(5), 421–433. https://doi.org/10.1016/j.chembiol.2010.04.012

Porter, I. M., Schleicher, K., Porter, M., & Swedlow, J. R. (2013). Bod1 regulates protein phosphatase 2A at mitotic kinetochores. *Nature Communications*, *4*, 2677. https://doi.org/10.1038/ncomms3677

Prakash, R., Zhang, Y., Feng, W., & Jasin, M. (2015). Homologous recombination and human health: the roles of BRCA1, BRCA2, and associated proteins. *Cold Spring Harbor Perspectives in Biology*, *7*(4), a016600. https://doi.org/10.1101/cshperspect.a016600

Preiss, D., Lloyd, S. M., Ford, I., McMurray, J. J., Holman, R. R., Welsh, P., Fisher, M., Packard, C. J., & Sattar, N. (2014). Metformin for non-diabetic patients with coronary heart disease (the CAMERA study): a randomised controlled trial. *The Lancet. Diabetes & Endocrinology*, *2*(2), 116–124. https://doi.org/10.1016/S2213-8587(13)70152-9

Puustinen, P., & Jäättelä, M. (2014). KIAA1524/CIP2A promotes cancer growth by coordinating the activities of MTORC1 and MYC. *Autophagy*, *10*(7), 1352–1354. https://doi.org/10.4161/auto.29076

Puustinen, P., Rytter, A., Mortensen, M., Kohonen, P., Moreira, J. M., & Jäättelä, M. (2014). CIP2A oncoprotein controls cell growth and autophagy through mTORC1 activation. *The Journal of Cell Biology*, *204*(5), 713–727. https://doi.org/10.1083/jcb.201304012

Qu, Y., Han, B., Yu, Y., Yao, W., Bose, S., Karlan, B. Y., Giuliano, A. E., & Cui, X. (2015). Evaluation of MCF10A as a Reliable Model for Normal Human Mammary Epithelial Cells. *PloS One*, *10*(7), e0131285. https://doi.org/10.1371/journal.pone.0131285

Raffaghello, L., Lee, C., Safdie, F. M., Wei, M., Madia, F., Bianchi, G., & Longo, V. D. (2008). Starvation-dependent differential stress resistance protects normal but not cancer cells against high-dose chemotherapy. *Proceedings of the National Academy of Sciences of the United States of America*, *105*(24), 8215–8220. https://doi.org/10.1073/pnas.0708100105

Ramos, F., Villoria, M. T., Alonso-Rodríguez, E., & Clemente-Blanco, A. (2019). Role of protein phosphatases PP1, PP2A, PP4 and Cdc14 in the DNA damage response. *Cell Stress*, *3*(3), 70–85. https://doi.org/10.15698/cst2019.03.178

Rice, L. M., Donigan, M., Yang, M., Liu, W., Pandya, D., Joseph, B. K., Sodi, V., Gearhart, T. L., Yip, J., Bouchard, M., & Nickels, J. T. (2014). Protein phosphatase 2A (PP2A) regulates low density lipoprotein uptake through regulating sterol response element-binding protein-2 (SREBP-2) DNA binding. *The Journal of Biological Chemistry*, *289*(24), 17268–17279. https://doi.org/10.1074/jbc.M114.570390

Robey, R. B., & Hay, N. (2006). Mitochondrial hexokinases, novel mediators of the antiapoptotic effects of growth factors and Akt. *Oncogene*, *25*(34), 4683–4696. https://doi.org/10.1038/sj.onc.1209595

Robson, M., Goessl, C., & Domchek, S. (2017). Olaparib for Metastatic Germline BRCA-Mutated Breast Cancer. *The New England Journal of Medicine*, *377*(18), 1792–1793. https://doi.org/10.1056/NEJMc1711644

Robson, M., Im, S.-A., Senkus, E., Xu, B., Domchek, S. M., Masuda, N., Delaloge, S., Li, W., Tung, N., Armstrong, A., Wu, W., Goessl, C., Runswick, S., & Conte, P. (2017). Olaparib for Metastatic Breast Cancer in Patients with a Germline BRCA Mutation. *The New England Journal of Medicine*, *377*(6), 523–533. https://doi.org/10.1056/NEJMoa1706450

Roesch, A., Vultur, A., Bogeski, I., Wang, H., Zimmermann, K. M., Speicher, D., Körbel, C., Laschke, M. W., Gimotty, P. A., Philipp, S. E., Krause, E., Pätzold, S., Villanueva, J., Krepler, C., Fukunaga-Kalabis, M., Hoth, M., Bastian, B. C., Vogt, T., & Herlyn, M. (2013). Overcoming intrinsic multidrug resistance in melanoma by blocking the mitochondrial respiratory chain of slow-cycling JARID1B(high) cells. *Cancer Cell*, *23*(6), 811–825. https://doi.org/10.1016/j.ccr.2013.05.003

Rohban, S., & Campaner, S. (2015). Myc induced replicative stress response: How to cope with it and exploit it. *Biochimica et Biophysica Acta*, *1849*(5), 517–524. https://doi.org/10.1016/j.bbagrm.2014.04.008

Rouse, J., & Jackson, S. P. (2002). Interfaces between the detection, signaling, and repair of DNA damage. *Science (New York, N.Y.)*, *297*(5581), 547–551. https://doi.org/10.1126/science.1074740

Ruvolo, P. P., Qui, Y. H., Coombes, K. R., Zhang, N., Ruvolo, V. R., Borthakur, G., Konopleva, M., Andreeff, M., & Kornblau, S. M. (2011). Low expression of PP2A regulatory subunit B55α is associated with T308 phosphorylation of AKT and shorter complete remission duration in acute myeloid leukemia patients. *Leukemia*, *25*(11), 1711–1717. https://doi.org/10.1038/leu.2011.146

Sabharwal, S. S., & Schumacker, P. T. (2014). Mitochondrial ROS in cancer: initiators, amplifiers or an Achilles' heel? *Nature Reviews. Cancer*, *14*(11), 709–721. https://doi.org/10.1038/nrc3803

Sablina, A. A., Chen, W., Arroyo, J. D., Corral, L., Hector, M., Bulmer, S. E., DeCaprio, J. A., & Hahn, W. C. (2007). The tumor suppressor PP2A Abeta regulates the RalA GTPase. *Cell*, *129*(5), 969–982. https://doi.org/10.1016/j.cell.2007.03.047

Sachlos, E., Risueño, R. M., Laronde, S., Shapovalova, Z., Lee, J.-H., Russell, J., Malig, M., McNicol, J. D., Fiebig-Comyn, A., Graham, M., Levadoux-Martin, M., Lee, J. B., Giacomelli, A. O., Hassell, J. A., Fischer-Russell, D., Trus, M. R., Foley, R., Leber, B., Xenocostas, A., … Bhatia, M. (2012). Identification of drugs including a dopamine receptor antagonist that selectively target cancer stem cells. *Cell*, *149*(6), 1284–1297. https://doi.org/10.1016/j.cell.2012.03.049

Saito, Y., Chapple, R. H., Lin, A., Kitano, A., & Nakada, D. (2015). AMPK Protects Leukemia-Initiating Cells in Myeloid Leukemias from Metabolic Stress in the Bone Marrow. *Cell Stem Cell*, *17*(5), 585–596. https://doi.org/10.1016/j.stem.2015.08.019

Sangodkar, J., Farrington, C. C., McClinch, K., Galsky, M. D., Kastrinsky, D. B., & Narla, G. (2016). All roads lead to PP2A: exploiting the therapeutic potential of this phosphatase. *The FEBS Journal*, *283*(6), 1004–1024. https://doi.org/10.1111/febs.13573

Schafer, Z. T., Grassian, A. R., Song, L., Jiang, Z., Gerhart-Hines, Z., Irie, H. Y., Gao, S., Puigserver, P., & Brugge, J. S. (2009). Antioxidant and oncogene rescue of metabolic defects caused by loss of matrix attachment. *Nature*, *461*(7260), 109–113. https://doi.org/10.1038/nature08268

Schmitz, M. H. A., Held, M., Janssens, V., Hutchins, J. R. A., Hudecz, O., Ivanova, E., Goris, J., Trinkle-Mulcahy, L., Lamond, A. I., Poser, I., Hyman, A. A., Mechtler, K., Peters, J.-M., & Gerlich, D. W. (2010). Live-cell imaging RNAi screen identifies PP2A-B55alpha and importin-beta1 as key mitotic exit regulators in human cells. *Nature Cell Biology*, *12*(9), 886–893. https://doi.org/10.1038/ncb2092

Segurado, M., & Diffley, J. F. X. (2008). Separate roles for the DNA damage checkpoint protein kinases in stabilizing DNA replication forks. *Genes & Development*, *22*(13), 1816–1827. https://doi.org/10.1101/gad.477208

Shechter, D., Costanzo, V., & Gautier, J. (2004). ATR and ATM regulate the timing of DNA replication origin firing. *Nature Cell Biology*, *6*(7), 648–655. https://doi.org/10.1038/ncb1145

Shi, Q., Le, X., Wang, B., Abbruzzese, J. L., Xiong, Q., He, Y., & Xie, K. (2001). Regulation of vascular endothelial growth factor expression by acidosis in human cancer cells. *Oncogene*, *20*(28), 3751–3756. https://doi.org/10.1038/sj.onc.1204500

Shim, H. S., Wei, M., Brandhorst, S., & Longo, V. D. (2015). Starvation promotes REV1 SUMOylation and p53-dependent sensitization of melanoma and breast cancer cells. *Cancer Research*, *75*(6), 1056–1067. https://doi.org/10.1158/0008-5472.CAN-14-2249

Shimada, M., & Nakanishi, M. (2013). Response to DNA damage: why do we need to focus on protein phosphatases? *Frontiers in Oncology*, *3*, 8. https://doi.org/10.3389/fonc.2013.00008

Smetana, J. H. C., & Zanchin, N. I. T. (2007). Interaction analysis of the heterotrimer formed by the phosphatase 2A catalytic subunit, alpha4 and the mammalian ortholog of yeast Tip41 (TIPRL). *The FEBS Journal*, *274*(22), 5891–5904. https://doi.org/10.1111/j.1742-4658.2007.06112.x

So, S., Davis, A. J., & Chen, D. J. (2009). Autophosphorylation at serine 1981 stabilizes ATM at DNA damage sites. *The Journal of Cell Biology*, *187*(7), 977–990. https://doi.org/10.1083/jcb.200906064

Song, D.-G., Ye, Q., Poussin, M., Chacon, J. A., Figini, M., & Powell, D. J. (2016). Effective adoptive immunotherapy of triple-negative breast cancer by folate receptor-alpha redirected CAR T cells is influenced by surface antigen expression level. *Journal of Hematology & Oncology*, *9*(1), 56. https://doi.org/10.1186/s13045-016-0285-y

Sørlie, T., Perou, C. M., Tibshirani, R., Aas, T., Geisler, S., Johnsen, H., Hastie, T., Eisen, M. B., van de Rijn, M., Jeffrey, S. S., Thorsen, T., Quist, H., Matese, J. C., Brown, P. O., Botstein, D., Lønning, P. E., & Børresen-Dale, A. L. (2001). Gene expression patterns of breast carcinomas distinguish tumor subclasses with clinical implications. *Proceedings of the National Academy of Sciences of the United States of America*, *98*(19), 10869–10874. https://doi.org/10.1073/pnas.191367098

Sporikova, Z., Koudelakova, V., Trojanec, R., & Hajduch, M. (2018). Genetic Markers in Triple-Negative Breast Cancer. *Clinical Breast Cancer*, *18*(5), e841–e850. https://doi.org/10.1016/j.clbc.2018.07.023

St Onge, R. P., Besley, B. D. A., Pelley, J. L., & Davey, S. (2003). A role for the phosphorylation of hRad9 in checkpoint signaling. *The Journal of Biological Chemistry*, *278*(29), 26620–26628. https://doi.org/10.1074/jbc.M303134200

Steelman, L. S., Navolanic, P. M., Sokolosky, M. L., Taylor, J. R., Lehmann, B. D., Chappell, W. H., Abrams, S. L., Wong, E. W. T., Stadelman, K. M., Terrian, D. M., Leslie, N. R., Martelli, A. M., Stivala, F., Libra, M., Franklin, R. A., & McCubrey, J. A. (2008). Suppression of PTEN function increases breast cancer chemotherapeutic drug resistance while conferring sensitivity to mTOR inhibitors. *Oncogene*, *27*(29), 4086–4095. https://doi.org/10.1038/onc.2008.49

Strohecker, A. M., & White, E. (2014). Autophagy promotes BrafV600E-driven lung tumorigenesis by preserving mitochondrial metabolism. *Autophagy*, *10*(2), 384–385. https://doi.org/10.4161/auto.27320

Sun, W. Y., Lee, Y. K., & Koo, J. S. (2016). Expression of PD-L1 in triple-negative breast cancer based on different immunohistochemical antibodies. *Journal of Translational Medicine*, *14*(1), 173. https://doi.org/10.1186/s12967-016-0925-6

Sun, Y., Jiang, X., Chen, S., Fernandes, N., & Price, B. D. (2005). A role for the Tip60 histone acetyltransferase in the acetylation and activation of ATM. *Proceedings of the National Academy of Sciences of the United States of America*, *102*(37), 13182–13187. https://doi.org/10.1073/pnas.0504211102

Sun, Y., Xu, Y., Roy, K., & Price, B. D. (2007). DNA damage-induced acetylation of lysine 3016 of ATM activates ATM kinase activity. *Molecular and Cellular Biology*, *27*(24), 8502–8509. https://doi.org/10.1128/MCB.01382-07

Tacar, O., & Dass, C. R. (2013). Doxorubicin-induced death in tumour cells and cardiomyocytes: is autophagy the key to improving future clinical outcomes? *The Journal of Pharmacy and Pharmacology*, *65*(11), 1577–1589. https://doi.org/10.1111/jphp.12144

Taffs, R. E., Redegeld, F. A., & Sitkovsky, M. v. (1991). Modulation of cytolytic T lymphocyte functions by an inhibitor of serine/threonine phosphatase, okadaic acid. Enhancement of cytolytic T lymphocyte-mediated cytotoxicity. *Journal of Immunology (Baltimore, Md. : 1950)*, *147*(2), 722–728.

Tagde, A., Singh, H., Kang, M. H., & Reynolds, C. P. (2014). The glutathione synthesis inhibitor buthionine sulfoximine synergistically enhanced melphalan activity against preclinical models of multiple myeloma. *Blood Cancer Journal*, *4*, e229. https://doi.org/10.1038/bcj.2014.45

Tan, D. S. P., Marchió, C., Jones, R. L., Savage, K., Smith, I. E., Dowsett, M., & Reis-Filho, J. S. (2008). Triple negative breast cancer: molecular profiling and prognostic impact in adjuvant anthracycline-treated patients. *Breast Cancer Research and Treatment*, *111*(1), 27–44. https://doi.org/10.1007/s10549-007-9756-8

Tan, E. Y., Yan, M., Campo, L., Han, C., Takano, E., Turley, H., Candiloro, I., Pezzella, F., Gatter, K. C., Millar, E. K. A., O'Toole, S. A., McNeil, C. M., Crea, P., Segara, D., Sutherland, R. L., Harris, A. L., & Fox, S. B. (2009). The key hypoxia regulated gene CAIX is upregulated in basal-like breast tumours and is associated with resistance to chemotherapy. *British Journal of Cancer*, *100*(2), 405–411. https://doi.org/10.1038/sj.bjc.6604844

ten Klooster, J. P., Leeuwen, I. v, Scheres, N., Anthony, E. C., & Hordijk, P. L. (2007). Rac1-induced cell migration requires membrane recruitment of the nuclear oncogene SET. *The EMBO Journal*, *26*(2), 336–345. https://doi.org/10.1038/sj.emboj.7601518

Tseng, L.-M., Liu, C.-Y., Chang, K.-C., Chu, P.-Y., Shiau, C.-W., & Chen, K.-F. (2012). CIP2A is a target of bortezomib in human triple negative breast cancer cells. *Breast Cancer Research : BCR*, *14*(2), R68. https://doi.org/10.1186/bcr3175

Tsuji, S., Kohyanagi, N., Mizuno, T., Ohama, T., & Sato, K. (2021). Perphenazine exerts antitumor effects on HUT78 cells through Akt dephosphorylation by protein phosphatase 2A. *Oncology Letters*, *21*(2), 113. https://doi.org/10.3892/ol.2020.12374

Tubbs, J. L., Pegg, A. E., & Tainer, J. A. (2007). DNA binding, nucleotide flipping, and the helix-turn-helix motif in base repair by O6-alkylguanine-DNA alkyltransferase and its implications for cancer chemotherapy. *DNA Repair*, *6*(8), 1100–1115. https://doi.org/10.1016/j.dnarep.2007.03.011

Turenne, G. A., Paul, P., Laflair, L., & Price, B. D. (2001). Activation of p53 transcriptional activity requires ATM's kinase domain and multiple N-terminal serine residues of p53. *Oncogene*, *20*(37), 5100–5110. https://doi.org/10.1038/sj.onc.1204665

Tutt, A., Robson, M., Garber, J. E., Domchek, S. M., Audeh, M. W., Weitzel, J. N., Friedlander, M., Arun, B., Loman, N., Schmutzler, R. K., Wardley, A., Mitchell, G., Earl, H., Wickens, M., & Carmichael, J. (2010). Oral poly(ADP-ribose) polymerase inhibitor olaparib in patients with BRCA1 or BRCA2 mutations and advanced breast cancer: a proof-of-concept trial. *Lancet (London, England)*, *376*(9737), 235–244. https://doi.org/10.1016/S0140-6736(10)60892-6

Ueng, S.-H., Chen, S.-C., Chang, Y.-S., Hsueh, S., Lin, Y.-C., Chien, H.-P., Lo, Y.-F., Shen, S.-C., & Hsueh, C. (2012). Phosphorylated mTOR expression correlates with poor outcome in early-stage triple negative breast carcinomas. *International Journal of Clinical and Experimental Pathology*, *5*(8), 806–813.

Ugi, S., Imamura, T., Maegawa, H., Egawa, K., Yoshizaki, T., Shi, K., Obata, T., Ebina, Y., Kashiwagi, A., & Olefsky, J. M. (2004). Protein phosphatase 2A negatively regulates insulin's metabolic signaling pathway by inhibiting Akt (protein kinase B) activity in 3T3-L1 adipocytes. *Molecular and Cellular Biology*, *24*(19), 8778–8789. https://doi.org/10.1128/MCB.24.19.8778-8789.2004

Ugi, S., Imamura, T., Ricketts, W., & Olefsky, J. M. (2002). Protein phosphatase 2A forms a molecular complex with Shc and regulates Shc tyrosine phosphorylation and downstream mitogenic signaling. *Molecular and Cellular Biology*, *22*(7), 2375–2387. https://doi.org/10.1128/MCB.22.7.2375-2387.2002

Valvona, C. J., Fillmore, H. L., Nunn, P. B., & Pilkington, G. J. (2016). The Regulation and Function of Lactate Dehydrogenase A: Therapeutic Potential in Brain Tumor. *Brain Pathology (Zurich, Switzerland)*, *26*(1), 3–17. https://doi.org/10.1111/bpa.12299

vande Voorde, J., Ackermann, T., Pfetzer, N., Sumpton, D., Mackay, G., Kalna, G., Nixon, C., Blyth, K., Gottlieb, E., & Tardito, S. (2019). Improving the metabolic fidelity of cancer models with a

physiological cell culture medium. *Science Advances*, *5*(1), eaau7314. https://doi.org/10.1126/sciadv.aau7314
vander Heiden, M. G. (2011). Targeting cancer metabolism: a therapeutic window opens. *Nature Reviews. Drug Discovery*, *10*(9), 671–684. https://doi.org/10.1038/nrd3504
vander Heiden, M. G., Cantley, L. C., & Thompson, C. B. (2009). Understanding the Warburg effect: the metabolic requirements of cell proliferation. *Science (New York, N.Y.)*, *324*(5930), 1029–1033. https://doi.org/10.1126/science.1160809
Varadkar, P., Abbasi, F., Takeda, K., Dyson, J. J., & McCright, B. (2017). PP2A-B56γ is required for an efficient spindle assembly checkpoint. *Cell Cycle (Georgetown, Tex.)*, *16*(12), 1210–1219. https://doi.org/10.1080/15384101.2017.1325042
Venkitaraman, A. R. (2014). Cancer suppression by the chromosome custodians, BRCA1 and BRCA2. *Science (New York, N.Y.)*, *343*(6178), 1470–1475. https://doi.org/10.1126/science.1252230
Vernieri, C., Fucà, G., Ligorio, F., Huber, V., Vingiani, A., Iannelli, F., Raimondi, A., Rinchai, D., Frigè, G., Belfiore, A., Lalli, L., Chiodoni, C., Cancila, V., Zanardi, F., Ajazi, A., Cortellino, S., Vallacchi, V., Squarcina, P., Cova, A., … de Braud, F. (2022). Fasting-Mimicking Diet Is Safe and Reshapes Metabolism and Antitumor Immunity in Patients with Cancer. *Cancer Discovery*, *12*(1), 90–107. https://doi.org/10.1158/2159-8290.CD-21-0030
Vervoort, S. J., Welsh, S. A., Devlin, J. R., Barbieri, E., Knight, D. A., Offley, S., Bjelosevic, S., Costacurta, M., Todorovski, I., Kearney, C. J., Sandow, J. J., Fan, Z., Blyth, B., McLeod, V., Vissers, J. H. A., Pavic, K., Martin, B. P., Gregory, G., Demosthenous, E., … Johnstone, R. W. (2021). The PP2A-Integrator-CDK9 axis fine-tunes transcription and can be targeted therapeutically in cancer. *Cell*, *184*(12), 3143-3162.e32. https://doi.org/10.1016/j.cell.2021.04.022
von Minckwitz, G., Untch, M., Blohmer, J.-U., Costa, S. D., Eidtmann, H., Fasching, P. A., Gerber, B., Eiermann, W., Hilfrich, J., Huober, J., Jackisch, C., Kaufmann, M., Konecny, G. E., Denkert, C., Nekljudova, V., Mehta, K., & Loibl, S. (2012). Definition and impact of pathologic complete response on prognosis after neoadjuvant chemotherapy in various intrinsic breast cancer subtypes. *Journal of Clinical Oncology : Official Journal of the American Society of Clinical Oncology*, *30*(15), 1796–1804. https://doi.org/10.1200/JCO.2011.38.8595
Wang, J., Okkeri, J., Pavic, K., Wang, Z., Kauko, O., Halonen, T., Sarek, G., Ojala, P. M., Rao, Z., Xu, W., & Westermarck, J. (2017). Oncoprotein CIP2A is stabilized via interaction with tumor suppressor PP2A/B56. *EMBO Reports*, *18*(3), 437–450. https://doi.org/10.15252/embr.201642788
Wang, Y.-H., Israelsen, W. J., Lee, D., Yu, V. W. C., Jeanson, N. T., Clish, C. B., Cantley, L. C., vander Heiden, M. G., & Scadden, D. T. (2014). Cell-state-specific metabolic dependency in hematopoiesis and leukemogenesis. *Cell*, *158*(6), 1309–1323. https://doi.org/10.1016/j.cell.2014.07.048
Wang, Z., Zhang, X., Shen, P., Loggie, B. W., Chang, Y., & Deuel, T. F. (2005). Identification, cloning, and expression of human estrogen receptor-alpha36, a novel variant of human estrogen receptor-alpha66. *Biochemical and Biophysical Research Communications*, *336*(4), 1023–1027. https://doi.org/10.1016/j.bbrc.2005.08.226
Wang, Z., Zhang, X., Shen, P., Loggie, B. W., Chang, Y., & Deuel, T. F. (2006). A variant of estrogen receptor-{alpha}, hER-{alpha}36: transduction of estrogen- and antiestrogen-dependent membrane-initiated mitogenic signaling. *Proceedings of the National Academy of Sciences of the United States of America*, *103*(24), 9063–9068. https://doi.org/10.1073/pnas.0603339103
WARBURG, O. (1956). On respiratory impairment in cancer cells. *Science (New York, N.Y.)*, *124*(3215), 269–270.
Wei, D., Parsels, L. A., Karnak, D., Davis, M. A., Parsels, J. D., Marsh, A. C., Zhao, L., Maybaum, J., Lawrence, T. S., Sun, Y., & Morgan, M. A. (2013). Inhibition of Protein Phosphatase 2A Radiosensitizes Pancreatic Cancers by Modulating CDC25C/CDK1 and Homologous Recombination Repair. *Clinical Cancer Research*, *19*(16), 4422–4432. https://doi.org/10.1158/1078-0432.CCR-13-0788
Wei, H., Zhang, H.-L., Wang, X.-C., Xie, J.-Z., An, D.-D., Wan, L., Wang, J.-Z., Zeng, Y., Shu, X.-J., Westermarck, J., Lu, Y.-M., Ohlmeyer, M., & Liu, R. (2020). Direct Activation of Protein Phosphatase 2A (PP2A) by Tricyclic Sulfonamides Ameliorates Alzheimer's Disease Pathogenesis in Cell and Animal Models. *Neurotherapeutics : The Journal of the American Society for Experimental NeuroTherapeutics*, *17*(3), 1087–1103. https://doi.org/10.1007/s13311-020-00841-6
Westermarck, J., & Neel, B. G. (2020). Piecing Together a Broken Tumor Suppressor Phosphatase for Cancer Therapy. *Cell*, *181*(3), 514–517. https://doi.org/10.1016/j.cell.2020.04.005

Wheaton, W. W., Weinberg, S. E., Hamanaka, R. B., Soberanes, S., Sullivan, L. B., Anso, E., Glasauer, A., Dufour, E., Mutlu, G. M., Budigner, G. S., & Chandel, N. S. (2014). Metformin inhibits mitochondrial complex I of cancer cells to reduce tumorigenesis. *ELife*, *3*, e02242. https://doi.org/10.7554/eLife.02242

Wilson, J. E. (2003). Isozymes of mammalian hexokinase: structure, subcellular localization and metabolic function. *The Journal of Experimental Biology*, *206*(Pt 12), 2049–2057. https://doi.org/10.1242/jeb.00241

Wilson, W. R., & Hay, M. P. (2011). Targeting hypoxia in cancer therapy. *Nature Reviews. Cancer*, *11*(6), 393–410. https://doi.org/10.1038/nrc3064

Wong, P.-M., Feng, Y., Wang, J., Shi, R., & Jiang, X. (2015). Regulation of autophagy by coordinated action of mTORC1 and protein phosphatase 2A. *Nature Communications*, *6*, 8048. https://doi.org/10.1038/ncomms9048

Xie, H., Hanai, J.-I., Ren, J.-G., Kats, L., Burgess, K., Bhargava, P., Signoretti, S., Billiard, J., Duffy, K. J., Grant, A., Wang, X., Lorkiewicz, P. K., Schatzman, S., Bousamra, M., Lane, A. N., Higashi, R. M., Fan, T. W. M., Pandolfi, P. P., Sukhatme, V. P., & Seth, P. (2014). Targeting lactate dehydrogenase--a inhibits tumorigenesis and tumor progression in mouse models of lung cancer and impacts tumor-initiating cells. *Cell Metabolism*, *19*(5), 795–809. https://doi.org/10.1016/j.cmet.2014.03.003

Xing, Y., Xu, Y., Chen, Y., Jeffrey, P. D., Chao, Y., Lin, Z., Li, Z., Strack, S., Stock, J. B., & Shi, Y. (2006). Structure of protein phosphatase 2A core enzyme bound to tumor-inducing toxins. *Cell*, *127*(2), 341–353. https://doi.org/10.1016/j.cell.2006.09.025

Xu, Y., Xing, Y., Chen, Y., Chao, Y., Lin, Z., Fan, E., Yu, J. W., Strack, S., Jeffrey, P. D., & Shi, Y. (2006). Structure of the protein phosphatase 2A holoenzyme. *Cell*, *127*(6), 1239–1251. https://doi.org/10.1016/j.cell.2006.11.033

Yamada, A., Ishikawa, T., Ota, I., Kimura, M., Shimizu, D., Tanabe, M., Chishima, T., Sasaki, T., Ichikawa, Y., Morita, S., Yoshiura, K., Takabe, K., & Endo, I. (2013). High expression of ATP-binding cassette transporter ABCC11 in breast tumors is associated with aggressive subtypes and low disease-free survival. *Breast Cancer Research and Treatment*, *137*(3), 773–782. https://doi.org/10.1007/s10549-012-2398-5

Yan, L., Mieulet, V., Burgess, D., Findlay, G. M., Sully, K., Procter, J., Goris, J., Janssens, V., Morrice, N. A., & Lamb, R. F. (2010). PP2A T61 epsilon is an inhibitor of MAP4K3 in nutrient signaling to mTOR. *Molecular Cell*, *37*(5), 633–642. https://doi.org/10.1016/j.molcel.2010.01.031

Ye, J., Fan, J., Venneti, S., Wan, Y.-W., Pawel, B. R., Zhang, J., Finley, L. W. S., Lu, C., Lindsten, T., Cross, J. R., Qing, G., Liu, Z., Simon, M. C., Rabinowitz, J. D., & Thompson, C. B. (2014). Serine catabolism regulates mitochondrial redox control during hypoxia. *Cancer Discovery*, *4*(12), 1406–1417. https://doi.org/10.1158/2159-8290.CD-14-0250

Yin, L., Duan, J.-J., Bian, X.-W., & Yu, S.-C. (2020). Triple-negative breast cancer molecular subtyping and treatment progress. *Breast Cancer Research : BCR*, *22*(1), 61. https://doi.org/10.1186/s13058-020-01296-5

Young, M. R. I., Kolesiak, K., & Meisinger, J. (2002). Protein phosphatase-2A regulates endothelial cell motility and both the phosphorylation and the stability of focal adhesion complexes. *International Journal of Cancer*, *100*(3), 276–282. https://doi.org/10.1002/ijc.10491

Young, M. R. I., Liu, S. W., & Meisinger, J. (2003). Protein phosphatase-2A restricts migration of Lewis lung carcinoma cells by modulating the phosphorylation of focal adhesion proteins. *International Journal of Cancer*, *103*(1), 38–44. https://doi.org/10.1002/ijc.10772

Yu, G., Yan, T., Feng, Y., Liu, X., Xia, Y., Luo, H., Wang, J.-Z., & Wang, X. (2013). Ser9 phosphorylation causes cytoplasmic detention of I2PP2A/SET in Alzheimer disease. *Neurobiology of Aging*, *34*(7), 1748–1758. https://doi.org/10.1016/j.neurobiolaging.2012.12.025

Zeman, M. K., & Cimprich, K. A. (2014). Causes and consequences of replication stress. *Nature Cell Biology*, *16*(1), 2–9. https://doi.org/10.1038/ncb2897

Zhang, J., Jiang, W., Liu, W., Wu, J.-J., Song, L., Cheng, J.-X., Yao, M., Yang, L.-P., & Yao, D.-F. (2016). Effective targeting of colorectal cancer cells using TORC1/2 kinase inhibitors in vitro and in vivo. *Future Oncology (London, England)*, *12*(4), 515–524. https://doi.org/10.2217/fon.15.248

Zhang, X. T., Kang, L. G., Ding, L., Vranic, S., Gatalica, Z., & Wang, Z.-Y. (2011). A positive feedback loop of ER-α36/EGFR promotes malignant growth of ER-negative breast cancer cells. *Oncogene*, *30*(7), 770–780. https://doi.org/10.1038/onc.2010.458

Zhao, H., & Piwnica-Worms, H. (2001). ATR-mediated checkpoint pathways regulate phosphorylation and activation of human Chk1. *Molecular and Cellular Biology*, *21*(13), 4129–4139. https://doi.org/10.1128/MCB.21.13.4129-4139.2001

Zheng, H., Qi, Y., Hu, S., Cao, X., Xu, C., Yin, Z., Chen, X., Li, Y., Liu, W., Li, J., Wang, J., Wei, G., Liang, K., Chen, F. X., & Xu, Y. (2020). Identification of Integrator-PP2A complex (INTAC), an RNA polymerase II phosphatase. *Science (New York, N.Y.)*, *370*(6520). https://doi.org/10.1126/science.abb5872

Zheng, L., Cardaci, S., Jerby, L., MacKenzie, E. D., Sciacovelli, M., Johnson, T. I., Gaude, E., King, A., Leach, J. D. G., Edrada-Ebel, R., Hedley, A., Morrice, N. A., Kalna, G., Blyth, K., Ruppin, E., Frezza, C., & Gottlieb, E. (2015). Fumarate induces redox-dependent senescence by modifying glutathione metabolism. *Nature Communications*, *6*, 6001. https://doi.org/10.1038/ncomms7001

Zhou, P., Shaffer, D. R., Alvarez Arias, D. A., Nakazaki, Y., Pos, W., Torres, A. J., Cremasco, V., Dougan, S. K., Cowley, G. S., Elpek, K., Brogdon, J., Lamb, J., Turley, S. J., Ploegh, H. L., Root, D. E., Love, J. C., Dranoff, G., Hacohen, N., Cantor, H., & Wucherpfennig, K. W. (2014). In vivo discovery of immunotherapy targets in the tumour microenvironment. *Nature*, *506*(7486), 52–57. https://doi.org/10.1038/nature12988

Zhou, S., Schuetz, J. D., Bunting, K. D., Colapietro, A. M., Sampath, J., Morris, J. J., Lagutina, I., Grosveld, G. C., Osawa, M., Nakauchi, H., & Sorrentino, B. P. (2001). The ABC transporter Bcrp1/ABCG2 is expressed in a wide variety of stem cells and is a molecular determinant of the side-population phenotype. *Nature Medicine*, *7*(9), 1028–1034. https://doi.org/10.1038/nm0901-1028

Zhu, D., Yuan, Y., Qiao, J., Yu, C., Yang, X., Wang, L., Zhang, Z., & Zhong, L. (2015). Enhanced anticancer activity of a protein phosphatase 2A inhibitor on chemotherapy and radiation in head and neck squamous cell carcinoma. *Cancer Letters*, *356*(2 Pt B), 773–780. https://doi.org/10.1016/j.canlet.2014.10.024

Zou, L., & Elledge, S. J. (2003). Sensing DNA damage through ATRIP recognition of RPA-ssDNA complexes. *Science (New York, N.Y.)*, *300*(5625), 1542–1548. https://doi.org/10.1126/science.1083430

Acknowledgements

First and foremost, I would like to thank Prof. Saverio Minucci for his guidance, support, and trust that allowed me to pursue this project.

I want to express my gratitude to my internal and external advisors, Prof. Marco Foiani and Dr. Saverio Tardito, for their advices and helpful discussions.

I also thank the reviewers of the present thesis, Dr. Claudio Vernieri and Prof. Jukka Westermarck, for their feedback and comments.

Finally, I would like to thank all the members of the Minucci's group and people in IEO, friends more than colleagues, for sharing this journey with me.